UiT The Arctic University of Norway

Faculty of Health Science

Modern corneal imaging technology in cataract and refractive surgery

Total corneal astigmatism and corneal epithelial thickness measurements for surgical planning in lens exchange- and laser vision correction surgery

Yue Feng

A dissertation for the degree of Doctor of Philosophy (PhD) September 2024

Table of Contents

List of Tables

List of Figures

1. Acknowledgments

I would like to acknowledge all the individuals who have directly and indirectly contributed to this PhD project and express my sincere gratitude. Their unwavering support and involvement have been invaluable, and I am genuinely grateful to every one of them. The names listed below represent those to whom I am particularly thankful.

My deepest gratitude goes to Aleksandar Stojanovic and Geir Bertelsen, whose encouragement and support have provided constant inspiration throughout this endeavor. Aleksandar played a pivotal role in initiating this PhD project, while Geir graciously assumed the role of my primary supervisor from the University side. Collaborating with Aleksandar has been an extraordinary and enriching experience, thanks to his remarkable passion for scientific knowledge.

Tore Nitter consistently demonstrated exceptional scientific acumen, fearlessly tackling every scientific challenge that arose. His presence and contributions have been truly invaluable.

I am immensely grateful to Dan Z. Reinstein and Timothy J. Archer from the London Vision Clinic in the United Kingdom, who have been dedicated research partners. Their support has played a pivotal role in the successful execution of my studies.

Colm McAlinden has been instrumental in revising my manuscripts and has provided invaluable suggestions throughout my PhD journey. I am genuinely thankful for his assistance.

I would like to extend my gratitude to Tor Paske Utheim and Xiangjun Chen, the co-supervisors of this PhD project, for their generous support and guidance.

I would also like to thank those individuals whom I haven't mentioned but who also deserve recognition and appreciation.

2. Abbreviations

AL	Axial length
AS-OCT	Anterior segment optical coherence tomography
CDVA	Corrected distance visual acuity
CXL	Corneal collagen crosslinking
D	Diopter
ETM	Epithelial thickness mapping
HOAs	Higher-order aberrations
IOL	Intraocular lens
KC	Keratoconus
LASIK	Laser in situ keratomileusis
LoA	Limit of agreement
LogMAR	Logarithm of the minimum angle of resolution
LVC	Laser vision correction
PRK	Photorefractive keratectomy
RLE	refractive lens exchange
SD	Standard deviation
SD-OCT	Spectral Domain optical coherence tomography
SimK	Simulated keratometry
SMILE	Small incision lenticule extraction
SS-OCT	Swept-source optical coherence tomography
TCA	Total corneal astigmatism
TCP	Total corneal power
T-PTK	Transepithelial phototherapeutic keratectomy
UDVA	Uncorrected distance visual acuity
VHF	Very high-frequency
Paper 1	Repeatability and agreement of total corneal astigmatism measured in keratoconic eyes using four current devices
Paper 2	Heidelberg Anterion Swept-Source OCT Corneal Epithelial Thickness Mapping: Repeatability and Agreement with Optovue Avanti
Paper 3	Epithelial Thickness Mapping in Keratoconic Corneas: Repeatability and Agreement Between CSO MS-39, Heidelberg Anterion, and Optovue Avanti OCT Devices

3. Abstract

3.1 Background/Aim

The precision and accuracy of corneal imaging technology are crucial in contemporary cataract and refractive surgery. This thesis aims to assess the quality of measurements for total corneal astigmatism (TCA), axial length (AL) and corneal epithelial thickness mapping (ETM), that are curial for early detection and management of keratoconus (KC), as well as for planning and monitoring refractive surgery. Five modern optical coherence tomography (OCT) devices were tested across various the clinical conditions, including keratoconus, post-laser vision correction eyes, and in normal eyes.

3.2 Methods

We examined 392 eyes with three consecutive measurements using two swept-source (SS) OCTs (Anterion and Casia SS-1000), one spectral-domain (SD) OCT (Avanti), one SS-OCT combined with reflectometry (IOLMaster 700), and one SD-OCT combined with Placido imaging (MS-39). Repeatability was assessed by pooled within-subject standard deviation (S_w), and agreement was analyzed using paired t-tests, Bland-Altman plots, and the tolerance index were used for agreement (TA).

3.3 Results

TCA measurements demonstrated excellent repeatability across all devices. However, statistically significant differences in cylinder magnitude were observed for most pairs of devices, except IOLMaster 700 vs. MS-39 and Anterion vs. MS-39. Anterion and IOLMaster 700 exhibited high repeatability in AL measurements and the difference between them was not clinically significant. For ETM, Anterion demonstrated higher repeatability compared to Avanti and MS-39. The TA surpassed the cutoff in all sections for all pairs of devices, showing their non-interchangeability.

3.4 Conclusions

All devices demonstrated good repeatability in TCA-, AL- and ETM measurements. However, variations and low agreement in cylinder magnitude and ETM were observed, proving their non-interchangeability. On the other hand, AL measurements with Anterion and IOLMaster 700 were interchangeable. We expect that our findings may provide valuable

insights for a tailored approach in the use of the tested device in a broad spectrum of clinical situations.

4. Introduction

4.1 The Ocular surface

4.1.1 The Tear Film

The tear film is a vital component of the ocular surface and plays a crucial role in maintaining the health and functionality of the eye.[1] It consists of three layers (Figure 1): the lipid layer (0.1 µm), the aqueous layer (7 µm), and the mucin layer (0.02 to 0.05 µm).[2, 3] The lipid layer is primarily produced by the meibomian glands located in the eyelids. It forms a thin film on the surface, reducing the rate of tear evaporation and maintaining tear stability.[4] The aqueous layer is responsible for lubrication and provides the necessary nutrients to maintain osmolarity. The aqueous layer is produced by the lacrimal glands, which are located in the upper outer portion of the eye socket. The lacrimal glands secrete a watery fluid that contains electrolytes, proteins, and other substances essential for maintaining the health of the cornea and other ocular tissues.[5] Lastly, the mucin layer is produced by the goblet cells located in the conjunctiva, which is the thin membrane that covers the white part of the eye and lines the inside of the eyelids. The mucin layer plays a crucial role in protecting the corneal epithelium. It helps spread the tear film evenly across the cornea, ensuring that the corneal epithelium remains moist and protected.[2] These layers function synergistically to establish a stable tear film that plays a crucial role in ensuring ocular comfort and provides mechanical, environmental, and immune protection. Additionally, they are indispensable for maintaining epithelial health and creating a smooth refractive surface, essential for clear vision.[6]

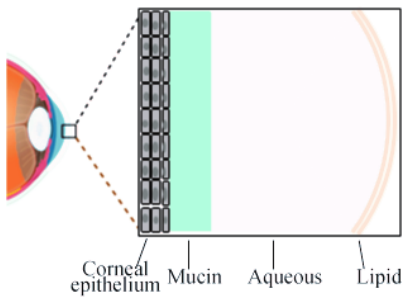

Figure 1 The tear film consists of three distinct layers: the lipid layer, the aqueous layer, and the mucin layer.

The air-tear film interface, the first refractive surface of the eye, contributes to the eye's refractive power the most, due to the large difference in refractive index between the air and the tear film. The tear film is crucial also because it fills and evens out the microscopic irregularities on the corneal surface.[7] This is essential for upholding a consistent and smooth optical surface.[8, 9] Hence, any disruption to the tear film may lead to compromised optical quality and diminished visual performance of the eye.[10] Compromised ocular surface and tear film condition ahead of refractive surgery may impact surgical outcomes, including postoperative dry eye as well as suboptimal refractive outcomes and optical quality.[11]

Among the complaints after refractive corneal surgery, dry eye stands as one of the most prevalent.[12, 13] Its origin is thought to be multifaceted, encompassing neurotrophic epitheliopathy, altered insufficient tear film, and inflammation-induced desiccation of the ocular surface.[14] Though typically transient, its adverse impact on quality of life is noteworthy, often emerging as the principal cause for patient discontentment with the refractive surgery results.[15] Individuals with dry eye following refractive surgery are also exposed to a heightened risk of regression in refraction and detriment to the ocular surface.[16] Identification of individuals with pre-existing dry eye pathology prior to surgery, coupled with preoperative and postoperative interventions, holds the potential for improving refractive surgery outcomes.[17]

4.1.2 The Cornea

The cornea is a dome-shaped, transparent, avascular tissue located at the eye's anterior surface with significant refractive and barrier functions.[18] The average adult cornea is about 520 μm thick in the center and 650 μm thick at the periphery.[7]

The cornea comprises five distinct layers (Figure 2), from anterior to posterior, namely the epithelium, Bowman's layer, stroma, Descemet's membrane, and endothelium. The corneal structure exhibits a complex arrangement tailored to its multiple functions.[19] Additionally, a sixth layer (Dua's layer) has recently been proposed, lying in the pre-Descemet's cornea.[20]

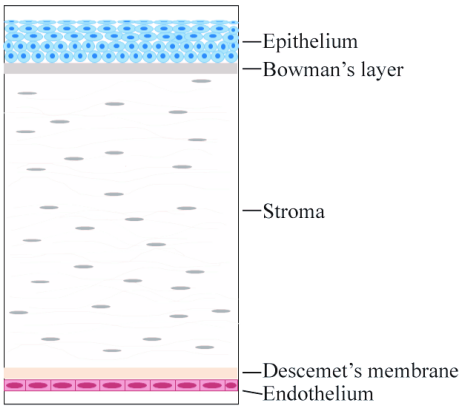

Figure 2 Five distinct layers of the cornea. From anterior to posterior: epithelium, Bowman's layer, stroma, Descemet's membrane, and endothelium.

The corneal epithelium plays an active role in determining the final power of the cornea. The refractive power of the epithelium is significant within the central cornea.[21] It accounts for an average of -1.03 D of the power of a normal virgin eye in the central 2-mm diameter zone.[22] It means that the removal of the epithelium leads to an increase in corneal refracting power since the radius of curvature of the Bowman's membrane is smaller than the cornea with epithelium.[21]

The epithelium does not form a layer of uniform thickness over the Bowman's surface. Epithelial profile is influenced by eyelid anatomy, mechanics and blinking, which occurs 300-1500 times per hour.[23] The eyelid applies more force on the superior than the inferior cornea, and friction during lid closure is greater temporally than nasally.[24] The mechanical stimuli lead to alterations in cell shape and junction integrity, and influence the remodeling of cell-cell junctions in epithelial tissues. Such mechanosensitive remodeling is vital for maintaining tissue homeostasis and barrier function, as cells respond to local mechanical cues by reorganizing their junctions and cytoskeleton.[25] All the mentioned factors dictate the physiological epithelial thickness profile, which shows slightly increased thickness inferiorly and nasally compare with superiorly and temporally. The mentioned forces as well as the smoothness of the stromal surface govern the process of "epithelial remodeling",[26] according to the following four rules: 1. Epithelium thickens to fill the stromal depressions; 2. Epithelium thins over the stromal peaks; 3. Epithelium changes are proportional to the stromal profile landscape;[22] 4. The amount of epithelial thickness variation is defined by the

rate of variation of the stromal curvature.[27] The clinical application of the epithelial remodeling will be elaborated in the discussion section "*7.2 Epithelial thickness*".

Apart from refracting and transmitting incoming light onto the retina, the cornea also safeguards the delicate intraocular structures from external irritants, pathogens, and mechanical trauma. The intricate interplay between the corneal layers, their specialized cellular components, and their extracellular matrix culminates in an optical interface that significantly influences the quality and acuity of vision.

4.1.3 The Corneal Optics

As a primary refractive element in the visual system, the corneal optic is essential in focusing light onto the retina to form a clear and discernible image. The corneal refractive power is determined by its curvature and refractive index, and the quality of the corneal optics is decided by its geometrical/optical regularity. Numerous attempts have been made to simplify the intricate optical system of the human eye, an example being the Gullstrand's eye model.[28] In this model, the total refractive power of the optical system is 58.64 diopters (D), with 43.05 D attributed to the cornea and 19.11 D to the crystalline lens, assuming an axial length of the eye of 24 mm.[29] In Gullstrand's model, the cornea is depicted as a single refractive surface.[30] However, in reality, the incoming light undergoes refraction not only at the anterior, but also at the posterior surface of the cornea, as well as at the interface between the epithelium and Bowman's surface. The anterior surface of the cornea is flatter than the posterior surface, with average radii of curvature measuring 7.7 mm and 6.8 mm, respectively. The anterior corneal surface exhibits significantly higher optical power (48.8 D) than the posterior surface (-5.8 D), due to the significant difference in refractive indexes between the air and the cornea, as opposed to the small difference between the cornea and the aqueous fluid.

Derived from Gullstrand's human cornea model, which establishes a fixed ratio between the anterior and posterior corneal radii of curvature and a theoretical refractive index of 1.3375 (known as the keratometric index of refraction), which presents cornea as a whole was introduced[31]. Building upon this index, Simulated Keratometry (SimK) was introduced in the 1980s as an integral component of computer-assisted video keratography technology[32]. The use of the SimK enables the calculation of the corneal power using the measurements of

only the anterior corneal surface. Until recently, this was a necessity because technology did not allow optical measurements of the posterior cornea, and this has been functioning quite well in eyes with normal, virgin corneas.

The total corneal power (TCP) refers to the optical power of the cornea based on measured curvatures of both the anterior and the posterior corneal surfaces and using the real refractive indexes of the two surfaces for calculating the corneal optics. Using the TCP is essential in cases where the assumption of a fixed relationship between anterior and posterior curvatures is invalid, like after corneal refractive surgery and in keratoconus (KC). Indeed, a study showed that an IOL formula, using direct measurements of both anterior and posterior corneal power, had a higher predictive accuracy for spherical equivalent refractive outcome in post-laser vision correction (LVC) cataract surgery, than the regression-based formulas based on the SimK.[33] In virgin eyes, the contribution of the posterior corneal astigmatism is not nearly as significant as the contribution of the anterior corneal astigmatism [34], and the SimK, which is based solely on anterior corneal measurements, has been used with success to assess the corneal optics in most traditional IOL calculations[35]. Still, the lack of data from the posterior cornea has been identified as the most important source of error in toric IOL calculations[36]. In KC, where the optics of the posterior corneal surface may be dominant and in cases who previously underwent LVC, TCP and total corneal astigmatism (TCA), both based on real measurements of both corneal surfaces, are crucial. An ever-increasing demand for precision in refractive predictability in lens exchange procedures relies on the correct power of the implanted IOL, which in turn depends on precise axial length (AL), corneal power, and corneal astigmatism measurements. By focusing on KC eyes, our first paper aims to address the specific needs of this population for best quality measurements that provide insights relevant for clinical management. Through this investigation, we attempt to address the gap in the current literature by assessing the repeatability and agreement of TCA measurements using four OCT-based devices not previously tested in KC eyes. By performing the measurements in a clinically relevant settings, our paper 1 also aims to aid clinicians' decision-making processes and ultimately help improve the treatment outcomes and visual quality for KC patients.

4.1.4 Keratoconus and epithelial remodeling

KC is a progressive keratoectatic disease with localized biomechanical failure, which leads to a local protrusion and can lead to significant visual impairment due to irregular corneal optics.[37, 38]

The local protrusion causes intense epithelial remodeling consisting of a compensatory thinning over the protruding part (cone) and thickening in the area of the surrounding annulus, giving the characteristic donut-shaped epithelial thickness pattern.[26] Epithelial thickness mapping (ETM) has become an essential tool for the early diagnosis of KC,[26, 39-49] by revealing the epithelial thickness pattern that smoothens and hides the underlying stromal shape. The ETM may be considered an imprint of the protruding stromal surface underneath the moldable epithelial tissue.[50]

In this thesis, one of the primary clinical purposes was to evaluate the use of ETM across different clinical scenarios, including KC eyes, post-refractive surgery eyes, and normal virgin eyes. By comparing three optical coherence tomographers (OCT) featuring different technologies: 1. Spectral-domain (SD) OCT combined with Placido disk corneal topography (MS-39), 2. Swept-source (SS) OCT (Anterion), and 3. SD-OCT (Avanti) —we aimed to determine the repeatability and agreement of these devices in measuring epithelial thickness.

ETM is crucial for the early detection and management of KC, and it is currently broadly used in the armamentarium for KC diagnosis as well as in treatment planning and it is very sensitive in evaluating the effect of the treatment. It is also used in planning and monitoring refractive surgery, both by differentiating true- from pseudo-ectasia in the screening process, and for customized treatment planning in therapeutic cases as well as in primary cases and enhancements. Furthermore, ETM is invaluable in post-refractive surgery monitoring, by providing explanations for unsatisfactory outcomes and potential solutions.

4.2 The Crystalline Lens

4.2.1 Structure and Function

The human crystalline lens is an essential ocular structure behind the iris and the pupil within the eye's anterior segment. It dynamically adjusts its shape to facilitate the focusing of

light onto the retina, at varying distances, a function called accomodation.[51] Comprising a clear, flexible, and avascular tissue, the crystalline lens is enveloped by a thin, elastic membrane known as the lens capsule. This capsule maintains the lens's structural integrity and shape. The lens is further divided into three distinct sections: the lens nucleus, the lens cortex, and the lens epithelium.

During the accommodation process[52], managed by the ciliary muscle, the lens changes its curvature. According to the Helmholtz theory, ciliary muscle contraction leads to relaxation of the lens capsule and relaxation of the zonules that anchor the lens. As a result, the lens becomes thicker and more spherical, enhancing its refractive power for focusing on near objects.

Over time, the lens may undergo age-related changes, including a gradual loss of flexibility and transparency, leading to a condition known as presbyopia. This condition impairs the lens's ability to adjust its shape effectively, resulting in difficulty in focusing on close objects. The advancing age of lens fiber cells, their limited cellular machinery, and elevated levels of crystallin proteins collectively play a role in the development of cataracts. The growing susceptibility of crystallin proteins to damage over time, leads to aggregation of the proteins, ultimately causing the formation of cataracts.[53]

4.2.2 The Lens Optics

The eye adapts its refractive power to achieve focus on nearby objects through accommodation. In the relaxed eye, the lens has a power of about 19 D, while in the fully accommodated state, it can temporarily increase to 33 D in young adults. In a relaxed accommodative state, the collective optical power of the cornea and crystalline lens must correspond to the eye's axial length for a clear focus of distant objects on the retina (emmetropia).[52] Deviations from this harmony result in unfocused images, a condition known as ametropia (refractive error).

4.3 Diagnostics- Corneal imaging technology

4.3.1 OCT and OCT-based topography

OCT is a non-contact optical imaging technique used to visualize and analyze biological tissues with exceptional precision and resolution. It employs the principles of

interferometry and low-coherence light and the backscattered light is measured with an interferometric set-up to reconstruct the depth profile of the sample at the selected location.[54] A scanning OCT beam allows for the acquisition of cross-sectional images of the tissue structure, including the cornea.[55] OCT constructs a depth-resolved profile of the tissue's internal structure by measuring the time delay or phase shift of light returning from various depths in the cornea. This technology allows for non-invasive, high-resolution visualization of the cornea's different layers, such as epithelium, stroma, and endothelium, with micrometer-level precision.[56]

OCT-based corneal imaging has transformed clinical practice in ophthalmology. It aids in diagnosing and monitoring corneal diseases like KC, Fuchs' endothelial dystrophy, and corneal edema. It also plays an increasingly vital role in planning and assessing refractive surgeries, such as LASIK and PRK, by providing accurate preoperative corneal thicknesses and shape measurements.

Three types of OCT technologies, Time-domain, Spectral-domain, and Swept-source have been used in ophthalmology. The first to appear, time-domain OCT (TD-OCT) was remarkable for its time, but it suffered low image resolution. Spectral-domain OCT (SD-OCT) technology achieves up to 100 times more A-scans per second than TD-OCT, minimizing the risk of missing critical pathology.[57] The more recently introduced swept-source OCT (SS-OCT) technology has a light source of longer wavelength than the SD-OCT, allowing greater image depth and high-contrast imaging of the entire anterior segment, achieving ten times faster image capture speeds than SD technology.[58]

Reinstein and colleagues pioneered ETM in 1994,[26, 43, 59] and they have described "epithelial remodeling" across the whole cornea in eyes with KC[26, 39] using very high-frequency (VHF) digital ultrasound scanning (Artemis Insight 100, *ArcScan Inc, Morrison, CO,* USA). OCT-based ETM appeared much later (2011)[41], without surpassing VHF digital ultrasound scanning in terms of repeatability. Still, OCT quickly became prevalent ETM technology in clinical practice due to its speed and ease of use. The first commercially available OCT-based instrument for ETM was the Optovue RT-100 (Optovue, Inc., Fremont, CA, USA), introduced in 2011, featuring SD-OCT technology that provided ETM of the central 6 mm of cornea. SD-OCT technology was later used in numerous other devices providing a larger diameter ETM, with the Avanti (Optovue, Inc., Fremont, CA, USA)

probably becoming the most commonly used one.[60] The Anterion (Heidelberg Engineering, Heidelberg, Germany) and Casia 2 (Tomey Corporation, Nagoya, Japan) are high-resolution anterior segment OCT devices featuring SS-OCT technology.[61]

4.3.2 Placido-based corneal topography

In Placido-based corneal topography, the ring of visible light is projected to the cornea. The reflected image of the corneal surface is captured by a camera. The captured image is then computer-analyzed to determine the distance between the rings and their distortion, which provides information about the anterior corneal curvature and its other optical properties.[62]

There are several constraints inherent to Placido-based technology. Firstly, the scope of corneal coverage is confined to approximately 60%,[63] since the peripheral and central areas of the maps are mostly based on interpolated data. Secondly, it lacks data from the posterior corneal surface, which may be crucial in conditions like KC.[64, 65] Lastly, the topographic curvature maps derived from Placido technology are aligned to a reference axis, and the position of the examined eye influences the reliability of the examination. Consequently, cases involving displaced corneal apex or significant corneal asymmetry can lead to errors, as their reference axis does not coincide with the corneal apex axis.

Different devices may exhibit variations in repeatability and agreement. Such discrepancies may have significant clinical implications in the diagnosis and management of KC eyes. Inconsistent measurements can lead to under- or over-diagnosing, suboptimal treatment choices, and suboptimal follow-up, potentially affecting visual outcomes. Therefore, understanding the clinical impact of measurement variability between devices is crucial for improved the precision of corneal assessments and better quality of subsequent management.

4.4 Lens exchange surgery

4.4.1 Cataract surgery

Cataract surgery, an important procedure in ophthalmology, involves the removal of a clouded crystalline lens (cataract) and its replacement with an artificial IOL to restore visual acuity.

The evolution of cataract surgery witnessed significant advancements in the 20th century. The introduction of extracapsular cataract extraction (ECCE) involved removing the lens while leaving the posterior capsule intact, enabling IOL implantation. However, the surgery still required a large incision and sutures.

The breakthrough came with phacoemulsification, pioneered by Charles Kelman in the 1960s.[66] This technique involved using ultrasonic energy to fragment the cataract, which could then be aspirated through a small incision. The introduction of foldable IOLs in the 1980s allowed for even smaller incisions and improved outcomes.

Modern cataract surgery employs a micro-incision technique, using ultrasound or laser to emulsify the crystalline lens. Patients experience quicker recovery, reduced complications compared to the earlier techniques, and improved visual outcomes. Although certain types of IOLs provide multifocality and capability for both distance and near vision, these lenses currently cannot fully revive the lens's ability to adjust focus.[67]

4.4.2 Lens exchange surgery

Lens exchange surgery, also known as refractive lens exchange (RLE) or clear lens extraction (CLE), is a procedure involving the removal of a clear crystalline lens and replacement with an artificial IOL to correct refractive errors, such as high myopia or hyperopia with or without astigmatism, as one of the refractive surgery procedures.[68] This procedure is technically identical to cataract surgery, but it addresses refractive issues rather than a clouded crystalline lens. RLE mostly involves the use of IOLs with multifocal or accommodating capabilities, offering the potential to correct refractive errors, with the resulting sharp vision at distance and at the same time provide improved functional vision at closer distances.

Evaluation for both cataract surgery and lens exchange surgery involves comprehensive preoperative assessment, to determine the patient's visual acuity, refractive error, ocular health, and potential comorbidities. A biometric analysis is performed to measure the eye's AL and corneal curvature, necessary for IOL power calculation. The patient's medical history, lifestyle, and visual expectations are also assessed.

4.5 Laser vision correction surgery

Corneal laser refractive surgery has been a groundbreaking procedure for correcting vision by reshaping the cornea since the 1980s. The foundation for corneal laser refractive surgery was laid by the development of the excimer laser, which could remove a controlled amount of tissue from the cornea without generating heat, in order to alter its curvature and accurately focus the light onto the retina.

Photorefractive Keratectomy (PRK): Developed in the 1980s[69], PRK was the earliest form of corneal laser refractive surgery, and the first clinical studies were conducted to evaluate its effectiveness in correcting myopia.[70] It involves removing the epithelial layer of the cornea mechanically or with alcohol, before reshaping the underlying stroma with a laser. PRK is effective for treating myopia but has a longer recovery time than the more recent procedures. It may lead to the development of subepithelial scaring (haze), is prone to regression, and can cause discomfort during the initial healing phase. PRK has been less successful in treating hyperopia and high-grade astigmatism. It should be noted that many of the mentioned drawbacks of the original PRK were inherent to the older excimer laser technology, like wide laser-beam of low frequency and lack of reliable eye-tracking.[71] With the advancement of the excimer laser technology after 2010, PRK has regained its popularity, especially if used transepithelially, where the epithelium is also removed by the laser.[71] With this modality most of the issues with the original PRK are solved and the procedure is particularly well suited for therapeutic refractive surgery where customized, corneal topo/tomography- and epithelial thickness map (ETM)- guided ablations are used.

Laser-Assisted in situ Keratomileusis (LASIK): Introduced in the 1990s,[72] LASIK quickly gained popularity due to its quicker visual recovery and reduced postoperative discomfort compared to PRK. In LASIK, a thin flap is created on the cornea's surface, reshaping the underlying tissue with a laser. The flap is then repositioned, allowing for quicker healing and visual improvement. LASIK is suitable for treating myopia, hyperopia, and astigmatism. The 1990s witnessed the rapid growth of refractive surgery popularity. In the early 2000s, LASIK continued to evolve, with surgical techniques and laser technology refinements to enhance outcomes and safety.

Small-Incision Lenticule Extraction (SMILE): SMILE has been introduced in the 2010s.[73] It involves creating a small incision on the cornea by femtosecond laser, to create a precise lenticule of tissue, which is removed to alter the corneal shape, and correcting refractive error. SMILE offers potential advantages, including less disruption to corneal nerves and corneal biomechanics, potentially reducing dry eye symptoms.

Accurate measurements of total corneal astigmatism and corneal epithelial thickness are essential for surgical planning in lens exchange and laser vision correction surgery. These measurements are crucial in selecting the most suitable intraocular lens (IOL) for optimal postoperative visual outcomes and in determining the appropriate surgical techniques in corneal refractive surgery.[71]

4.6 Concepts concerning measurement

4.6.1 Precision

Precision, in the context of measurements, refers to the degree of repeatability and reproducibility of results. It assesses how closely individual measurements agree with each other when performed under the same conditions (repeatability) and when performed by different operators or in different laboratories (reproducibility)[74]. It is a crucial aspect of measurements as it helps determine the reliability and trustworthiness of data. High precision implies that the measurements produce consistent results, which is essential to make correct clinical decisions[75].

4.6.2 Repeatability

Repeatability measures the consistency or precision of results when the same measurement or experiment is repeated multiple times by the same person or using the same equipment and conditions[76]. If the results are very close to each other in such repetitions, it indicates high precision or repeatability.

4.6.3 Reproducibility

Reproducibility assesses the consistency of results when the same measurement is conducted by different individuals, with different equipment, or in different locations. If the results remain consistent across these variations, it signifies high precision or reproducibility.

The current guideline from the International Standard recommends expressing estimates of repeatability and reproducibility using standard deviations[76]. When evaluating the repeatability of repeated measurements on multiple subjects, a one-way analysis of variance (ANOVA) should be performed to determine the within-subject standard deviation (S_w). The S_w is the repeatability of the measurements. Considering the 95% confidence intervals around this value, the repeatability limit (r) is reported as $1.96\sqrt{2} \cdot S_w$ which gives the likely limits within which 95% of measurements should be within.[77]

Comparison refers to the fundamental process of assessing the relationship between different measurements to determine their agreement (see 4.6.4) and interchangeability (see 4.6.5). This concept is crucial for ensuring the reliability and consistency of measurements in various scientific fields.

4.6.4 Agreement

Agreement in measurement refers to the degree of similarity or consistency between multiple measurements acquired by different devices of the same quantity. When measurements agree closely, it suggests that the measurement process is reliable and accurate. The agreement can be summarized by determining a bias, which is estimated by the mean difference *d*, and the standard deviation of the differences (*s*). If there is a consistent bias, it can be accounted for by subtracting *d* from the latter. It would be expected that most differences would lie between d −1.96*s* and d +1.96s assuming that differences follow a normal distribution. Provided the differences within d ± 1.96s are not clinically important (clinical interpretation is an essential attribute of this approach), the measurements of two devices could be used interchangeably.[77]

4.6.5 Interchangeability

Interchangeability refers to the possibility of using a measurement acquired by one device in place of another measurement, which is acquired by another device, with the expectation that it will yield comparable results for the same quantity. Interchangeability is essential for ensuring that measurements made by different instruments or in different locations can be considered equivalent. It involves assessing factors like calibration, standardization, and compatibility between measurement systems. The tolerance index for agreement (TA) is calculated as described by Bergin and colleagues to assess

Interchangeability.[78] TA is defined as TA=$ln\frac{95\%\ LoA}{r}$, where the 95% limits of agreement (LoA) is the difference between the upper and lower 95% LoA and r is the limit of repeatability.

4.6.6 Accuracy

Accuracy refers to how close a measured value is to the "true" value. It reflects the overall correctness of a measurement[74]. It is different to precision, which relates to the reproducibility or consistency of measurements. Precision is concerned with how close individual measurements are to each other, regardless of their closeness to the "true" value[75].

4.7 Study aims

Our aim was to identify clinically suitable technology for measurement of ETM, TCA and AL to assure reliable diagnosis treatment and follow up of keratoconus and other corneal conditions and for use in cataract and refractive surgery. Current corneal imaging technologies, such as traditional Placido imaging and reflectometry, focus on measuring the anterior corneal surface. This approach has significant limitations, particularly in assessing total corneal astigmatism (TCA) and total corneal power (TCP), as it does not account for the posterior corneal surface. For patients with keratoconus (KC) and those who have undergone laser refractive surgery, this oversight can lead to inaccuracies in diagnosis, treatment planning and outcomes. Accurate measurements improve the diagnosis and management of KC and other corneal conditions, while, inaccurate data can result in suboptimal treatment outcomes, affecting visual quality and patient satisfaction. Hence the clinical implications of our measuring corneal posterior surface are substantial. Due to the rapid advancements in imaging technology, there are gaps in literature in deeper understanding of the SD- and SS-OCT technology and its application in measurements of TCA and epithelial thickness in demanding clinical settings.

Lens and laser vision correction surgeries face several challenges, including the need for high accuracy and precision in ocular measurements (TCA, ETM and AL). Traditional intraocular lens (IOL) power calculations, based on anterior keratometry, overestimate corneal power in KC eyes, leading to postoperative refractive errors such as hyperopia. TCA and ETM are also especially important for therapeutic corneal refractive surgery.

Modern imaging technologies, particularly optical coherence tomography (OCT), offer solutions to these challenges. Swept-source OCT (SS-OCT) and spectral-domain OCT (SD-OCT) provide detailed imaging of the entire anterior segment, including both the anterior and posterior corneal surfaces within a short exam lasting couple of seconds, using non-disturbing infra-red light. These advancements enable more accurate TCA and ETM measurements, essential for early diagnosis of KC, differentiate true and pseudo- ectasia, and preoperative assessment in cataract and refractive surgery.

Our project is to identify the most clinically propriate technology among several corneal imaging devices for diagnostic and surgical tasks relevant to cataract and therapeutic cornea surgery, has been achieved by testing the following three hypotheses:

Hypothesis 1: Hybrid SD-OCT and Placido disk imaging technology is clinically applicable and compares favorably to validated SS-OCT and reflectometry technologies in measuring TCA in KC eyes.

Hypothesis 2: SS-OCT-based ETM provides good diagnostic capabilities for detecting and planning treatment for KC and PLRS eyes.

Hypothesis 3: Hybrid SD-OCT and Placido disk imaging technology and SS-OCT technologies for ETM in KC eyes offer similar precision and clinical applicability as the validated SD-OCT technology.

This thesis aims to provide insights into the clinical applications of the tested corneal imaging technology, or use in early diagnosis, differential diagnosis, and preoperative assessment, management, and follow-up in corneal, refractive, and cataract surgery. By understanding each device's strengths and limitations, clinicians may make more informed decisions, improving patient outcomes. Our findings are aimed to emphasize the importance of consistent device usage especially for preoperative and postoperative follow-up of KC progression and PLRS outcomes, and to validate the tested devices in filling the requirements for the very precise measurements of TCA and AL for premium IOL power calculations. Ultimately, our results may help improve overall surgical outcomes in corneal, refractive and cataract surgery.

5. Materials and Methods

5.1 Patients

The participants recruited to the studies were patients screened for candidacy for refractive surgery (Paper 2) or those already treated with refractive surgery at SynsLaser Clinic, Tromsø, Norway (Paper 2), and KC patients referred to CXL at the University Hospital of North Norway, Tromsø, Norway (Papers 1, 2 and 3).

Inclusion criteria for paper 1 were age 18 years or older and healthy corneas for the virgin eye group; age 18 years and older and previous corneal laser vision surgery (both myopic and hyperopic treated eyes) at least three months before the examination for the post laser refractive surgery (PLRS) eye group; and age 16 years or older and a diagnosis of KC and the spherical equivalent of myopia of 8.00 D or less for the KC group. Exclusion criteria included a history of previous ocular surgery (except for PLRS eyes); patients with pterygium or other conjunctival, limbal, or corneal diseases (except for KC); poor fixation or inability to complete the examination; and use of hard contact lenses.

For studies 2 and 3, inclusion criteria were: age 16 years or older; diagnosis of KC; and spherical equivalent of myopia of 8.00 D or less. Exclusion criteria were history of previous ocular surgery (except for CXL); patients with conjunctival, limbal, or corneal disease (except for KC); poor fixation or inability to complete the examination; and use of rigid gas permeable contact lens within two weeks of the examination day. In patients where both eyes met the inclusion criteria, one of each patient's eyes was randomly selected.

5.2 Instruments

5.2.1 Avanti

The Avanti SD-OCT (Optovue, Inc., Fremont, CA, USA; software version 6.11.0.12) generates images using a SLed light source at 840 nm. It features a 70,000-Hz scanning and obtains B-scans with an axial resolution of 5 μm and a transversal resolution of 15 μm.

5.2.2 Anterion

The Anterion SS-OCT (Heidelberg Engineering, Heidelberg, Germany; software version 2.5.2) generates images using a laser light source with a 1300 nm wavelength to obtain B-scans with an axial resolution of <10 μm and a transversal resolution of 45 μm. An active eye-tracker is utilized. The software version 2.5.2, with an activated investigational epithelium feature, provides corneal ETM.

5.2.3 MS-39

The MS-39 (CSO, Firenze, Italy; software Phoenix v.4.1.1.5) combines two illumination sources, for SD-OCT, a super luminescent diode (SLed) at 845 nm, and Placido disk, a SLed at 635 nm. It provides an axial resolution of 3.6 μm and a transversal resolution of 35 μm. For the anterior corneal topography, ring edges are detected on the Placido image, providing native curvature data, while the height and slope data are calculated using the arc-step method. Profiles of both the anterior and the posterior cornea are provided from the SD-OCT scans. Data representing the anterior corneal surface is provided by merging the Placido imaging and the SD-OCT, using the manufacturer's proprietary method, while the data for the posterior cornea is derived solely from the SD-OCT.

5.2.4 Casia SS-1000

The Casia SS-1000 (Tomey, Japan; software version 6Q.2) is also an SS-OCT, using a 1310 nm light source. Its axial and transverse resolution is 10 μm and 30 μm, respectively. It performs 16 radial scans with 512 A-scan lines centered on the corneal vertex within 10 mm diameter. The device performs 30000 A-scans per second and uses auto alignment to focus on the examined eye. Acquisition time is about 0.3 seconds.

5.2.5 IOLMaster 700

The IOLMaster 700 (Carl Zeiss Meditec, Jena, Germany) is an SS-OCT device combined with telecentric keratometry. The OCT uses a laser with a tunable wavelength ranging from 1035 nm to 1080 nm, centered on 1055 nm, while the keratometer uses a 950 nm light source. The SS-OCT generates B-scans with an acquisition speed of 2000 A-scans per second and a penetration depth of 44 mm, providing 6-line scans with 22 μm axial resolution. These B-scans are displayed as full-length OCT images showing anatomical

details on a longitudinal section through the entire eye. The telecentric keratometer measures 18 points arranged on three rings radially from the corneal center. The optical axes of the SS-OCT and the keratometer are identical. This ensures that the B-scan passes through the measuring points. The anterior and posterior corneal curvatures are measured by telecentric keratometry and SS-OCT, respectively. Measurements can be done in Auto/ Manual mode. In the current thesis, the auto mode was selected.

5.3 Clinical measurements

5.3.1 General Ophthalmologic Evaluation

All patients underwent complete ophthalmologic evaluation, including slit lamp bio-microscopy, Anterior segment optical coherence tomography (Avanti, Optovue, Inc., Fremont, CA, USA; Anterion, Heidelberg Engineering, Heidelberg, Germany), Placido-based corneal topography and wavefront aberrometer (Nidek OPD II, Nidek Co. Ltd, Aichi, Japan) or a luminescent diode based total ocular wavefront aberrometer (Osiris, CSO, Firenze, Italy), eye tonometry (Icare tonometer, Revenio Group Corporation, Helsinki, Finland), fundoscopy (EasyScan, Medicolle, Tyresö, SWEDEN; Canon CR-2 AF, Canon Medical Systems, USA), subjective spectacle refraction, UDVA, and CDVA.

5.3.2 Total corneal astigmatism measurements

We employed the MS-39, Anterion SS-OCT, Casia SS-1000, and IOLMaster 700 to measure total corneal astigmatism. The technical specifications of the devices are summarized in Table 1. The TCA values were given for a central 3.0 mm zone for all devices except for IOLMaster 700, which gave the values for a 2.5 mm zone.

For MS-39 and Anterion, the steep and flat keratometry readings and axis for a central 3.0 mm zone are given by the manufacturers with Microsoft Excel 2019 (Microsoft Corporation, Redmond, WA). For Casia SS-1000, the readings were exported directly from the software. For IOLMaster 700, the Keratometry values are calculated by analyzing the anterior corneal curvature at 18 reference points in hexagonal patterns at 1.5-, 2.5-, and 3.5-mm optical zones. The keratometry values analyzed in the current thesis were at the 2.5-mm zone. The keratometry values were read from the reports, and then recorded in Excel sheets.

Table 1 Specifications of the four devices for TCA

Table 1. Specifications of the four devices for TCA				
Device	Anterion	Casia SS-1000	IOLMaster 700	MS-39
Light source wavelength (nm)	1300	1310	OCT: 1055; keratometer: 950	OCT: 845; Placido: 635
A-scan speed (scan/s)	50000	30000	2000	102,400
Axial resolution (μm)	<10	10	22	3.6
Transverse resolution (μm)	<45	30	24	35
A-scan depth (mm)	14 ± 0.5	6	44	7.5
Maximum Scan width (mm)	16.5	10	6	6
Number of B-scans	65 × 1	16	18	12 × 5*
Number of A-scans per B-scan	256	512	128	1024**
Acquisition time (s)	0.33	0.3	1.2	2

*OCT = optical coherence tomography; TCA = total corneal astigmatism; *: Customized in this thesis as recommended by the manufacture; **: 1600 A-scan on 16 mm and 800 A-scan on 8 mm*

5.3.3 Epithelial Thickness Measurements

We employed the Avanti SD-OCT (Paper 2 and 3), Anterion SS-OCT (Paper 2 and 3) and MS-39 (Paper 3) to measure epithelial thickness.

The measurements with the three devices were performed in a random order according to a randomized list generated by Microsoft Excel 2016. Three consecutive measurements were taken with each device. For each device, a single measurement was acquired within 20 seconds. All measurements with all three devices were acquired within 10 minutes.

The patients were asked to fixate on the device's fixation target to achieve a coaxial position with the infrared camera and the corneal vertex. During each measurement, the examiner centered the scan on the corneal vertex by adjusting the joystick until a bright vertical flare line was seen at the center of the real-time OCT image. Patients were instructed to blink immediately before each measurement to ensure that the tear film would be spread out evenly and to keep their eyes wide open during the measurement. After each measurement, patients were then asked to sit back and look away from the fixation light. No eye drops were applied during testing.

With Avanti, corneal thickness mapping and ETM are produced using the "Pachymetry Wide" scan pattern mode and attaching the "long adaptor lens" to the instrument. The ETM measurement consists of 8 radial scans at 22.5° intervals, repeated five times for each meridian,

with 1,024 A-scan lines over a 9 mm diameter. The acquisition time is 0.58 seconds. ETM, as well as the corneal pachymetry maps, are generated by an automatic algorithm and divided into a total of 25 sections over a 9-mm diameter: a central 2 mm diameter zone and eight sections equally distributed within three annular rings (2-5 mm, 5-7 mm, and 7-9 mm). The mean epithelial thickness of each section is presented in Figure 3.

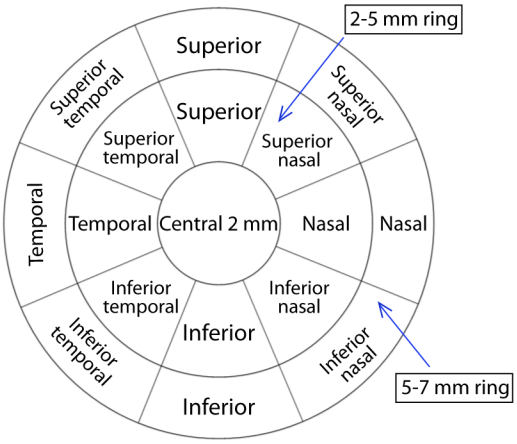

Figure 3 17 sections and two rings used in the analysis of the measurements.

With Anterion, the ETMs are acquired quickest using the "Cornea APP" mode on the device, but the same data can also be obtained with the "Cataract APP" mode; both perform 65 radial scans with 256 A-scan lines centered on the corneal vertex within a 7 mm diameter. The acquisition time with the Cornea APP is <1 second. After the acquisition, the instrument presents ETM, displaying the mean thicknesses at 41 points evenly distributed across the map.

With MS-39, the "Corneal topography" mode "12 × 5 @10 mm" was used for ETM as recommended by the manufacturer, as it provides a higher resolution than the "25 × 1 @16 mm" mode, which has been used in previous studies.[79-81] In the 12 x 5 mode, the ETM measurement consists of 12 radial B-scans repeated 5 times for each of the 12 meridians, with 800 A-scan lines per B-scan over an 8 mm diameter. The acquisition time is about 1 second. It calculates the epithelial thickness within the 8 mm diameter and provides ETM, divided into a total of 25 sections: a central 2 mm diameter zone and eight sections equally distributed (superior (S), superior temporal (ST), temporal (T), inferior temporal (IT), inferior (I), inferior nasal (IN), nasal (N) and superior nasal (SN)) within three annular rings (2-4-, 4-6- and 6-8

mm). The mean, maximum, and minimum values as well as the standard deviation (SD) of each section, are presented on the map.

For all three devices, the user may measure the epithelium thickness at any point on the map by mouse pointing. To compare the three devices, the mean values of the same 17 sections (including the central 2 mm zone) within 7 mm diameter, as well as for the whole 2-5 mm and 5-7 mm rings, were calculated (Figure 3). Only high-quality images centered at the corneal vertex, with complete coverage and free of motion artifacts, were accepted for analysis. The technical specifications of the devices are summarized in Table 2. Three measurements were obtained on a single visit, and the average value was used for further analysis.

Table 2 Technical specifications of the three devices for ETM

Table 2. Technical specifications of the three devices for ETM

Device	MS-39	Anterion	Avanti
Light source wavelength (nm)	OCT: 845 Placido: 635	1300	840
A-scan speed	102,400	50000	70000
Axial resolution (μm)	3.6	<10	5
Transverse resolution (μm)	35	<45	15
A-scan depth (mm)	7.5	14	3
Maximum Scan width (mm)	16	16.5	12
B scan	10 × 5*	65 × 1	8 × 5
Number of A-scans per B-scan	1024**	256	1024
Acquisition time (s)	1	0.33	0.58

*OCT = optical coherence tomography; ETM = epithelial thickness mapping; *: Customized in this thesis as recommended by the manufacturer; **: 1600 A-scan on16 mm and 800 A-scan on 8 mm*

5.3.4 Measurement Quality and Image Selection Criteria

To ensure the accuracy and reliability of our study's findings, stringent criteria were implemented for selecting high-quality images and measurements for TCA, AL, and ETM across all devices used. All measurements were conducted by the same experienced examiner (YF) using standardized protocols to minimize variability. The measurements were performed between 10 AM and 2 PM to reduce diurnal variations, and only data meeting strict quality criteria were included in the final analysis.

For TCA measurements, images needed to be well-centered on the corneal vertex with clear visualization of the corneal curvature. The tear film had to be uniform and free from

significant distortions or motion artifacts, and the devices' specific quality indices were used to verify image acceptability. AL measurements were taken concurrently with TCA measurements using the Anterion and IOLMaster 700 devices, ensuring consistency in patient positioning and fixation. Multiple images were captured, and only the eyes for which each device captured three high-quality images were included in the analysis.

For ETM measurements, images needed to clearly delineate the epithelial layer with minimal noise and artifacts. Scans were centered on the corneal vertex, confirmed by a bright vertical flare line on the real-time OCT image. Only eyes with three high-quality ETM measurements from each device were included in the analysis.

The percentage of high-quality measurements was documented in Table 3 to reflect the reliability of the data and ensure transparency.

Table 3 Proportion of acceptable quality measurements per device used in the three papers

Table 3. Proportion of acceptable quality measurements per device used in the three papers

Paper	Population	Device			
Paper 1		Anterion	MS-39	Casia SS-1000	IOLMaster 700
	KC	90.91%	87.88%	92.12%	82.42%
Paper 2		Anterion	Avanti		
	Virgin	98.91%	97.83%		
	PLRS	96.00%	92.00%		
	KC	87.41%	85.31%		
Paper 3		Anterion	Avanti	MS-39	
	KC	88.89%	83.33%	84.72%	

KC = keratoconus; PLRS = post-laser refractive surgery

5.4 Data Analysis

5.4.1 Astigmatism Components Analysis

The TCA values were decomposed into two components by using the following equations[82]:

$$J_0 = \frac{C}{2} \times cos\ 2\alpha$$

$$J_{45} = \frac{C}{2} \times sin\ 2\alpha$$

Where c is the negative cylindrical power and α is the cylindrical axis. J_0 refers to a Jackson cross-cylinder power set orthogonally at 90° and 180° meridians. Positive values of J_0 indicate with-the-rule (WTR) astigmatism, and negative values of J_0 indicate against-the-rule (ATR) astigmatism. J_{45} refers to a Jackson cross-cylinder power set orthogonally at 45° and 135°, representing oblique astigmatism.

5.4.2 Statistical analysis

Data was entered into Microsoft Excel 2019 and then imported into the statistical package SPSS (IBM SPSS Statistics for Windows, Version 20.0. IBM Corp) for analysis. Descriptive statistics were done for continuous variables. Visual inspections of P-P plots and Kolmogorov–Smirnov tests were used to confirm that the data were normally distributed. The level of statistical significance was set at $p < 0.05$.

We used vertically mirrored symmetry superimposition: thickness values for left eyes were reflected in the vertical axis and superimposed onto the right eye values to combine nasal/temporal characteristics.[83]

To assess the repeatability, we calculated the pooled within-subject standard deviation (S_w) (lower values of S_w indicate better repeatability).[84] The repeatability limit (r), defined as $1.96\sqrt{2} \times S_w$ (= $2.77 \times S_w$), gives the value below which the absolute difference between two measurements of S_w would lie with 0.95 probability.[77, 84]

To assess the agreement, we calculated the following parameters: 1. Difference in thickness readings, 2. The 95% LoA, defined as the mean difference in thickness ± 1.96 × standard deviation, and 3. Paired two-tailed t-tests. Bland-Altman plots were generated to visualize the agreement between any two devices.

To assess ETM measurement interchangeability between devices, the tolerance index for agreement (TA) is calculated as described by Bergin and colleagues.[78] TA is defined as:

$$\text{TA}=ln\frac{95\%\ LoA}{r}$$

where the 95% LoA is the difference between the upper and lower 95% LoA and r is the limit of repeatability. From the formula, we observe that a value of 0 represents a perfect alignment

between the limits of agreement and repeatability, and therefore the corresponding devices can be considered fully interchangeable. For two devices, A and B, we use the 95% LoA in the numerator and the limit of repeatability of device A (r_A) in the denominator. If the resulting TA value is below the corresponding cutoff value (shown in Table 4) in the paper by Bergin and colleagues,[78] device A can be replaced by device B. Vice versa, if we want to evaluate whether device B can be replaced by device A, then we use the same difference in the numerator, but in the denominator, we use the limit of repeatability of device B (r_B). Then we check again if the TA value is below the same cutoff value.

Table 4 Tolerance Index Cutoff Based on Sample Size

Table 4. Tolerance Index Cutoff Based on Sample Size

		Sample 2									
	n	10	20	30	40	50	75	100	150	250	1000
Sample 1	CI	31%	22%	18%	15%	14%	11%	10%	8%	6%	3%
10	31%	0.48	0.42	0.40	0.38	0.37	0.35	0.34	0.33	0.32	0.29
20	22%	0.42	0.36	0.34	0.32	0.31	0.29	0.28	0.26	0.25	0.22
30	18%	0.40	0.34	0.31	0.29	0.28	0.26	0.24	0.23	0.22	0.19
40	15%	0.38	0.32	0.29	0.28	0.26	0.24	0.23	0.22	0.2	0.17
50	14%	0.37	0.31	0.28	0.26	0.24	0.23	0.22	0.2	0.18	0.16
75	11%	0.35	0.29	0.26	0.24	0.22	0.22	0.19	0.18	0.16	0.13
100	10%	0.34	0.28	0.24	0.23	0.21	0.19	0.18	0.16	0.15	0.12
150	8%	0.33	0.26	0.23	0.21	0.20	0.18	0.16	0.15	0.13	0.11
250	6%	0.32	0.25	0.22	0.20	0.18	0.16	0.15	0.13	0.12	0.09
1000	3%	0.29	0.22	0.19	0.17	0.16	0.13	0.12	0.11	0.09	0.06

* This table was originally made by Bergin and colleagues[78], and reproduced here with the permission of the authors.

5.4.3 Sample size estimation

To achieve a 15% confidence in the estimate (a number used in similar repeatability studies of ETM in eyes with KC[79, 80, 85]), the required sample size, n is given by the formula[86]:

$$1.96\frac{Sw}{\sqrt{2n(n\prime-1)}}=0.15S_w$$

where n' is the number of repeated measurements. Solving this equation for n' = 3 gives n= 43.

Paper 1 enrolled 136 KC eyes (n=136), paper 2 enrolled 90 virgin, 46 PLRS, and 122 KC eyes (n=258), and paper 3 enrolled 60 KC eyes (n=60), which all give a higher than 15% confidence.

6. Results

6.1 Paper 1

In paper 1, we evaluated repeatability and agreement of measurements of TCA in KC eyes, obtained by two SS-OCT-based devices (Anterion and Casia SS-1000), one SS-OCT combined with reflectometry (IOLMaster 700) and one SD-OCT combined with Placido imaging (MS-39). Three qualified measurements were acquired with each of the four devices in 136 eyes (OD/OS: 81/55) of 136 patients (41.66 years ± 15.15 [SD], range 16 to 75 years; male/female: 87/49). TCA values were transformed into TCA components (J_0/J_{45}). The acquisitions from the Anterion and the IOLMaster 700 also provided AL measurements.

According to Amsler-Krumeich KC classification, the 136 eyes included in this paper were Grade I: 103 eyes, Grade II: 30 eyes, Grade III: 3 eyes, and Grade IV: 0 eyes. For all four devices, the repeatability of TCA measurements showed $S_w \leq 0.23$ D for TCA magnitude, ≤ 0.14 D for J_0, and ≤ 0.12 D for J_{45}. Anterion had the best S_w for TCA magnitude, J_0 and J_{45}, followed by Casia SS-1000, IOLMaster 700 and MS-39. Anterion had the best S_w with 4.26° for the TCA axis, followed by IOLMaster 700 with 7.21°, MS-39 with 8.73° and Casia SS-1000 with 9.23°. All of them had an S_w statistically significant ($p< 0.001$) negative Pearson correlation (with r from -0.491 to -0.359) with the TCA magnitude, which means, that as the magnitude increases, the S_w tends to decrease (better repeatability).

Casia SS-1000 had the lowest mean TCA magnitude with 1.52 ± 1.31 D, followed by Anterion with 1.89 ± 1.52 D, MS-39 with 1.99 ± 1.73 D, while IOLMaster 700 had the highest with 2.15 ± 1.81 D. The means of J_{45} values were similar for all four devices (from 0.124 to 0.189 D), while the mean of J_0 for Anterion and Casia SS-1000 was higher than for IOLMaster 700 and MS-39. There were statistically significant differences in TCA magnitude in all pairs except for Anterion vs. MS-39 and IOLMaster 700 vs. MS-39, but only the difference between Casia SS-1000 and IOLMaster 700 was clinically significant by exceeding 0.50 D (0.631 D, $p =0.000$). There were no statistically significant differences in TCA components in any pairs except in J_0 for IOLMaster 700 vs. Anterion with a mean difference of -0.191 D ($p =0.000$), and in Anterion vs. MS-39 with a mean difference of 0.196 D ($p =0.004$).

Both Anterion and IOLMaster 700 had high repeatability in AL measurements (S_w: 0.007 mm for Anterion and 0.009 mm for IOLMaster 700). The difference in AL between the two was 0.015 ± 0.033 mm ($p < 0.001$).

6.2 Paper 2

In paper 2, we assessed the repeatability of corneal epithelial thickness mapping in virgin, PLRS, and keratoconic eyes using a novel SS-OCT and to determine the agreement of the measurements with a validated SD-OCT. We Analyzed 90 virgin, 46 PLRS, and 122 keratoconic eyes. Three consecutive measurements of each eye were acquired with the Anterion SS-OCT and Avanti SD-OCT devices, and averages of the epithelial thickness mapping were calculated in the central 2-mm zone and in the 2- to 5-mm and 5- to 7-mm diameter rings.

The repeatability ranges of the Anterion and Avanti epithelial thickness mapping measurements were S_w: 0.60 to 1.36 µm and S_w: 0.75 to 1.96 µm, respectively. The 95% limits of agreement of the Anterion and Avanti were 0.826 to 8.297. All values of the thickness measurements with the Anterion were lower than those of the Avanti, with the mean differences being 4.06 ± 1.81, 3.26 ± 2.52, and 3.68 ± 2.51 µm in virgin, PLRS, and keratoconic eyes, respectively ($P < 0.001$ for all).

6.3 Paper 3

In paper 3, we assessed the repeatability and agreement of corneal ETM in KC eyes using three OCT instruments featuring different technologies: 1. SD-OCT combined with Placido disk corneal topography (MS-39), 2. SS-OCT (Anterion), and 3. SD-OCT (Avanti). Three consecutive measurements were acquired with the three devices in 60 KC eyes. The mean epithelial thickness was calculated in the central 2 mm zone and 2-5- and 5-7 mm diameter rings.

The repeatability (S_w) of the epithelial thickness for the central 2 mm zone was 0.91, 0.71, and 0.93 µm for MS-39, Anterion, and Avanti, respectively. All thicknesses with MS-39 were greater than Anterion's and Avanti's, with differences of 4.11 ± 1.34 µm ($p<0.001$) and 0.52 ± 1.30 µm ($p=0.003$), respectively. The 95% LoA for the MS-39 and Anterion were 1.484 to 6.736 µm, for Avanti and MS-39 –3.068 to 2.028 µm and for Avanti and Anterion 1.258 to 5.922 µm.

6.4 Other results (not included in the papers)

Based on the data in Paper 1, Double Angle plots were made for visualizing TCA measurements in 60 KC eyes. Figure 4 (A-D) shows the Double Angle plots of TCA for the four devices. Figure 5 (A-F) shows Double Angle plots for the difference in astigmatism for each pair of devices.

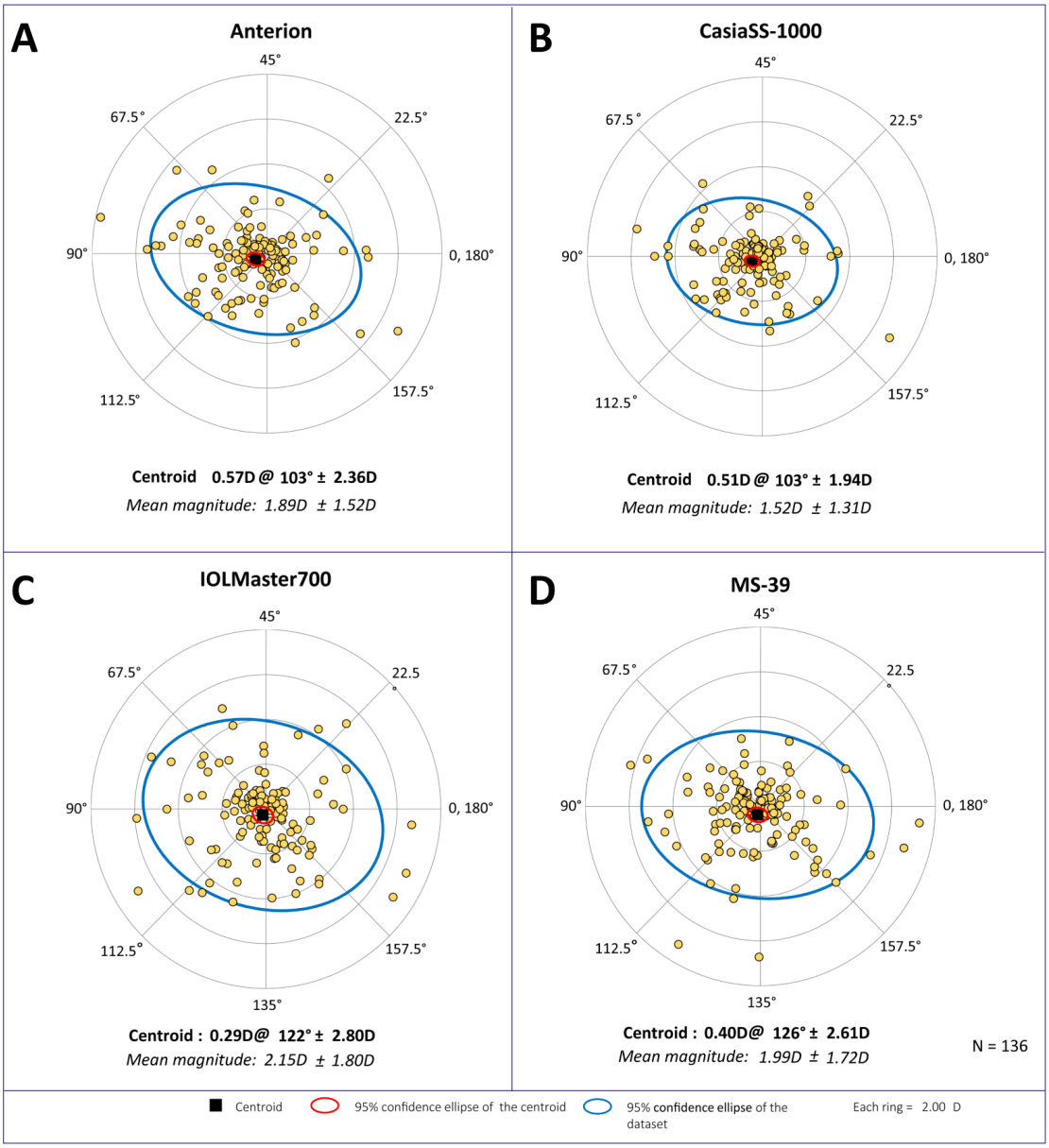

Figure 4 Double-angle plots of the TCA measurements in KC eyes (n=136) using four measuring devices: (A) Anterion, (B) Casia SS-1000, (C) IOLMaster 700, and (D) MS-39
(TCA = total corneal astigmatism; KC= keratoconus; The black squares represent the centroid, which is the vectoral center of the dataset, the red circles represent the 95% confidence ellipse of the centroid, and the blue circles represent the 95% confidence ellipse of the dataset.)

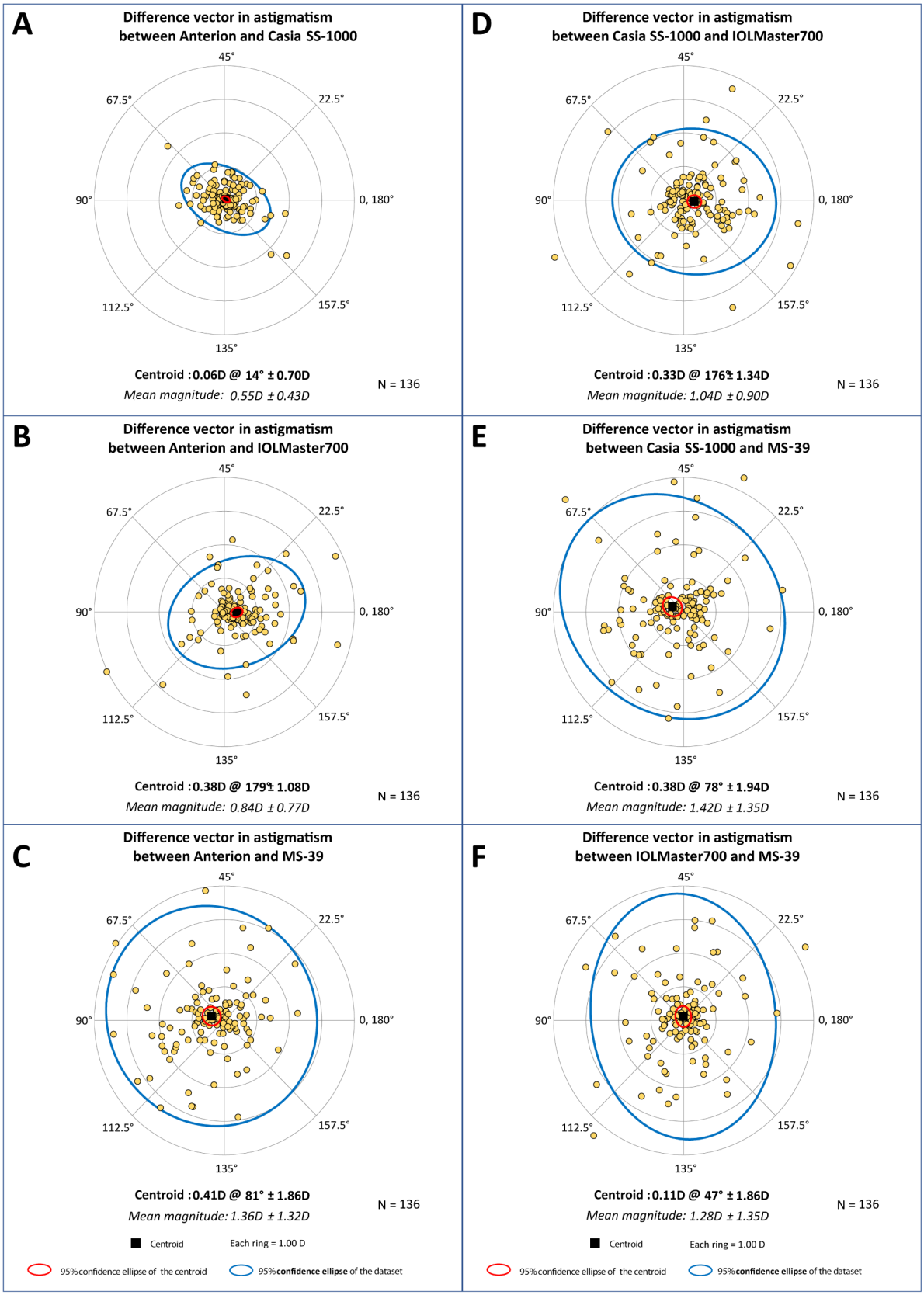

Figure 5 Double-angle plots of the difference in TCA measured by (A) Anterion and Casia SS-1000, (B) Anterion and IOLMaster 700, (C) Anterion and MS-39, (D) Casia SS-1000 and IOLMaster 700, (E) Casia SS-1000 and MS-39, (F) IOLMaster 700 and MS-39

(TCA = total corneal astigmatism; The black squares represent the centroid, which is the vectoral center of the dataset, the red circles represent the 95% confidence ellipse of the centroid, and the blue circles represent the 95% confidence ellipse of the dataset.)

The centroid in each plot represents the vectoral center of the dataset. The double-angle plots show the best agreement in results between Anterion and Casia SS-1000, with a very similar 95% confidence ellipse of the dataset (Figure 4A and B) and the smallest 95% confidence ellipse in the difference plot (Figure 5 A). Comparison between MS-39 and any of the other three devices showed weaker agreement with a wider 95% confidence ellipse of the difference (Figure 5 C, E and F).

Based on the data in Paper 3, we assessed the interchangeability between the devices-tolerance index for agreement (TA). The TA for all pairs of devices was larger than our cutoff of 0.24 for the sample size used in this study (Table 5), rendering the three devices not interchangeable for ETMs in KC eyes.

Table 5 Tolerance index for agreement (TA) of ETM measurements for each device

Table 5. Tolerance index for agreement (TA) of ETM measurements for each device

	TA= ln (95% LoA / r)					
	MS-39-Anterion		Avanti - MS-39		Avanti - Anterion	
	(1) MS-39	(2) Anterion	(3) MS-39	(4) Avanti	(5) Anterion	(6) Avanti
Zone 0-2 mm						
Central	1.43	1.61	1.12	1.03	1.36	1.09
Ring 2-5 mm						
Nasal	1.20	1.16	1.27	0.92	1.13	0.81
Superior nasal	1.02	0.99	1.14	0.80	0.90	0.59
Superior	1.08	1.06	0.97	0.80	1.02	0.87
Superior temporal	1.07	1.19	0.80	0.86	1.08	1.02
Temporal	0.88	1.20	0.87	0.60	1.11	0.52
Inferior temporal	0.94	1.26	0.81	0.68	1.08	0.64
Inferior	0.93	1.18	0.88	0.75	1.22	0.84
Inferior nasal	1.09	1.21	0.88	0.56	1.16	0.72
Ring 5-7 mm						
Nasal	1.35	1.39	0.91	0.70	1.34	1.09
Superior nasal	1.09	1.03	0.85	0.84	0.89	0.94
Superior	0.79	0.86	0.79	0.94	0.91	0.99
Superior temporal	1.08	1.00	0.89	0.81	1.02	1.02
Temporal	0.85	0.73	0.84	0.55	0.76	0.58
Inferior temporal	1.28	1.39	0.88	0.56	1.31	0.88
Inferior	1.20	0.73	1.06	1.06	0.76	1.23
Inferior nasal	1.72	1.32	1.04	1.13	1.27	1.76

ETM = epithelial thickness mapping; LoA= limits of agreement; Repeatability limit (r)= 2.77 × S_w; S_w= Pooled within-subject standard deviation; (1): TA for replacing MS-39 by Anterion; (2): TA for replacing Anterion by MS-39; (3): TA for replacing MS-39 by Avanti; (4): TA for replacing Avanti by MS-39; (5): TA for replacing Anterion by Avanti; (6): TA for replacing Avanti by Anterion.

7. Discussion

7.1 Total corneal astigmatism

The irregular corneal optics in keratoconus (KC) presents a challenge in achieving precise measurements of the magnitude and axis of Total Corneal Astigmatism (TCA), while the dominance of the posterior corneal surface optics in KC eyes amplifies the significance of TCA compared to normal eyes. In paper 1, we assessed the repeatability of TCA measurements within a cohort of KC eyes using four different devices, as detailed in Table 1. To evaluate the variability between three consecutive measurements, we performed the calculation of the pooled within-subject standard deviation (S_w).

In addition to the special need of the keratoconus population for high quality of measurements of the TCA, ETM and AL, this population chosen for this study due to the inherent difficulties in measurements of its corneal irregularities. Unlike normal corneas, the KC cornea has more pronounced variations in curvature, particularly on the posterior surface, as well as a great variation in its stromal and epithelial thickness. Assessing the repeatability and agreement of TCA measurements in KC eyes is crucial for ensuring reliable data important for clinical decisions. To better guide interventions such as CXL, intracorneal ring segments, and toric intraocular lenses requires highly precise corneal and axial length assessments. Finally, earlier studies[80] reported worse repeatability in KC eyes compared with virgin eyes, highlighting the need for dedicated research in this area.

Our paper found that while all four devices demonstrated acceptable repeatability and agreement for TCA measurements, there were significant differences among them. The Anterion and IOLMaster 700 exhibited superior repeatability for TCA magnitude and for the components J0 and J45 compared with the Casia SS-1000 and MS-39. The Anterion and IOLMaster 700 also provided highly reliable AL measurements.

The study published in paper 1 revealed that the pooled within-subject standard deviation (S_w) for the cylinder magnitude was 0.12 D for Anterion, 0.18 D for Casia SS-1000, 0.19 D for IOLMaster 700, and 0.23 D for MS-39. It is important to note that higher values of S_w indicate poorer outcomes, signifying less consistent measurements. The S_w values for J_0

and J_{45} were found to be ≤ 0.14 D and ≤ 0.12 D, respectively. Among the four devices, Anterion exhibited the most favorable repeatability in measuring the cylinder magnitude and vector components. In normal eyes, previous studies[87-91] have shown that OCT-based devices generally provide good repeatability and agreement for TCA measurements. In these studies, Anterion had an S_w for TCA magnitude varying from 0.07 D to 0.13 D, and IOLMaster 700 had an S_w of 0.15 D. The relatively inferior repeatability observed in our paper was anticipated due to the inclusion of KC corneas with irregular corneal optics. Gjerdrum et al.[92] evaluated the repeatability of Anterion and Casia SS-1000 in patients with hyperosmolar (n=31) and normal (n=63) tear film, demonstrating S_w values for TCA varying from 0.15 D to 0.16 D for Anterion and from 0.18 D to 0.28 D for Casia SS-1000. However, KC eyes are more challenging to measure due to their irregular corneal topography. Schiano-Lomoriello et al.[80] assessed the repeatability of MS-39 in KC eyes (n=44), yielding an S_w of 0.55 D for TCA magnitude, which is more than twice the S_w observed in our results.

Piñero and colleagues[93] reported pooled within-subject standard deviations (S_w) of 0.09 D for J_0 and 0.07 D for J_{45} in a study involving healthy eyes (n=35) utilizing the Cassini system (i-Optics, The Hague, Netherlands, distributed by Ophthec). The Cassini system employs 679 colored light-emitting diodes (LEDs) for the specular reflection to generate topographic maps of the anterior corneal surface, but only seven additional infrared LEDs for measuring the curvature of the posterior corneal surface. Their findings using the Cassini system demonstrated superior repeatability compared to our results with the MS-39 (S_w: 0.14 D for J_0 and 0.12 D for J_{45}), and were similar to our findings with the Casia SS-1000 (S_w: 0.10 D for J_0 and 0.10 D for J_{45}) and IOLMaster 700 (S_w: 0.10 D for J_0 and 0.09 D for J_{45}), but inferior to our results with the Anterion (S_w: 0.07 D for J_0 and 0.06 D for J_{45}). The limitation of only 7 points representing the posterior corneal surface must be taken into account when interpreting the Cassini results.

Table 6 Repeatability of TCA measurements reported by previous investigators

Table 6. Repeatability of TCA measurements reported by previous investigators

Authors/ Year	Eyes (n)	Parameter	Repeatability, S_w Normal	KC	Areas	Instrument used
Tañá-Rivero P and colleagues (2021)	Normal: 74	Cylinder magnitude	0.0712		3-mm	Anterion SS- OCT
			0.0558		6-mm	
Schiano-Lomoriello D and colleagues (2021)	Normal: 96	Cylinder magnitude	0.13		3-mm	Anterion SS- OCT
	Normal: 25	Cylinder magnitude (>1 D)	0.1		3-mm	
Cheng SM and colleauges (2022)	Normal: 101	J0	0.084		3-mm	
		J45	0.071		3-mm	
Shajari and colleagues (2022)	Normal: 93	Cylinder magnitude	0.14		3-mm	IOLMaster 700
Gjerdrum and colleagues (2020)	Normal: 32	Cylinder magnitude	0.155		3-mm	Anterion SS- OCT
	Hyperosmolar: 16		0.148		3-mm	
	Normal: 62		0.282		3-mm	Casia SS-1000
	Hyperosmolar: 31		0.184		3-mm	
Schiano-Lomoriello and colleagues (2020)	KC: 44	Cylinder magnitude		0.55	3-mm	MS-39 SD- OCT
Piñero and colleagues (2019)	Normal: 35	Cylinder magnitude	0.16		3-mm	Cassini
		J0	0.09		3-mm	
		J45	0.07		3-mm	
The current paper 1	KC: 136	Cylinder magnitude		0.12	3-mm	Anterion SS- OCT
		J0		0.07	3-mm	
		J45		0.06	3-mm	
		Cylinder magnitude		0.18	3-mm	Casia SS- 1000
		J0		0.1	3-mm	
		J45		0.1	3-mm	
		Cylinder magnitude		0.19	3-mm	IOLMaster 700
		J0		0.1	3-mm	
		J45		0.09	3-mm	
		Cylinder magnitude		0.23	3-mm	MS-39 SD- OCT
		J0		0.14	3-mm	
		J45		0.12	3-mm	

TCA= total corneal astigmatism; S_w= Pooled within-subject standard deviation; KC= keratoconus; SD= Spectral-domain; SS= Swept source; OCT = optical coherence tomographer; Uint: Diopter

So far, there are no publications about the repeatability of TCA axis measurements in KC eyes with the current four devices. Paper 1 showed the best repeatability in Anterion with S_w 4.26° and the worst in Casia SS-1000 with S_w of 9.23°. de Luis Eguileor and colleagues[94, 95] found an S_w range from 7.70° to11.78° for the astigmatism axis in a Scheimpflug-based tomographer, Pentacam HR (Oculus; Optikgeräte GmbH, Wetzlar, Germany), in KC eyes. Their results were close to ours with Casia SS-1000 (S_w: 9.23°), IOLMaster 700 (S_w: 7.21°) and MS-39 (S_w: 8.73°), while far worse than ours with Anterion. Kanellopoulos and colleague[96] reported in normal eyes, the greater the cylinder magnitude, the better the repeatability of the axis with Cassini. We found the same trend in KC eyes. Pearson correlation shows the TCA axis measurement repeatability improved with increasing TCA magnitude in all four devices. In our paper, Anterion and Casia SS-1000 showed a moderate correlation, while IOLMaster 700 and MS-39 showed a weak correlation. The low cylinder measurements are generally more likely than the high cylinder to be influenced by general

noise in the readings, such as tear film surface irregularities[97], which can obscure the precise detection of the axis.

In terms of the agreement in Total Corneal Astigmatism (TCA) measurements between any pair of devices, most exhibited statistically significant variances in cylinder magnitude. Specifically, the mean difference in cylinder magnitude between the Casia SS-1000 and IOLMaster 700 was 0.631 D ($p < 0.001$). Conversely, the mean difference for the remaining pairs did not surpass 0.50 D. It is noteworthy that a variance of 0.50 D in corneal power estimation can lead to an error in intraocular lens (IOL) power calculations of less than 0.50 D at the corneal plane. Moreover, 0.50 D represents the minimum IOL power increment offered by most manufacturers[98]. Consequently, only the variance in cylinder magnitude between the Casia SS-1000 and IOLMaster 700 holds clinical significance. The 95% LoA ranges were broad for all device pairs, indicating poor statistical agreement, although the variance in vector components was not statistically significant, except for J_0 for IOLMaster 700 compared to Anterion and Anterion compared to MS-39.

TCA analysis revealed that the most favorable agreement in the mean magnitude of astigmatism was observed between Anterion and Casia SS-1000, exhibiting a mean difference of 0.55 ± 0.43 D and a notably similar 95% confidence ellipse of the dataset (Figure 5 A and B). Conversely, the comparison between Casia SS-1000 and MS-39 (difference of 1.42 ± 1.35 D), and between Anterion and MS-39 (difference of 1.36 ± 1.32 D) demonstrated weaker agreement (Figure 6 C and E). In comparing the IOLMaster 700 and MS-39, it was observed that while the 95% confidence ellipse of the dataset was wide, the 95% confidence ellipse of the centroid was relatively small, measuring 0.11 ± 1.86D @ 47° (Figure 6 F). This could potentially be attributed to the very small differences in the centroid meridians (@122 vs. @126) from both devices (Figure 5 C and D). These findings indicate that Anterion and Casia SS-1000, both utilizing SS-OCT technology, are the most comparable devices, despite the distinct methods employed for calculating total corneal power. Specifically, Casia SS-1000 utilizes a vectorial sum of the anterior and posterior surface with corneal thickness correction, while Anterion employs ray-tracing ray-tracing.[99, 100]

The need for precision in corneal measurements for effective KC management underscores the clinical relevance of our findings. The superior repeatability demonstrated by the Anterion, and the good agreement in TCA between Anterion and Casia SS-1000, as well

as the good agreement in AL between Anterion and IOLMaster 700 suggest that these devices are particularly well-suited for the KC population and will provide clinicians with more reliable data for clinical decision-making. Additionally, the differences observed between devices highlight the importance of understanding each device's capabilities and limitations. Clinicians should consider these factors when choosing diagnostic tools.

In practical terms, the use of devices with high repeatability and agreement for TCA and AL measurements can lead to better management with better treatment outcomes for KC patients. Accurate TCA measurements are critical for determining the correct power and alignment of toric IOLs, which can significantly improve postoperative visual acuity in lens exchange surgery in KC eyes. Similarly, reliable AL measurements are also essential for selecting the appropriate lens power. Moreover, understanding the clinical implications of measurement variability can help in developing standardized protocols for KC management.

7.2 Epithelial thickness

In the current project, we evaluated the repeatability of Epithelial Thickness Mapping (ETM) measurements using the Anterion SS-OCT and its agreement with the Avanti SD-OCT in healthy virgin, PLRS, and keratoconic eyes (published in paper 2). Additionally, we compared the repeatability and agreement between the MS-39 SD-OCT, Anterion SS-OCT, and Avanti SD-OCT (published in paper 3). The evaluation of ETM is crucial for early detection and management of KC, as well as for planning and monitoring refractive surgery.

In paper 2, we observed that the repeatability of the Heidelberg Anterion SS-OCT in the three cohorts of eyes (virgin, PLRS, and KC) was very good, surpassing that of the commonly utilized SD-OCT, the Avanti. Furthermore, the Anterion's measurements of the mean epithelial thickness in all three cohorts of eyes were lower than those obtained using the Avanti. In paper 3, we conducted the first investigation of the ETM obtained by the MS-39 hybrid device, which is based on SD-OCT corneal topography/tomography and Placido disk anterior surface corneal topography. The "12 x 5 @ 10 mm" averaged mode was employed. We compared the instrument’s repeatability with the SS-OCT-based Anterion and the SD-OCT-based Avanti in a cohort of 60 KC eyes. In addition to assessing the repeatability and agreement in our published article, we also analyzed the interchangeability between the devices in measuring ETM. Although all three devices exhibited high repeatability of the

ETM measurements, the concordance between the devices was low and did not meet the interchangeability criteria. The repeatability (S_w) in the central 2 mm zone and 2-5 mm ring was optimal for the Anterion (0.71 and 0.91 μm), followed by the MS-39 (0.91 and 1.06 μm) and the Avanti (0.93 and 1.28 μm).

Repeatable measurements of corneal epithelial thickness play a crucial role in the diagnosis and management of KC,[26, 39, 46, 101] and are equally vital in corneal refractive surgery. The initial ETM conducted by Reinstein and colleagues using the Artemis VHF digital ultrasound in 1994 demonstrated a within-subject standard deviation (S_w) of 0.58 μm at the corneal vertex and 0.43-1.36 μm in 90% of locations within the central 6-mm diameter after five consecutive measurements of ten eyes of 10 patients one year after LASIK. Notably, the S_w of Artemis in PLRS eyes within the 7 mm diameter was comparable to our findings with Anterion (0.60-1.36 μm) but superior to our measurements with Avanti (0.75-1.96 μm). However, it is essential to consider repeatability in the context of the device's measurement resolution; VHF digital ultrasound can measure epithelial thickness with a resolution of less than 1 μm, whereas OCT devices have a resolution closer to ~5 μm for Avanti and ~8 μm for Anterion. Therefore, while repeatability may be similar, it is reasonable to anticipate that the accuracy of OCT devices might be lower than that of VHF digital ultrasound.

Introduced 17 years after the Artemis, the SD-OCT Optovue RT-100 has demonstrated good repeatability and reproducibility of ETM in both normal and abnormal eyes, including those with dry eye syndrome, contact lens wear, post-laser refractive surgery, and KC.[41, 102, 103] Table 7 presents the repeatability of ETM measurements as reported by previous researchers. In virgin eyes, the ETM measured by SD-OCT Optovue RT-100 showed similar results to those obtained with the Anterion (S_w: 0.64, 1.01 μm), but lower than those obtained with the Avanti (S_w: 0.98, 1.14 μm) for the central 2 mm zone and the outer 5-7 mm ring. Sedaghat and colleagues calculated the repeatability of ETM with the Avanti before and after PRK and found a S_w of 1.73 μm preoperatively and 4.50 μm six months postoperatively.[104] Within the 7 mm zone, our data in paper 2 showed a lower S_w than that reported by Sedaghat in our PLRS eyes obtained with both the Anterion (S_w: 0.60, 1.36 μm) and the Avanti (S_w: 0.75, 1.96 μm). Even when including all eyes in paper 2, our data indicated that the S_w of the Avanti (1.34 μm) was lower than that reported by Sedaghat and colleagues (1.73 μm). Lu and colleagues[105] measured ETM with Optovue Avanti SD-OCT,

showing S_w: (1.31, 2.43) μm in mild KC eyes and S_w: (1.90, 3.89) μm in advanced KC eyes. In contrast, the current paper 3 found better repeatability of ETM measured with Avanti, S_w: (0.75, 1.68) μm, and Anterion, S_w: (0.71, 1.59) μm in 60 KC eyes. These results were consistent with the repeatability reported in paper 2 for Avanti, S_w: (0.75, 1.96) μm, and Anterion, S_w: (0.60, 1.36) μm in KC eyes.[85] Vega-Estrada and colleagues, using the MS 39 SD-OCT[79], found an S_w of 1.24 μm in virgin eyes and an S_w of 2.03 μm in KC eyes, while paper 2 found an S_w of 0.64 μm in virgin eyes and an S_w of 0.98 μm in KC eyes with the Anterion and an S_w of 1.18 μm in virgin eyes and an S_w of 1.37 μm in KC eyes with the Avanti. Schiano-Lomoriello and colleagues[80] reported an S_w of 1.57 μm in KC eyes with the MS-39. Paper 3 showed better repeatability with MS-39 with an S_w of 0.91 μm in the central 2 mm zone, and S_w ranges (0.53, 1.62) μm in the 2-5 mm and (0.73, 1.79) μm in the 5-7 mm ring, which were better than the results from the two mentioned studies.

Table 7 Repeatability of ETM measurements reported by previous investigators

Table 7. Repeatability of ETM measurements reported by previous investigators

		Repeatability, S_w				
Authors/ Year	Eyes (n)	Normal	PLRS	KC	Areas	Instrument used
Reinstein and colleagues (2010)	KC: 10		0.58		vertex	Very-high frequency ultrasound
			0.43-1.36		central 6 mm	
Ma and colleagues (2013)	Normal: 35 PLRS: 45	0.7	0.7		central 2 mm	Optovue RT-100 SD-OCT
		0.6-0.9	0.8-1.7		2-5 mm	
		0.8-1.2	1.4-2.2		5-6 mm	
Sella and colleagues (2019)	Normal: 12 PLRS: 48	0.9	1.2		central 2 mm	
		0.9-1.3	1.3-1.5		2-5 mm	
		1.0-1.4	1.5-1.9		5-6 mm	
Lu and colleagues (2019)	Normal: 75 PLRS: 204 KC:73	0.89	1.35-2.34	1.41-2.42	central 2 mm	Optovue Avanti SD-OCT
		0.99-1.24	1.2-3.56	1.36-3.89	2-5 mm	
		1-1.26	1.42-3.04	1.31-3.83	5-7 mm	
		0.92-1.62	1.57-2.94	1.02-4.01	7-9 mm	
Savini and colleagues (2018)	Normal: 96 PLRS: 43	0.99	1.84		central 3 mm	MS-39 SD OCT
		1.06-1.57	1.50-2.10		3-6 mm	
Vega-Estrada and colleagues (2019)	Normal: 60 KC:170	2.03		1.24	central 3 mm	
		0.84-1.18		1.16-1.69	3-6 mm	
		0.99-2.72		1.42-2.70	6-8 mm	
Schiano-Lomoriello and colleagues (2020)	KC: 43			1.57	central 3 mm	
The current paper 2	Normal: 90 PLRS: 46 KC:122	0.98	0.75	1.15	central 2 mm	Optovue Avanti SD-OCT
		1.08-1.19	1.07-1.49	1.17-1.52	2-5 mm	
		0.94-1.27	1.70-2.40	1.29-1.72	5-7 mm	
		0.64	0.6	0.91	central 2 mm	Anterion SS- OCT
		0.69-0.89	0.79-0.96	0.91-1.09	2-5 mm	
		0.86-1.11	1.07-2.05	1.10-1.47	5-7 mm	
The current paper 3	KC: 60			0.93	central 2 mm	Optovue Avanti SD-OCT
				1.04-1.68	2-5 mm	

	0.75-1.79	5-7 mm	
	0.71	central 2 mm	Anterion SS- OCT
	0.81-0.98	2-5 mm	
	0.86-1.59	5-7 mm	
	0.91	central 2 mm	MS-39 SD OCT
	0.53-1.62	2-5 mm	
	0.73-1.79	5-7 mm	

ETM= epithelial thickness mapping; S_w= Pooled within-subject standard deviation; PLRS= post-laser refractive surgery; KC= keratoconus; SD= Spectral-domain; SS= Swept source; OCT = optical coherence tomographer; Unit: μm

Reinstein and colleagues, utilizing very high-frequency ultrasound[43, 106, 107], reported a central epithelial thickness of 53.4 ± 4.6 μm in virgin eyes[106] and 45.7 ± 5.9 μm in eyes with KC[43]. These measurements excluded the pre-corneal tear film thickness. In contrast, our measurements of the central epithelial thickness in virgin eyes with the Avanti, which include the tear film[104], showed 55.60 ± 3.26 μm, while the Anterion exhibited 51.59 ± 3.27 μm. The manufacturer of the Anterion has not provided definitive information regarding the inclusion of the tear film. In both virgin and PLRS eyes, both the Avanti and Anterion measured a thicker epithelium inferiorly than superiorly, consistent with findings from other researchers.[43, 104, 108, 109] In KC eyes, both devices measured a thinner epithelium inferiorly than superiorly, with the differences in thickness between the superior and inferior sections being more pronounced than in the other two groups of eyes. Additionally, in KC eyes, the thinnest part of the epithelium, as measured by both devices, was located in the inferior temporal section within the 2-5 mm ring, aligning with the findings of other researchers.[41, 43]

In paper 2, a significant difference in mean epithelial thickness was observed between the Anterion and the Avanti across all sections in all three groups of eyes, with the Avanti exhibiting a thickness 3.74 ± 2.33 μm greater than the Anterion ($p < 0.001$). In paper 3, the epithelium of keratoconic eyes measured by the MS-39 was notably thicker than that measured by the Anterion (4.11 ± 1.34 μm, $p < 0.001$), and slightly thicker than the Avanti (0.52 ± 1.30 μm, $p < 0.001$). Furthermore, the epithelial measurements obtained with the Anterion were significantly thinner than those obtained with the Avanti (3.59 ± 1.19 μm, $p < 0.001$). The agreement between the Anterion and Avanti was consistent with the results in paper 2.[85] Additionally, we assessed the agreement in 17 sections of the ETM, revealing the differences in measured thicknesses between the Anterion and Avanti in the three groups of eyes. Our findings demonstrated a close correlation in the thickness distribution between the devices, resulting in similar recognizable ETM patterns that are crucial for diagnosing pathological conditions in clinical practice. However, in keratoconus screening, where

measurements need to be precise within a few microns, understanding the precise difference between the two devices is essential if their interchangeability is being considered.

7.2.1 Mechanisms of Epithelial Remodeling

The corneal epithelium plays an active role in determining the final power of the cornea. As mentioned in the introduction, it accounts for an average of -1.03 D of the power in the central 2-mm diameter zone,[22] and it does not form a uniform layer but varies in thickness to smoothen the effect of the irregularities in the underlying stromal surface. This phenomenon is known as epithelial remodeling.[26] The process of epithelial remodeling follows the four rules mentioned in the introduction section "*4.1.2 The Cornea*". The remodeling process is leading to regularizing the corneal refractive properties.[110, 111] In extreme cases, a sharp spike on the stroma would be totally compensated by the epithelial remodeling, while very gradual stromal irregularities would not be compensated at all and would appear unchanged on the anterior corneal surface. Figure 6 is showing how the underlying stroma decides the compensatory capacity of the epithelial remodeling. Generally, the epithelium regularizes the corneal refractive properties leading to less total corneal astigmatism, less prolate total corneal asphericity, and fewer total corneal high-order aberrations,[110, 111]compared to the same parameters measured on the stromal surface. Knowing the epithelial thickness profile will therefore benefit corneal refractive surgery planning.[112]

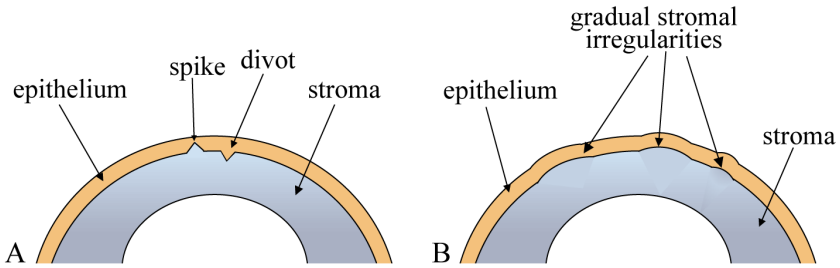

Figure 6 Epithelial remodeling as a function of rate of change of stromal curvature.

A: Sharp spikes and divots on top of the stroma are totally compensated by the epithelial remodeling.
B: Gradual stromal irregularities are not compensated for at all and appear unchanged at surface

7.2.2 Diagnostic Value of Epithelial Thickness Patterns

Our paper's findings have potentially significant implications for the early diagnosis of corneal ectasia and its differentiation from the curvature profiles caused by the epithelial

changes that may simulate keratoconus. The epithelial remodeling in KC results in a characteristic donut-shaped epithelial thickness pattern, which is a typical diagnostic sign of KC. In contrast, inferior corneal epithelium thickening causing the inferior steepening of the anterior corneal surface differentiates contact lens warpage, dry eye, corneal dystrophy and other conditions that lead to inferior epithelial hypertrophy from keratoconus. Hence, the epithelial thickening over an area of topographic steepening indicates that the steepening is not caused by an ectatic surface beneath, but rather represents "pseudo-ectasia". Such insights are crucial in clinical ophthalmology, refractive cataract, and corneal laser vision surgery, making the high quality ETM a significant contribution. Specifically, in PLRS and KC (presented in Paper 2, Figure C and D), epithelium thickens in areas where the stromal tissue has been removed by excimer laser or flattened by CXL, and thins over the untouched regions that became relatively elevated,[26, 27] after the treatment. ETM in such cases represents an invaluable source of information about the effect of the previous surgery, identifying the reason for over/under correction, or visual disturbances due to decentration of the LVC, or the effect/lack of effect of CXL in KC eyes.

7.2.3 Role of ETM in Evaluation of KC Progression before and after CXL

Even a minor epithelial thinning localized over the highest point of the posterior surface and stroma may reveal subclinical changes indicative of KC, not shown yet on the anterior surface elevation or curvature maps. This is vital for timely intervention and management to prevent progression to more severe stages. The presence of progressive epithelial thinning over the cone during a follow-up of initially diagnosed KC will help make a correct decision about the indication for CXL. Likewise, the follow-up of the epithelial thickness over the cone after the CXL will give us a clear sign of the surgical success. Keratoconus stabilization characterized by an increase of the epithelial thickness over the cone, compared to preoperative, will indicate surgical success, while continuous thinning will mean an insufficient effect of the surgery.

7.2.4 Role of ETM in Surgical Planning and Follow-up in Therapeutic- and Elective Laser Refractive Surgery

Given that certain topographic patterns are associated with a higher risk of ectasia, their interpretation may be difficult and may vary depending on the clinician's experience, impacting the inclusion/exclusion criteria in corneal refractive surgery. Integrating epithelial

maps into routine screening for refractive surgery candidacy reduces the risk of missing the diagnosis of early KC, and consequently the development of postoperative ectasia. Understanding and measuring the corneal epithelial profile assists in decision-making and planning therapeutic corneal surgeries, with respect to the choice of the type of laser procedure to be used. Compensatory epithelial modifications, i.e., its remodeling will negatively affect the outcome of the topography-guided (TG) ablations (programmed according to the anterior surface topography) if they are not performed transepithelially. the true stromal irregularity is partially masked by the smoothing effect of the epithelium[22] and will not show on the anterior corneal topography. However, it will become manifest if the epithelium is totally removed mechanically or by use of alcohol. Hence, using TG treatments after mechanical or alcohol epithelial removal will only partially regularize the corneal surface. Performing transepithelial phototherapeutic keratectomy (PTK, lamellar ablation), programmed to the depth of the thickest point on ETM, before the TG ablation, will however remove the epithelium along with the protruding peaks of the irregular stroma, and that way the TG ablation will result in regularized stromal surface (Figure 7, reproduced with the permission of the authors).[113]

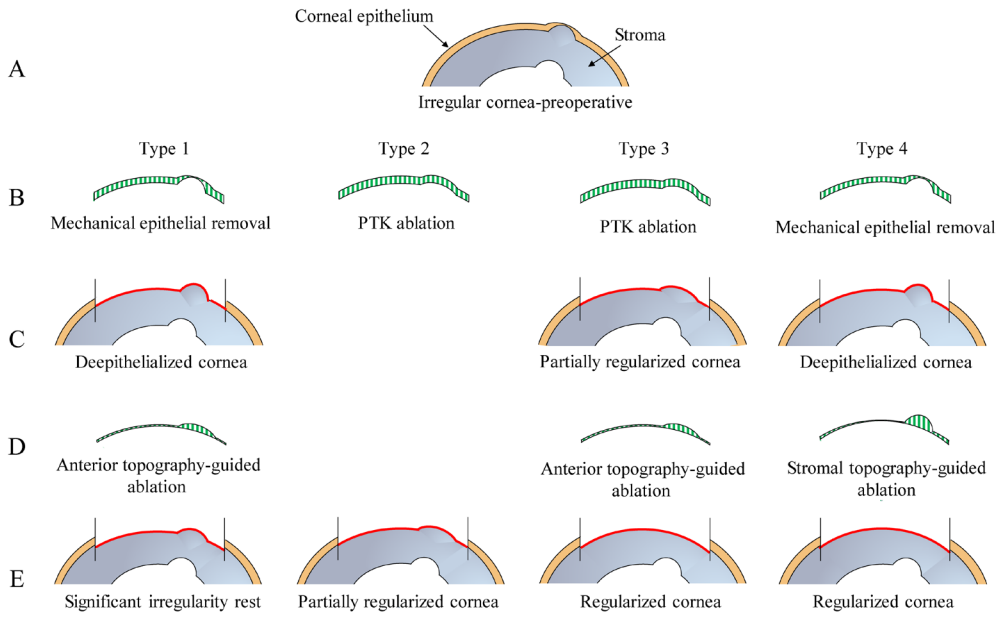

Figure 7 Schematic illustration of four surface ablation treatment types in the treatment of irregular corneas

Row A: Preoperative corneal bulging; Row B: Mechanical epithelial removal in types 1 and 4, and PTK ablation of the epithelium and the protruding stroma within the lamellar ablation in types 2 and

3. Row C: Stromal surface outlined in red after epithelial removal in types 1, 3 and 4; Row D: Ablation profiles of anterior topography-guided PRK used in types 1 and 3 and stromal topography-guided PRK used in type 4; Row E: Stromal surface outlined in red after completed treatment with the four types.

Type 1: Conventional anterior topography-guided PRK; Type 2: Trans-epithelial PTK; Type 3: Trans-epithelial topography-guided PRK; Type 4: Stromal topography-guided PRK; PTK= photo-therapeutic keratectomy; PRK= photorefractive keratectomy

For post-refractive surgery eyes, ETM provides valuable information for monitoring of the healing process and early detection of complications. Central epithelial thickening after myopic treatment is expected because of the epithelial remodeling, and is including in the ablation nomogram,[114] but if it is excessive it will lead to regression of the treatment. In hyperopia treatments, epithelial thickening is expected to happen in the mid- periphery in the ablation area, but a central epithelial thinning over the steepened area will show regression if the epithelium has reached its compensatory capacity, a phenomenon known as “apical syndrome”, which may result in recurrent corneal erosions.[115]

7.2.5 Technological Considerations and Measurement Variability

The tear film can introduce measurement variability, especially in cases of dry eyes. Although each device's protocol includes having patients blink before measurement to standardize the tear film, minor inconsistencies may still influence the results,[6, 7] which will be discussed in the discussion section “*7.5.3 Tear Film Influence*”. The MS-39, Anterion, and Avanti use their own proprietary methods for their respective segmentation algorithms. The question arises as to whether the tear film is included in ETM measurements. Corneal epithelial thickness measured by very high-frequency ultrasound excludes the pre-corneal tear film thickness.[43, 106, 107] The MS-39 measures the distance between the tear film layer and Bowman's layer claimed by the manufacturer. According to Heidelberg Engineering, the segmentation used in Anterion is "looking for the highest intensity of the anterior surface, which can provide the ability to reliably find the underlying structure in a repeatable way" (*Sandro Gunkel, Heidelberg Engineering, personal communication, November 19, 2021*).[85] Since the axial resolution of the Anterion is limited to ~8 µm, the tear film probably cannot be imaged/resolved, and that is possibly why it is uncertain whether the tear film is included in the Anterion's OCT measurements. The Avanti has an axial resolution of ~5 µm and the manufacturer claims that its ETM measurements include the tear film.[104, 116] The impact of including or excluding the tear film in ETM measurements is currently unclear. Future studies

should consider assessing the impact of tear film variability on epithelial thickness measurements, by comparing measurements performed using a technology that definitely includes the tear film (SD-OCT, Avanti) and with a technology that definitely excludes the tear film (VHF ultra-sound, Artemis).

In this project, all three OCT devices use fourier domain detection, utilizing proprietary software, but feature different imaging and technical solutions to enhance the axial and lateral resolution. The software integrates advanced imaging algorithms to refine the raw data collected by the OCT systems, producing high-resolution images for accurate epithelial thickness measurements. For example, Anterion uses a tunable swept laser light source (center wavelength of 1300 nm),[117, 118] the Avanti and MS-39 use a broadband near-infrared SLed as their light source (center wavelength of 840 nm and 845 nm, respectively). This results in different axial and transversal resolutions (3.6 × 35 μm for MS-39, 10 × 45 μm for Anterion, and 5 × 15 μm for Avanti), which presumably leads to different performances. Both SS- and SD-OCT technologies record an interference spectrum that carries the information of the sample, but SS-OCT features a light source that sweeps the wavelength in time, while SD-OCT uses a spectrometer for wavelength separation. SS-OCT imaging features a denser scan pattern, due to its higher acquisition speed, as well as a greater scan depth, due to the use of a longer wavelength and reduced sensitivity roll-off. Hence, SS-OCT may quickly acquire the images of the whole anterior segment,[117] while SD-OCT provides higher contrast and resolution within a shorter depth range.

The proprietary software of each device plays a significant role in optimizing image resolution and accuracy. For instance, the Anterion SS-OCT's software enhances the signal-to-noise ratio, providing clearer delineation of the epithelial layer. Similarly, the Avanti SD-OCT's software incorporates algorithms that correct motion artifacts and enhance lateral resolution. The MS-39's software combines the Placido-based corneal topography with data obtained by SD-OCT scanning. The CSO designers deemed it necessary to equip their SD-OCT device with a Placido disc, which detects ring edges and provides high-quality native curvature data, to achieve the best possible resolution of the curvature of the anterior surface, with the height calculated as secondary data, using the arc-step method. The final anterior corneal surface elevation profile of the MS-39 is derived by merging the secondary data from the Placido imaging and the native SD-OCT data, whereas the posterior cornea data is

provided solely from the SD-OCT. At the same time, the combination of curvature data with native elevation data from the SD-OCT for the anterior surface may be subject to cumulative errors inherent to the arc-step.

In contrast to the other two devices, the Anterion features real-time eye-tracking during the acquisition of multiple B-scans, which allows precise alignment and enhanced detailed imaging.[61] We assume that 65 radial scans used by the Anterion versus the 12 radial scans used by the MS-39 and 8 radial scans used by the Avanti (both repeated five times for each meridian), as well as the Anterion's eye-tracking ability, are the likely factors explaining the better repeatability with the Anterion. We hypothesize that the repeated, wider-spread radial scans used by the MS-39 and the Avanti do not provide as dense coverage as the Anterion provides. For a given cornea, it appears that multiple factors may influence the repeatability of a device, such as axial resolution, image contrast, penetration rate, tracking, scanning speed, and scanning density. The mentioned technological differences among the devices may contribute to the variations in the measured epithelial thickness profiles. So, just by looking at the technical specifications, one cannot decide which device is superior, which emphasizes the importance of clinical evaluations.

Our findings indicate that the measurements obtained by the Anterion SS-OCT and SD-OCT MS-39 and Avanti devices are not interchangeable without compensatory adjustment. This discrepancy underscores the importance of using the same OCT device for both longitudinal studies and clinical follow-ups to ensure consistency and reliability. However, it seems that the mentioned devices may be conditionally interchangeable if a linear correction (e.g., 4 um) is included, since the Anterion gave consistently thinner epithelium compared to the MS-39 and Avanti with a mean difference within the central 2-mm zone, (3.58 μm and 4.11 μm, respectively).[85, 119] A detailed understanding of these technological differences and their impact on measurement accuracy is essential for clinicians and researchers when interpreting OCT data and making informed clinical decisions.

7.3 Lens exchange surgery

Lens exchange surgery, which includes procedures such as cataract surgery, refractive lens exchange surgery, or clear lens extraction, involves removing the natural crystalline lens, which is then replaced with an IOL. This procedure presents unique considerations for

individuals with corneal issues, as the challenge of obtaining precise corneal measurements-vital for accurate IOL calculation-becomes a noteworthy aspect that may potentially influence total corneal astigmatism and overall surgical outcomes.

Several studies[120-122] have provided comprehensive insights into calculating IOL power, particularly focusing on which keratometry value (SimK or TCP) to be incorporated into IOL power calculation formulas. The SimK, based solely on anterior corneal measurements, has been used to assess the corneal optics in most traditional IOL calculations[35], even though lack of data from the posterior cornea has been identified as the most important source of error in toric IOL calculations[36]. Notably, determining the keratometry power poses the most significant challenge, as relying solely on anterior keratometry with a refractive index of 1.3375 typically overestimates the corneal power in keratoconic eyes, potentially resulting in postoperative hyperopia[123-126]. Indeed, a study showed that an IOL formula, using direct measurements of both anterior and posterior corneal power, had a higher predictive accuracy for spherical equivalent refractive outcome in LVC cataract surgery, than the regression-based formulas based on the SimK[33]. The use of TCP has been suggested to yield improved outcomes; however, there is no consensus on the specific corneal location for this measurement in keratoconus eyes, with some advocating for a central location and others favoring more peripheral sites[120, 127, 128].

Our study (Paper 1) focuses on the TCA measurements on keratoconic eyes, where the typical anterior/posterior ratios observed in regular eyes may not be applicable. Given the significant differences in both TCA magnitude and meridian for KC eyes among devices utilizing different technologies, spherical IOLs may be more suitable for KC patients with cataracts. Using the ray-tracing type IOL-calculation, used in formulas, such as Okulix[129]and Olsen[130] that involve the exact Snell's law and ray-tracing calculated TCA, not relying on any assumptions in the calculation, may be beneficial. For more accurate IOL power calculation and astigmatism correction in keratoconic eyes, it is essential to employ keratoconus-specific formulas. In addition to ray-tracing-based formulas, non-ray tracing formulas including the Barrett True-K for keratoconus, the Kane formula for keratoconus, the Holladay II keratoconus mode, the Toric Barrett True-K (for toric IOL), utilizing keratometry measurements. Notable options utilizing TCP including the Barrett True-K keratoconus

formula with total K (TK) for all severities of KC and Emmetropia Verifying Optical (EVO) formula with TK or K in eyes with non-severe disease ($K \leq 50.00$ D)[122].

The SRK/T (T for theoretical) formula, representing a combination of linear regression method with a theoretical eye model[131], has been shown to yield superior outcomes compared to other third-generation formulas and even a fourth-generation formula, such as the Barrett Universal II.[124] Alternatively, custom-designed toric IOLs may be necessary to address corneal and lenticular astigmatism. Some studies[132-134] have advocated for the use of a fairly new IOL, the IC-8 (Acufocus Inc., Irvine, California, USA), which incorporates a pinhole, to enhance visual acuity in patients with irregular corneas and HOAs that cannot be treated with customized refractive surgery. These specialized formulas take into account the unique corneal characteristics associated with keratoconus, providing more accurate and tailored results for IOL power and astigmatism correction.

As observed in paper 1, the difference in AL measurements between Anterion and IOLMaster 700 was statistically significant (0.015 ± 0.033 mm). However, since a variation in AL measurement of 0.015 mm would be clinically irrelevant and would produce a very negligible difference (less than 0.1 D) in postoperative refractive errors, the AL measured by the two instruments may be used interchangeably for IOL power calculation[135]. However, the significant discrepancies in TCA measurements for KC eyes among different technologies (Paper 1), may have a critical impact on toric correction procedures at the IOL plane. The variations observed underscore the importance of careful consideration in clinical decision-making, suggesting that a consistent use of the same device is necessary for accurate and reliable monitoring of keratoconus progression. Moreover, a personalized, device-specific A-constants to minimize systematic prediction errors.

Despite careful planning, residual astigmatism may persist after lens exchange surgery in keratoconus patients. Addressing this residual astigmatism may require additional surgical procedures, such as astigmatic keratotomy, laser vision correction (e.g., PRK), and even CXL. These interventions should be approached cautiously, as the compromised corneal structure in keratoconus can increase the susceptibility to complications.

7.4 Laser vision correction surgery

In individuals with a history of laser vision correction, the corneal epithelium can undergo significant changes due to epithelial remodeling, as evidenced in paper 2 and paper 3. These variations in epithelial thickness post-surgery can significantly impact refractive outcomes and may contribute to suboptimal results. Accurate Epithelial Thickness Mapping (ETM) measurement is also crucial in planning therapeutic laser surgery for keratoconus and irregular corneal optics in general. Besides ETM, Total Corneal Astigmatism (TCA) remains a critical consideration in addressing post-surgical astigmatism, significant coma or coma-like Higher Order Aberrations (HOAs). Zhou and coleagues[136] investigated the astigmatism correction strategy, suggesting that topography-guided custom ablation aiming to correct TCA independent of manifest refractive cylinder (MRC) is preferable in cases with significant coma or coma-like HOAs and low estimated lenticular astigmatism. Conversely, in lenticular exchange surgery, the toric IOL cylinder, which aims to correct MRC, appears to be more suitable.

Patients with a history of LASIK are at an increased risk of developing post-LASIK ectasia. Precise preoperative assessment and monitoring of corneal thickness and ETM are essential to minimize the risk of ectasia in these individuals. Our findings in paper 2 and paper 3 revealed discrepancies in ETM repeatability and agreement among different devices (Avant, Anterion, and MS-39). This underscores the importance of understanding the precise differences between the devices before making surgical decisions, especially considering they are interchangeability.

7.5 Limitations

7.5.1 Sample Size and Diversity

While the thesis included a significant number of participants, the diversity of the sample could have been greater. A more diverse sample in terms of age, ethnicity, and severity of keratoconus would potentially provide a more comprehensive understanding of TCA and ETM across different demographic groups.

7.5.2 Device Variability

This study used multiple OCT devices, each with different imaging protocols. This variability may have introduced challenges in ensuring consistency and comparability of

measurements across devices. Although efforts were made to standardize the measurement procedures as much as possible, minor discrepancies might have influenced the results.

7.5.3 Tear Film Influence

As mentioned in the section "*7.2.5 Technological Considerations and Measurement Variability*", the manufacturers of the three devices had a different approach concerning the tear film inclusion in their measurements. In addition, the variability in tear film thickness of the same eye at different measuring times exists and the eyes with increased or decreased tear production could affect the accuracy of ETM. Further research should investigate the impact of tear film on epithelial thickness measurements and explore methods to control or account for this variability.

7.5.4 Observer Variability

Although all measurements were acquired by one experienced examiner and all the measurements for each patient were performed within half an hour to minimize variability, some degree of variability is inevitable in clinical studies. Improving automated measurement techniques could reduce observer variability, increasing measurement reliability and should be encouraged.

7.6 Reflections on Initial Protocol and Study Design

The initial protocol served as the foundational blueprint for the study, outlining key objectives, methodologies, and anticipated outcomes. As the study progressed, we chose to adjust the following aspect of the protocol.

The initial protocol was aimed to identify the clinically most suitable technology among several currently available corneal imaging devices for various diagnostic and surgical tasks relevant to cataract and therapeutic cornea surgery. This led to the hypothesis that "Modern infra-red-light OCT imaging technology is clinically applicable in measurement of TCA in modern cataract and refractive surgery in virgin eyes and eyes with keratoconus". For testing this hypothesis, we chose to exclude virgin eyes and focus solely on eyes with keratoconus, where different technological approaches might yield different measurement quality. Including virgin eyes would, in the authors' opinion, dilute the focus of the study. Moreover, the testing of virgin eyes, which has already been extensively reported in the literature, makes our study more impactful by concentrating on the less frequently examined keratoconus

population. Excluding virgin eyes to focus on keratoconus (KC) in the TCA study (Paper 1) ensured focus, however, it excluded comparative insights from a wider population and the understanding of device performance across different conditions.

7.7 Ethics

All studies were conducted in accordance with the principles of the Declaration of Helsinki. The examinations mentioned in this project are standard routine procedures at the clinic. Approvals from The Regional Ethics Committee (REK) were obtained for the prospective study, and the use of data for retrospective studies was reported to the Norwegian Data Protection Authority (reference number: 311856 and 72084). Informed consent for the anonymous use of data for analysis and publication was obtained from all study participants.

8. Conclusions

The success of lens exchange surgery and laser vision correction surgery hinges on precise measurements and thorough consideration of various factors to achieve optimal outcomes. This study specifically focused on Total Corneal Astigmatism (TCA), Epithelial Thickness Mapping (ETM), and Axial Length (AL) measurements, which are critical for accurate intraocular lens (IOL) selection and predictable refractive surgery outcomes.

Recent technological advancements, as exemplified by the five devices investigated in this study, have increased the anticipated quality of refractive outcomes in contemporary cataract and refractive surgery. Our investigation revealed that four devices (Anterion, MS-39, Casia SS-1000, and IOLMaster 700) demonstrated good repeatability in measuring TCA in eyes with KC, with Anterion exhibiting the highest repeatability. However, disparities in fundamental technology among the devices led to low agreement in their measurements. Therefore, it is important to note that SS-OCT-based devices should not be used interchangeably with hybrid technologies. In contrast, for AL measurements, both Anterion and IOLMaster 700, which utilize SS-OCT technology, demonstrated good repeatability and clinical agreement, suggesting their interchangeability.

Accurate IOL power calculation is crucial for achieving optimal refractive outcomes, especially in KC and PLRS eyes. Standard formulas like SRK/T and Barrett Universal II are generally accurate for virgin eyes, but the traditional IOL calculations using only anterior

keratometry that includes a compensation for the posterior corneal power, often overestimate corneal power in keratoconic eyes, leading to postoperative hyperopia. Specialized formulas such as ray-tracing-based formulas incorporating total corneal power measurements and Barrett True-K for keratoconus (when based on measured instead of estimated posterior cornea) improve predictive accuracy of the refractive outcomes in KC eyes.

Our findings indicate that Anterion showed superior repeatability in ETM measurements compared to Avanti and MS-39. Similar to TCA measurements, ETM measurements showed low agreement and interchangeability among devices. In areas where tissue has been removed or the curvature has been flattened like PLRS and post CXL eyes, the ETM will show characteristic patterns that contrast with those seen in eyes without prior surgical intervention, highlighting significant variations in epithelial remodeling across different conditions. Recognizing the distinct ETM patterns in virgin, KC, and PLRS eyes is vital for accurate diagnosis and tailored treatment planning. Different devices, using varied technologies, may present these patterns differently, underscoring the importance of understanding the specific characteristics and limitations of each device, which is essential for clinicians when interpreting results and planning surgical interventions.

In conclusion, it is essential to understand the limitations and differences among devices for accurate interpretation of results. Consistent use of the same device for pre- and postoperative measurements is vital for reliable monitoring of keratoconus progression and PLRS outcomes. Collaboration between corneal and cataract surgeons is imperative in complex cases, ensuring tailored approaches based on the specific characteristics of each device and the patient's conditions.

9. References

1 Mishima S, Gasset A, Klyce SD, Jr., Baum JL. Determination of tear volume and tear flow. Invest Ophthalmol 1966; 5: 264-276

2 Holly FJ. Tear film physiology. Am J Optom Physiol Opt 1980; 57: 252-257

3 Holly FJ, Lemp MA. Tear physiology and dry eyes. Surv Ophthalmol 1977; 22: 69-87

4 Gipson IK. The ocular surface: the challenge to enable and protect vision: the Friedenwald lecture. Invest Ophthalmol Vis Sci 2007; 48: 4390; 4391-4398

5 Dartt DA. Neural regulation of lacrimal gland secretory processes: relevance in dry eye diseases. Prog Retin Eye Res 2009; 28: 155-177

6 Holland EJ, Mannis MJ, Lee WB. Ocular surface disease: cornea, conjunctiva and tear film: expert consult-online and print. Elsevier Health Sciences, 2013

7 Worthington CR. The structure of cornea. Q Rev Biophys 1984; 17: 423-451

8 Dursun D, Monroy D, Knighton R, Tervo T, Vesaluoma M, Carraway K, Feuer W, Pflugfelder SC. The effects of experimental tear film removal on corneal surface regularity and barrier function. Ophthalmology 2000; 107: 1754-1760

9 Rolando M, Zierhut M. The ocular surface and tear film and their dysfunction in dry eye disease. Surv Ophthalmol 2001; 45 Suppl 2: S203-210

10 Tiffany JM. The normal tear film. Dev Ophthalmol 2008; 41: 1-20

11 Albietz JM, Lenton LM. Management of the ocular surface and tear film before, during, and after laser in situ keratomileusis. J Refract Surg 2004; 20: 62-71

12 Labbé A, Alalwani H, Van Went C, Brasnu E, Georgescu D, Baudouin C. The relationship between subbasal nerve morphology and corneal sensation in ocular surface disease. Invest Ophthalmol Vis Sci 2012; 53: 4926-4931

13 Pflugfelder SC, Solomon A, Stern ME. The diagnosis and management of dry eye: a twenty-five-year review. Cornea 2000; 19: 644-649

14 Ambrósio R, Jr., Tervo T, Wilson SE. LASIK-associated dry eye and neurotrophic epitheliopathy: pathophysiology and strategies for prevention and treatment. J Refract Surg 2008; 24: 396-407

15 Behrens A, Doyle JJ, Stern L, Chuck RS, McDonnell PJ, Azar DT, Dua HS, Hom M, Karpecki PM, Laibson PR, Lemp MA, Meisler DM, Del Castillo JM, O'Brien TP, Pflugfelder SC, Rolando M, Schein OD, Seitz B, Tseng SC, van Setten G, Wilson SE, Yiu SC. Dysfunctional tear syndrome: a Delphi approach to treatment recommendations. Cornea 2006; 25: 900-907

16 Albietz JM, Lenton LM, McLennan SG. Chronic dry eye and regression after laser in situ keratomileusis for myopia. J Cataract Refract Surg 2004; 30: 675-684

17 Torricelli AA, Santhiago MR, Wilson SE. Topical cyclosporine a treatment in corneal refractive surgery and patients with dry eye. J Refract Surg 2014; 30: 558-564

18 DelMonte DW, Kim T. Anatomy and physiology of the cornea. J Cataract Refract Surg 2011; 37: 588-598

19 Cogan DG. Applied anatomy and physiology of the cornea. Trans Am Acad Ophthalmol Otolaryngol 1951; 55: 329-359

20 Dua HS, Faraj LA, Said DG, Gray T, Lowe J. Human corneal anatomy redefined: a novel pre-Descemet's layer (Dua's layer). Ophthalmology 2013; 120: 1778-1785

21 Simon G, Legeais JM, Parel JM. [Optical power of the corneal epithelium]. J Fr Ophtalmol 1993; 16: 41-47

22 Simon G, Ren Q, Kervick GN, Parel JM. Optics of the corneal epithelium. Refract Corneal Surg 1993; 9: 42-50

23 Fatt I, Weissman BA. Physiology of the eye: an introduction to the vegetative functions. Butterworth-Heinemann, 2013

24 Shaw AJ, Collins MJ, Davis BA, Carney LG. Eyelid Pressure: Inferences From Corneal Topographic Changes. Cornea 2009; 28: 181-188

25 Varadarajan S, Chumki SA, Stephenson RE, Misterovich ER, Wu JL, Dudley CE, Erofeev IS, Goryachev AB, Miller AL. Mechanosensitive calcium flashes promote sustained RhoA activation during tight junction remodeling. J Cell Biol 2022; 221
26 Reinstein DZ, Archer TJ, Gobbe M. Corneal epithelial thickness profile in the diagnosis of keratoconus. J Refract Surg 2009; 25: 604-610
27 Reinstein DZ, Srivannaboon S, Gobbe M, Archer TJ, Silverman RH, Sutton H, Coleman DJ. Epithelial thickness profile changes induced by myopic LASIK as measured by Artemis very high-frequency digital ultrasound. J Refract Surg 2009; 25: 444-450
28 Gullstrand A. How I found the mechanism of intracapsular accommodation. In: Physiol Med. Stockholm, Sweden, Nobel Lect., 1911
29 Bair HL, Martens TG. ANNUAL REVIEW: REFRACTION AND VISUAL PHYSIOLOGY. Arch Ophthalmol 1964; 71: 889-915
30 Ayres BD, Rapuano CJ. Refractive power of the cornea. Compr Ophthalmol Update 2006; 7: 243-251; discussion 253-245
31 Ferdi AC, Nguyen V, Gore DM, Allan BD, Rozema JJ, Watson SL. Keratoconus Natural Progression: A Systematic Review and Meta-analysis of 11 529 Eyes. Ophthalmology 2019; 126: 935-945
32 Alpins N, Ong JK, Stamatelatos G. New method of quantifying corneal topographic astigmatism that corresponds with manifest refractive cylinder. J Cataract Refract Surg 2012; 38: 1978-1988
33 Huang D, Tang M, Wang L, Zhang X, Armour RL, Gattey DM, Lombardi LH, Koch DD. Optical coherence tomography-based corneal power measurement and intraocular lens power calculation following laser vision correction (an American Ophthalmological Society thesis). Trans Am Ophthalmol Soc 2013; 111: 34-45
34 Balparda K, Maya-Naranjo MI, Mesa-Mesa S, Herrera-Chalarca T. Corneal and Whole-Eye Higher Order Aberrations Do Not Correlate With Ocular Residual Astigmatism in Prepresbyopic Refractive Surgery Candidates. Cornea 9900: 10.1097/ICO.0000000000003160
35 Mendes J, Ribeiro FJ, Ferreira TB. Evaluation of posterior and total corneal astigmatism with colour-LED topography. Eye 2021; 35: 2585-2593
36 Savini G, Naeser K. An analysis of the factors influencing the residual refractive astigmatism after cataract surgery with toric intraocular lenses. Invest Ophthalmol Vis Sci 2015; 56: 827-835
37 Rabinowitz YS. Keratoconus. Survey of ophthalmology 1998; 42: 297-319
38 Padmanabhan P, Lopes BT, Eliasy A, Abass A, Elsheikh A. In vivo biomechanical changes associated with Keratoconus progression. Current eye research 2022: 1-19
39 Silverman RH, Urs R, Roychoudhury A, Archer TJ, Gobbe M, Reinstein DZ. Epithelial remodeling as basis for machine-based identification of keratoconus. Invest Ophthalmol Vis Sci 2014; 55: 1580-1587
40 Kanellopoulos AJ, Aslanides IM, Asimellis G. Correlation between epithelial thickness in normal corneas, untreated ectatic corneas, and ectatic corneas previously treated with CXL; is overall epithelial thickness a very early ectasia prognostic factor? Clin Ophthalmol 2012; 6: 789-800
41 Li Y, Tan O, Brass R, Weiss JL, Huang D. Corneal epithelial thickness mapping by Fourier-domain optical coherence tomography in normal and keratoconic eyes. Ophthalmology 2012; 119: 2425-2433
42 Rocha KM, Perez-Straziota CE, Stulting RD, Randleman JB. SD-OCT analysis of regional epithelial thickness profiles in keratoconus, postoperative corneal ectasia, and normal eyes. J Refract Surg 2013; 29: 173-179
43 Reinstein DZ, Gobbe M, Archer TJ, Silverman RH, Coleman DJ. Epithelial, stromal, and total corneal thickness in keratoconus: three-dimensional display with artemis very-high frequency digital ultrasound. J Refract Surg 2010; 26: 259-271

44 Rattan SA, Anwar DS. Comparison of corneal epithelial thickness profile in dry eye patients, keratoconus suspect, and healthy eyes. European journal of ophthalmology 2020; 30: 1506-1511
45 Masiwa LE, Moodley V. A review of corneal imaging methods for the early diagnosis of pre-clinical Keratoconus. Journal of optometry 2020; 13: 269-275
46 Haque S, Jones L, Simpson T. Thickness mapping of the cornea and epithelium using optical coherence tomography. Optom Vis Sci 2008; 85: E963-976
47 Temstet C, Sandali O, Bouheraoua N, Hamiche T, Galan A, El Sanharawi M, Basli E, Laroche L, Borderie V. Corneal epithelial thickness mapping using Fourier-domain optical coherence tomography for detection of form fruste keratoconus. J Cataract Refract Surg 2015; 41: 812-820
48 Sandali O, El Sanharawi M, Temstet C, Hamiche T, Galan A, Ghouali W, Goemaere I, Basli E, Borderie V, Laroche L. Fourier-domain optical coherence tomography imaging in keratoconus: a corneal structural classification. Ophthalmology 2013; 120: 2403-2412
49 Yang Y, Pavlatos E, Chamberlain W, Huang D, Li Y. Keratoconus detection using OCT corneal and epithelial thickness map parameters and patterns. J Cataract Refract Surg 2021; 47: 759-766
50 Randleman JB, Woodward M, Lynn MJ, Stulting RD. Risk assessment for ectasia after corneal refractive surgery. Ophthalmology 2008; 115: 37-50
51 Kumar B, Reilly MA. The Development, Growth, and Regeneration of the Crystalline Lens: A Review. Curr Eye Res 2020; 45: 313-326
52 Hartridge H. HELMHOLTZ'S THEORY OF ACCOMMODATION. Br J Ophthalmol 1925; 9: 521-523
53 Truscott RJ, Zhu X. Presbyopia and cataract: a question of heat and time. Prog Retin Eye Res 2010; 29: 487-499
54 Aumann S DS, Fischer J, et al. Optical Coherence Tomography (OCT): Principle and Technical. In: JF B ed, High Resolution Imaging in Microscopy and Ophthalmology: New Frontiers in Biomedical Optics. Cham (CH): Springer, 2019 Aug 14
55 Ramos JL, Li Y, Huang D. Clinical and research applications of anterior segment optical coherence tomography - a review. Clin Exp Ophthalmol 2009; 37: 81-89
56 Doors M, Berendschot TT, de Brabander J, Webers CA, Nuijts RM. Value of optical coherence tomography for anterior segment surgery. J Cataract Refract Surg 2010; 36: 1213-1229
57 Wojtkowski M, Bajraszewski T, Gorczyńska I, Targowski P, Kowalczyk A, Wasilewski W, Radzewicz C. Ophthalmic imaging by spectral optical coherence tomography. Am J Ophthalmol 2004; 138: 412-419
58 Shoji T, Kato N, Ishikawa S, Ibuki H, Yamada N, Kimura I, Shinoda K. In vivo crystalline lens measurements with novel swept-source optical coherent tomography: an investigation on variability of measurement. BMJ Open Ophthalmol 2017; 1: e000058
59 Reinstein DZ, Silverman RH, Coleman DJ. High-frequency ultrasound measurement of the thickness of the corneal epithelium. Refract Corneal Surg 1993; 9: 385-387
60 El Wardani M, Hashemi K, Aliferis K, Kymionis G. Topographic changes simulating keratoconus in patients with irregular inferior epithelial thickening documented by anterior segment optical coherence tomography. Clinical ophthalmology (Auckland, NZ) 2019; 13: 2103-2110
61 Asam JS PM, Tafreshi A, et al. . Anterior Segment OCT. In: JF B ed, High Resolution Imaging in Microscopy and Ophthalmology: New Frontiers in Biomedical Optics. Springer, 2019
62 Seitz B, Behrens A, Langenbucher A. Corneal topography. Curr Opin Ophthalmol 1997; 8: 8-24
63 Corneal topography. American Academy of Ophthalmology. Ophthalmology 1999; 106: 1628-1638

64 Schlegel Z, Hoang-Xuan T, Gatinel D. Comparison of and correlation between anterior and posterior corneal elevation maps in normal eyes and keratoconus-suspect eyes. J Cataract Refract Surg 2008; 34: 789-795
65 Saad A, Gatinel D. Topographic and tomographic properties of forme fruste keratoconus corneas. Invest Ophthalmol Vis Sci 2010; 51: 5546-5555
66 Kelman CD. Phaco-emulsification and aspiration. A new technique of cataract removal. A preliminary report. Am J Ophthalmol 1967; 64: 23-35
67 Ale J, Manns F, Ho A. Evaluation of the performance of accommodating IOLs using a paraxial optics analysis. Ophthalmic Physiol Opt 2010; 30: 132-142
68 Hoffman RS, Fine IH, Packer M. Refractive lens exchange as a refractive surgery modality. Curr Opin Ophthalmol 2004; 15: 22-28
69 Munnerlyn CR, Koons SJ, Marshall J. Photorefractive keratectomy: a technique for laser refractive surgery. J Cataract Refract Surg 1988; 14: 46-52
70 Alio JL, Soria FA, Abbouda A, Peña-García P. Fifteen years follow-up of photorefractive keratectomy up to 10 D of myopia: outcomes and analysis of the refractive regression. Br J Ophthalmol 2016; 100: 626-632
71 Gobbi PG, Carones F, Brancato R, Carena M, Fortini A, Scagliotti F, Morico A, Venturi E. Automatic eye tracker for excimer laser photorefractive keratectomy. J Refract Surg 1995; 11: S337-342
72 Pallikaris IG, Papatzanaki ME, Stathi EZ, Frenschock O, Georgiadis A. Laser in situ keratomileusis. Lasers Surg Med 1990; 10: 463-468
73 Blum M, Sekundo W. [Femtosecond lenticule extraction (FLEx)]. Ophthalmologe 2010; 107: 967-970
74 Accuracy I. of measurement methods and results—part 1: General principles and definitions. International Organization for Standardization, Geneva, Switzerland 1994
75 Menditto A, Patriarca M, Magnusson B. Understanding the meaning of accuracy, trueness and precision. Accreditation and Quality Assurance 2007; 12: 45-47
76 Standardization IOf. Guidance for the use of repeatability, reproducibility and trueness estimates in measurement uncertainty estimation. ISO, 2010
77 McAlinden C, Khadka J, Pesudovs K. Statistical methods for conducting agreement (comparison of clinical tests) and precision (repeatability or reproducibility) studies in optometry and ophthalmology. Ophthalmic Physiol Opt 2011; 31: 330-338
78 Bergin C, Guber I, Hashemi K, Majo F. Tolerance and Relative Utility: Two Proposed Indices for Comparing Change in Clinical Measurement Noise Between Different Populations (Repeatability) or Measurement Methods (Agreement). Invest Ophthalmol Vis Sci 2015; 56: 5543-5547
79 Vega-Estrada A, Mimouni M, Espla E, Alió Del Barrio J, Alio JL. Corneal Epithelial Thickness Intrasubject Repeatability and its Relation With Visual Limitation in Keratoconus. Am J Ophthalmol 2019; 200: 255-262
80 Schiano-Lomoriello D, Bono V, Abicca I, Savini G. Repeatability of anterior segment measurements by optical coherence tomography combined with Placido disk corneal topography in eyes with keratoconus. Sci Rep 2020; 10: 1124
81 Savini G, Schiano-Lomoriello D, Hoffer KJ. Repeatability of automatic measurements by a new anterior segment optical coherence tomographer combined with Placido topography and agreement with 2 Scheimpflug cameras. J Cataract Refract Surg 2018; 44: 471-478
82 Thibos LN, Horner D. Power vector analysis of the optical outcome of refractive surgery. J Cataract Refract Surg 2001; 27: 80-85
83 Zhou W, Stojanovic A. Comparison of corneal epithelial and stromal thickness distributions between eyes with keratoconus and healthy eyes with corneal astigmatism ≥ 2.0 D. PLoS One 2014; 9: e85994
84 Bland JM, Altman DG. Measurement error. Bmj 1996; 313: 744
85 Feng Y, Reinstein DZ, Nitter T, Archer TJ, McAlinden C, Chen X, Bertelsen G, Utheim TP, Stojanovic A. Heidelberg Anterion Swept-Source OCT Corneal Epithelial Thickness

Mapping: Repeatability and Agreement With Optovue Avanti. J Refract Surg 2022; 38: 356-363
86 McAlinden C, Khadka J, Pesudovs K. Precision (repeatability and reproducibility) studies and sample-size calculation. Journal of cataract and refractive surgery 2015; 41: 2598-2604
87 Tañá-Rivero P, Aguilar-Córcoles S, Ruiz-Mesa R, Montés-Micó R. Repeatability of whole-cornea measurements using a new swept-source optical coherence tomographer. European journal of ophthalmology 2021; 31: 1709-1719
88 Schiano-Lomoriello D, Hoffer KJ, Abicca I, Savini G. Repeatability of automated measurements by a new anterior segment optical coherence tomographer and biometer and agreement with standard devices. Scientific reports 2021; 11: 983
89 Cheng SM, Zhang JS, Shao X, Wu ZT, Li TT, Wang P, Lin JH, Yu AY. Repeatability of a new swept-source optical coherence tomographer and agreement with other three optical biometers. Graefe's archive for clinical and experimental ophthalmology = Albrecht von Graefes Archiv fur klinische und experimentelle Ophthalmologie 2022; 260: 2271-2281
90 Shajari M, Sonntag R, Ramsauer M, Kreutzer T, Vounotrypidis E, Kohnen T, Priglinger S, Mayer WJ. Evaluation of total corneal power measurements with a new optical biometer. Journal of cataract and refractive surgery 2020; 46: 675-681
91 Shajari M, Kolb CM, Mayer WJ, Agha B, Steinwender G, Dirisamer M, Priglinger S, Kohnen T, Schmack I. Characteristics of preoperative and postoperative astigmatism in patients having Descemet membrane endothelial keratoplasty. J Cataract Refract Surg 2019; 45: 1001-1006
92 Gjerdrum B, Gundersen KG, Lundmark PO, Aakre BM. Repeatability of OCT-Based versus Scheimpflug- and Reflection-Based Keratometry in Patients with Hyperosmolar and Normal Tear Film. Clin Ophthalmol 2020; 14: 3991-4003
93 Piñero DP, Molina-Martín A, Camps VJ, de Fez D, Caballero MT. Validation of corneal topographic and aberrometric measurements obtained by color light-emitting diode reflection topography in healthy eyes. Graefe's archive for clinical and experimental ophthalmology = Albrecht von Graefes Archiv fur klinische und experimentelle Ophthalmologie 2019; 257: 2437-2447
94 de Luis Eguileor B, Arriola-Villalobos P, Pijoan Zubizarreta JI, Feijoo Lera R, Santamaria Carro A, Diaz-Valle D, Etxebarria J. Multicentre study: reliability and repeatability of Scheimpflug system measurement in keratoconus. Br J Ophthalmol 2021; 105: 22-26
95 de Luis Eguileor B, Argaluza JE, Zubizarreta JIP, Carro AS, Ecenarro JE. Evaluation of the reliability and repeatability of scheimpflug system measurement in keratoconus. Cornea 2018; 37: 177-181
96 Kanellopoulos AJ, Asimellis G. Distribution and Repeatability of Corneal Astigmatism Measurements (Magnitude and Axis) Evaluated With Color Light Emitting Diode Reflection Topography. Cornea 2015; 34: 937-944
97 Kanellopoulos AJ, Asimellis G. Forme Fruste Keratoconus Imaging and Validation via Novel Multi-Spot Reflection Topography. Case Rep Ophthalmol 2013; 4: 199-209
98 Piñero DP, Camps VJ, Mateo V, Ruiz-Fortes P. Clinical validation of an algorithm to correct the error in the keratometric estimation of corneal power in normal eyes. J Cataract Refract Surg 2012; 38: 1333-1338
99 Tomey. Casia SS-1000 Instruction Manual for Analysis. In: Nishi-ku, Nagoya, Japan, Tomey Corporation, 2012
100 Heidelberg. Anterion User Manual, Software Version 1.1. In: Heidelberg, Germany, Heidelberg Engineering GmbH, 2019
101 Pircher N, Schwarzhans F, Holzer S, Lammer J, Schmidl D, Bata AM, Werkmeister RM, Seidel G, Garhöfer G, Gschließer A, Schmetterer L, Schmidinger G. Distinguishing Keratoconic Eyes and Healthy Eyes Using Ultrahigh-Resolution Optical Coherence Tomography-Based Corneal Epithelium Thickness Mapping. American journal of ophthalmology 2018; 189: 47-54

102 Ma XJ, Wang L, Koch DD. Repeatability of corneal epithelial thickness measurements using Fourier-domain optical coherence tomography in normal and post-LASIK eyes. Cornea 2013; 32: 1544-1548
103 Sella R, Zangwill LM, Weinreb RN, Afshari NA. Repeatability and Reproducibility of Corneal Epithelial Thickness Mapping With Spectral-Domain Optical Coherence Tomography in Normal and Diseased Cornea Eyes. Am J Ophthalmol 2019; 197: 88-97
104 Sedaghat MR, Momeni-Moghaddam H, Gazanchian M, Reinstein DZ, Archer TJ, Randleman JB, Hosseini SR, Nouri-Hosseini G. Corneal Epithelial Thickness Mapping After Photorefractive Keratectomy for Myopia. Journal of refractive surgery (Thorofare, NJ : 1995) 2019; 35: 632-641
105 Lu NJ, Chen D, Cui LL, Wang L, Chen SH, Wang QM. Repeatability of Cornea and Sublayer Thickness Measurements Using Optical Coherence Tomography in Corneas of Anomalous Refractive Status. Journal of refractive surgery (Thorofare, NJ : 1995) 2019; 35: 600-605
106 Reinstein DZ, Archer TJ, Gobbe M, Silverman RH, Coleman DJ. Epithelial thickness in the normal cornea: three-dimensional display with Artemis very high-frequency digital ultrasound. J Refract Surg 2008; 24: 571-581
107 Reinstein DZ, Archer TJ, Gobbe M, Silverman RH, Coleman DJ. Epithelial thickness after hyperopic LASIK: three-dimensional display with Artemis very high-frequency digital ultrasound. Journal of refractive surgery (Thorofare, NJ : 1995) 2010; 26: 555-564
108 Erie JC, Patel SV, McLaren JW, Ramirez M, Hodge DO, Maguire LJ, Bourne WM. Effect of myopic laser in situ keratomileusis on epithelial and stromal thickness: a confocal microscopy study. Ophthalmology 2002; 109: 1447-1452
109 Patel SV, Erie JC, McLaren JW, Bourne WM. Confocal microscopy changes in epithelial and stromal thickness up to 7 years after LASIK and photorefractive keratectomy for myopia. Journal of refractive surgery (Thorofare, NJ : 1995) 2007; 23: 385-392
110 Zhou W, Reinstein DZ, Archer TJ, Chen X, Utheim TP, Feng Y, Stojanovic A. Intraoperative Swept-Source OCT-Based Corneal Topography for Measurement and Analysis of Stromal Surface After Epithelial Removal. J Refract Surg 2021; 37: 484-492
111 Reinstein DZ, Silverman RH, Sutton HF, Coleman DJ. Very high-frequency ultrasound corneal analysis identifies anatomic correlates of optical complications of lamellar refractive surgery: anatomic diagnosis in lamellar surgery. Ophthalmology 1999; 106: 474-482
112 Reinstein DZ, Archer TJ, Gobbe M. Refractive and topographic errors in topography-guided ablation produced by epithelial compensation predicted by 3D Artemis VHF digital ultrasound stromal and epithelial thickness mapping. J Refract Surg 2012; 28: 657-663
113 Zhou W, Reinstein DZ, Archer TJ, Nitter T, Feng Y, Mule G, Stojanovic A. The Impact of Epithelial Remodeling on Surgical Techniques Used in Topography-guided Surface Ablation in Irregular Corneas. J Refract Surg 2022; 38: 529-537
114 Yue Feng TN, Xu Liu, Aleksandar Stojanovic Nominal and achieved stromal ablation depth after myopic transepithelial photorefractive keratectomy: implications for residual stromal thickness calculation. Eye and Vision 2024
115 Reinstein DZ, Carp GI, Archer TJ, Buick T, Gobbe M, Rowe EL, Jukic M, Brandon E, Moore J, Moore T. LASIK for the Correction of High Hyperopic Astigmatism With Epithelial Thickness Monitoring. J Refract Surg 2017; 33: 314-321
116 Azartash K, Kwan J, Paugh JR, Nguyen AL, Jester JV, Gratton E. Pre-corneal tear film thickness in humans measured with a novel technique. Molecular vision 2011; 17: 756-767
117 Aumann S, Donner S, Fischer J, Müller F. Optical Coherence Tomography (OCT): Principle and Technical Realization. In: Bille JF ed, High Resolution Imaging in Microscopy and Ophthalmology: New Frontiers in Biomedical Optics. Cham (CH), Springer

 2019; 59-85
118 Potsaid B, Baumann B, Huang D, Barry S, Cable AE, Schuman JS, Duker JS, Fujimoto JG. Ultrahigh speed 1050nm swept source/Fourier domain OCT retinal and anterior segment imaging at 100,000 to 400,000 axial scans per second. Opt Express 2010; 18: 20029-20048

119 Feng Y, Reinstein DZ, Nitter T, Archer TJ, McAlinden C, Bertelsen G, Stojanovic A. Epithelial Thickness Mapping in Keratoconic Corneas: Repeatability and Agreement Between CSO MS-39, Heidelberg Anterion, and Optovue Avanti OCT Devices. J Refract Surg 2023; 39: 474-480
120 Park DY, Lim DH, Chung TY, Chung ES. Intraocular lens power calculations in a patient with posterior keratoconus. Cornea 2013; 32: 708-711
121 Tamaoki A, Kojima T, Hasegawa A, Nakamura H, Tanaka K, Ichikawa K. Intraocular lens power calculation in cases with posterior keratoconus. J Cataract Refract Surg 2015; 41: 2190-2195
122 Heath MT, Mulpuri L, Kimiagarov E, Patel RP, Murphy DA, Levine H, Tonk RS, Cooke DL, Riaz KM. Intraocular Lens Power Calculations in Keratoconus Eyes Comparing Keratometry, Total Keratometry, and Newer Formulae. Am J Ophthalmol 2023; 253: 206-214
123 Kamiya K, Iijima K, Nobuyuki S, Mori Y, Miyata K, Yamaguchi T, Shimazaki J, Watanabe S, Maeda N. Predictability of Intraocular Lens Power Calculation for Cataract with Keratoconus: A Multicenter Study. Sci Rep 2018; 8: 1312
124 Savini G, Abbate R, Hoffer KJ, Mularoni A, Imburgia A, Avoni L, D'Eliseo D, Schiano-Lomoriello D. Intraocular lens power calculation in eyes with keratoconus. J Cataract Refract Surg 2019; 45: 576-581
125 Camps VJ, Piñero DP, Caravaca E, De Fez D. Preliminary validation of an optimized algorithm for intraocular lens power calculation in keratoconus. Indian J Ophthalmol 2017; 65: 690-699
126 Piñero DP, Camps VJ, Caravaca-Arens E, Pérez-Cambrodí RJ, Artola A. Estimation of the central corneal power in keratoconus: theoretical and clinical assessment of the error of the keratometric approach. Cornea 2014; 33: 274-279
127 Hashemi H, Heidarian S, Seyedian MA, Yekta A, Khabazkhoob M. Evaluation of the Results of Using Toric IOL in the Cataract Surgery of Keratoconus Patients. Eye Contact Lens 2015; 41: 354-358
128 Celikkol L, Ahn D, Celikkol G, Feldman ST. Calculating intraocular lens power in eyes with keratoconus using videokeratography. J Cataract Refract Surg 1996; 22: 497-500
129 Ghoreyshi M, Khalilian A, Peyman M, Mohammadinia M, Peyman A. Comparison of OKULIX ray-tracing software with SRK-T and Hoffer-Q formula in intraocular lens power calculation. Journal of Current Ophthalmology 2018; 30: 63-67
130 Savini G, Taroni L, Hoffer KJ. Recent developments in intraocular lens power calculation methods-update 2020. Ann Transl Med 2020; 8: 1553
131 Retzlaff JA, Sanders DR, Kraff MC. Development of the SRK/T intraocular lens implant power calculation formula. J Cataract Refract Surg 1990; 16: 333-340
132 Franco F, Branchetti M, Vicchio L, Serino F, Piergentili M, Spagnuolo V, Santoro F, Virgili G, Giansanti F. Implantation of a Small Aperture Intraocular Lens in Eyes with Irregular Corneas and Higher Order Aberrations. J Ophthalmic Vis Res 2022; 17: 317-323
133 Shajari M, Mackert MJ, Langer J, Kreutzer T, Wolf A, Kohnen T, Priglinger S, Mayer WJ. Safety and efficacy of a small-aperture capsular bag-fixated intraocular lens in eyes with severe corneal irregularities. J Cataract Refract Surg 2020; 46: 188-192
134 Dick HB, Elling M, Schultz T. Binocular and Monocular Implantation of Small-Aperture Intraocular Lenses in Cataract Surgery. J Refract Surg 2018; 34: 629-631
135 Eibschitz-Tsimhoni M, Tsimhoni O, Archer SM, Del Monte MA. Effect of axial length and keratometry measurement error on intraocular lens implant power prediction formulas in pediatric patients. Journal of AAPOS : the official publication of the American Association for Pediatric Ophthalmology and Strabismus 2008; 12: 173-176
136 Zhou W, Stojanovic F, Reinstein DZ, Archer TJ, Chen X, Feng Y, Stojanovic A. Coma Influence on Manifest Astigmatism in Coma-Dominant Irregular Corneal Optics. J Refract Surg 2021; 37: 274-282

Paper 1

Repeatability and agreement of total corneal astigmatism measured in keratoconic eyes using four current devices

Received: 13 May 2024 | Revised: 8 July 2024 | Accepted: 9 July 2024

DOI: 10.1111/ceo.14423

ORIGINAL ARTICLE-CLINICAL SCIENCE

Clinical & Experimental Ophthalmology WILEY

Repeatability and agreement of total corneal astigmatism measured in keratoconic eyes using four current devices

Yue Feng MD, MSc[1] | **Tore Nitter MD, PhD** | **Geir Bertelsen MD, PhD**[1,2] | **Aleksandar Stojanovic MD, PhD**[2,3]

[1]Institute of Community Medicine, Faculty of Health Sciences, University in Tromsø, Tromsø, Norway

[2]Department of Ophthalmology, University Hospital North Norway, Tromsø, Norway

[3]Institute of Clinical Medicine, Faculty of Health Sciences, University in Tromsø, Tromsø, Norway

Correspondence
Aleksandar Stojanovic, Department of Ophthalmology, University Hospital North Norway, Sykehusveien 38, 9019 Tromsø, Norway.
Email: aleks@online.no

Funding information
Norwegian research council, Grant/Award Number: 311910

Abstract

Background: To evaluate repeatability and agreement in measurements of total corneal astigmatism (TCA) in keratoconic eyes, using four optical coherence tomography (OCT)-based devices: Anterion, Casia SS-1000, IOLMaster 700, and MS-39.

Methods: Three consecutive measurements were taken with each device in 136 eyes. TCA values were converted into components J_0 and J_{45}. The Anterion and the IOLMaster 700 also provided axial length (AL) measurements. The repeatability was calculated using pooled within-subject standard deviation (S_w). The agreement among the four devices was assessed by pairwise comparisons and Bland–Altman plots.

Results: For all devices, the repeatability of TCA measurements showed $S_w \leq 0.23$ D for TCA magnitude, ≤ 0.14 D for J_0, and ≤ 0.12 D for J_{45}. There were statistically significant differences in TCA magnitude for each pair, except for IOLMaster 700 with MS-39, and Anterion with MS-39. The repeatability (S_w) of axis measurements had a statistically significant negative correlation with the TCA magnitude ($p < 0.001$ for all devices). Both Anterion and IOLMaster 700 had high repeatability in AL measurements (S_w: 0.007 mm for Anterion and 0.009 mm for IOLMaster 700). The difference in AL between the two was 0.015 ± 0.033 mm ($p < 0.001$).

Conclusions: All four devices showed good repeatability in TCA measurements in keratoconic eyes, the agreement for TCA measurements between the tested devices was generally low. Anterion and IOLMaster 700 showed good repeatability and agreement in AL measurements.

KEYWORDS

axial length, keratoconus, optical coherence tomography, total corneal astigmatism

1 | INTRODUCTION

Keratoconus (KC) is characterised by a local corneal biomechanical failure, which results in progressive corneal steepening and thinning that cause optical irregularity leading to decreased visual quality and acuity.[1,2]

Corneal topography and tomography have been the basic diagnostic methods for keratoconus detection,[3] with a recent addition of corneal epithelial mapping[4] and biomechanical assessment.[5,6] KC treatment varies depending on its severity and progression. Mild non-progressive cases are typically only observed and corrected for their refractive error by spectacles or contact lenses. In moderate cases with pronounced irregular optics, hard contact lenses have been used, while the advanced and severe cases that could not be visually managed with scleral contact lenses, corneal transplantation has been required. Since its introduction at the beginning of this century, corneal cross-linking (CXL)[7] has been used to provide biomechanical stabilisation and halt the progression in mild to moderate cases of KC.[8] To improve the eye optics, CXL has often been combined with laser ablation[9] or intracorneal rings,[10] while in stabilised KC, implantation of phakic intraocular lenses (IOL), or refractive exchange of crystalline lens, has been used.[11] Treatments aiming to improve the irregular optics of KC may benefit from a better precision of corneal refractive analysis. Measuring the total corneal astigmatism (TCA) involves the optics of the posterior corneal surface and the corneal thickness, rather than only the anterior corneal surface. TCA can be determined by ray tracing or by utilising real measured data of the anterior and posterior corneal curvatures and corneal thickness.

In KC, where the optics of the posterior corneal surface may be dominant and in cases with previous post-laser vision correction (LVC), the determination of total corneal power (TCP) and TCA are crucial.[12–14] The Simulated Keratometry (SimK), which is based solely on anterior corneal measurements, has been used to assess the corneal optics in most traditional IOL calculations,[15] although lack of data from the posterior cornea has been identified as the most important source of error in toric IOLs calculations.[16,17] Indeed, a study showed that an IOL formula, using direct measurements of both anterior and posterior corneal power, had a higher predictive accuracy for spherical equivalent refractive outcome in LVC cataract surgery, than the regression-based formulas based on the SimK.[18–20] In virgin eyes, the contribution of the posterior corneal astigmatism is not nearly as important as the contribution of the anterior corneal astigmatism.[21] An ever-increasing demand for high precision in refractive predictability in lens exchange procedures relies on the correct power of the implanted IOL, which in turn depends on precise measurements of AL, corneal power, and corneal astigmatism.

Previous studies[22–25] have shown good repeatability and agreement for some of the four devices used in the current study. However, these four devices have not been compared when measuring patients with KC. The current study assesses the repeatability and agreement of TCA measurements of the four current devices: Anterion (Heidelberg Engineering, Heidelberg, Germany), Casia SS-1000 (Tomey Corporation, Nagoya, Aichi, Japan), IOLMaster 700 (Carl Zeiss Meditec, Jena, Germany), and MS-39 (CSO, Firenze, Italy). Two of these devices (Anterion and IOLMaster 700) provide AL measurements as well, within the same examination, and the repeatability and agreement of those measurements were assessed as well.

2 | METHODS

This prospective study included 136 keratoconic eyes of 136 consecutive patients who satisfied our inclusion and exclusion criteria. All examinations were performed between March 2021 and December 2021 at Øyelegesenteret clinic in Tromsø, Norway. Inclusion criteria were: (1) Age ≥16 years; (2) confirmed diagnosis of KC; and (3) TCA ≤8 diopters (D). Exclusion criteria were: (1) History of previous ocular surgery (except CXL); (2) presence of eye diseases (except KC); (3) poor fixation or inability to complete the examination; and (4) use of contact lenses within 2 weeks before the examination day (the period of 2 weeks was considered sufficient since we knew in advance that only the soft- or mini-scleral contact lenses, and no rigid gas permeable lenses, are used in our KC population).

The patients were diagnosed as KC according to the following standard: (1) Topographic maps showing irregular astigmatism with localised steepening on curvature maps and with coinciding protrusion on the elevation maps; (2) corneal tomography showing more pronounced protrusion on the posterior compared with the anterior cornea, and both stromal and epithelial thinning in the area of protrusion.

Refraction, visual acuity, and standard ophthalmological slit lamp examination were performed before the corneal measurements.

The study was approved by the Norwegian Regional Committee for Medical & Health Research Ethics (REK Nord 72 084) and complied with the tenets of the Declaration of Helsinki. All patients provided informed consent for the anonymous use of their data in scientific

analyses and publications, following a detailed explanation of the study.

2.1 | The measurements

Only one eye of each patient who met the inclusion criteria was selected for measurement according to a randomization generated by Microsoft Excel 2019 (Microsoft Corporation, Redmond, WA). Three consecutive measurements were taken with each device and each measurement took about 20 s. All measurements were achieved within 15 min and were performed in an undilated state by the same experienced examiner (YF) between 10 AM and 2 PM.

All the measurements were performed according to the operating instructions for the devices. The measurements with the four devices were obtained in a random order according to a randomised list generated by Microsoft Excel 2019. The subjects were asked to place their chin on the chin rest and press their forehead against the forehead strap, to look at the fixation target of the relevant device, and to blink before each measurement to ensure that the tear film spread out evenly, and to keep their eyes wide open during the measurement. Between each measurement, to ensure that the measurements were independent of one another, the patients were asked to sit back, look away from the fixation light, and blink normally. The measurements were considered acceptable if they satisfied the quality criteria for the devices as defined by the manufacturers.

2.2 | Device description

The specifications of the four devices are shown in Table 1.

2.3 | Anterion

The Anterion SS-OCT (software version 2.5.2) generates images using a laser light source of 1300 nm wavelength to obtain B-scans with an axial resolution of <10 μm and a transversal resolution of 45 μm. The corneal measurements are acquired using the 'Cataract APP' mode of the device, which additionally provides eye biometry data. Sixty-five radial B-scans are performed, with 256 A-scan lines centred on the corneal vertex within a 9 mm diameter. The acquisition time with the Cataract APP is <2 s.

2.4 | Casia SS-1000

The Casia SS-1000 (Tomey, Japan; software version 6Q.2) is also an SS-OCT, using a 1310 nm light source. Its axial and transverse resolution is 10 and 30 μm, respectively. It performs 16 radial scans with 512 A-scan lines centred on the corneal vertex within 10 mm diameter. The device performs 30 000 A-scans per second and uses auto alignment to focus on the examined eye. Acquisition time is about 0.3 s.

2.5 | IOLMaster 700

The IOLMaster 700 (Carl Zeiss Meditec, Jena, Germany) is an SS-OCT device combined with telecentric keratometry. The OCT uses a laser with a tunable wavelength from 1035 to 1080 nm centred on 1055 nm, while the keratometer uses a 950 nm light source. The SS-OCT generates B-scans with an acquisition speed of 2000 A-scans per second and a penetration depth of 44 mm, providing 6-line scans with 22 μm axial resolution. These B-scans are displayed as full-length OCT images showing

TABLE 1 Specifications of the four devices for TCA.

Device	Anterion	Casia SS-1000	IOLMaster 700	MS-39
Light source wavelength (nm)	1300	1310	OCT: 1055; keratometer: 950	OCT: 845; Placido: 635
A-scan speed (scan/s)	50 000	30 000	2000	102 400
Axial resolution (μm)	<10	10	22	3.6
Transverse resolution (μm)	<45	30	24	35
A-scan depth (mm)	14 ± 0.5	6	44	7.5
Maximum Scan width (mm)	16.5	10	6	6
Number of B-scans	65 × 1	16	6 × 3	12 × 5[a]
Number of A-scans per B-scan	256	512	128	1024[b]
Acquisition time (s)	0.33	0.3	1.2	2

Abbreviations: OCT, optical coherence tomography; TCA, total corneal astigmatism.
[a]Customised in this study as recommended by the manufacturer.
[b]1600 A-scan on 16 mm and 800 A-scan on 8 mm.

anatomical details on a longitudinal section through the entire eye. The telecentric keratometer measures 18 points arranged on three rings radially from the corneal centre. The optical axes of the SS-OCT and the keratometer are identical. This ensures that the B-scan passes through the measuring points. The anterior and the posterior corneal curvatures are measured by telecentric keratometry and by the SS-OCT, respectively. Measurements can be done in Auto/Manual mode. In the current study, the auto mode was selected. The Keratometry readings are calculated by analysing the anterior corneal curvature at 18 reference points in hexagonal patterns at 1.5-, 2.5-, and 3.5-mm optical zones. The keratometry readings analysed in the current study were at the 2.5-mm zone.

2.6 | MS-39

The MS-39 (CSO, Firenze, Italy; software Phoenix v.4.1.1.5) combines SD-OCT- and Placido disk imaging technology. A superluminescent diode (SLed) at 845 nm is used as a light source for the OCT, while a SLed at 635 nm is used for Placido disk illumination. The device provides an axial resolution of 3.6 μm, a transversal resolution of 35 μm, and a maximum depth of 7.5 mm. The 'Corneal topography' mode '12 × 5 @10 mm'[26] was used in this study as recommended by the manufacturer, as it provides a higher resolution than the '25 × 1 @16 mm' mode, which has been used in previous studies.[27–29] In the '12 × 5 @10 mm' mode, the measurement consists of 12 radial B-scans repeated five times for each of the 12 meridians, with 800 A-scan lines per B-scan over an 8 mm diameter. The acquisition time is about 2 s.

For the anterior corneal topography, ring edges are detected on the Placido image, providing native curvature data, while the height and slope data are calculated using the arc-step method. Profiles of both the anterior and the posterior cornea are provided from the SD-OCT scans. Data representing the anterior corneal surface are provided by merging the Placido imaging and the SD-OCT, using the manufacturer's proprietary method, while the data for the posterior cornea is derived solely from the SD-OCT.

2.7 | Statistical analysis

The TCA values were measured in a central 3.0 mm zone for all devices except for IOLMaster 700, where we used the values for a 2.5 mm zone. Data were analysed using the statistical package SPSS (IBM SPSS Statistics for Windows, Version 20.0. IBM Corp.). Descriptive statistics were done for continuous variables. Visual inspections of P–P plots and Kolmogorov–Smirnov tests were used to confirm that the data were normally distributed. The level of statistical significance was set at $p < 0.05$.

The TCA values were decomposed into two components by using the following equations[30]:

$$J_0 = \frac{C}{2} \times \cos 2\alpha$$

$$J_{45} = \frac{C}{2} \times \sin 2\alpha$$

where c is the negative cylindrical power and α is the cylindrical axis. J_0 refers to a Jackson cross-cylinder power set orthogonally at 90° and 180° meridians. Positive values of J_0 indicate with-the-rule (WTR) astigmatism, and negative values of J_0 indicate against-the-rule (ATR) astigmatism. J_{45} refers to a Jackson cross-cylinder power set orthogonally at 45° and 135°, representing oblique astigmatism.

To assess the repeatability, we calculated the pooled within-subject standard deviation (S_w) (lower values of S_w indicate better repeatability).[31] The repeatability limit (r), defined as $1.96\sqrt{2} \times S_w$ ($=2.77 \times S_w$), gives the value below which the absolute difference between two measurements of S_w would lie with 0.95 probability.[31,32] The Pearson correlation coefficient was calculated to assess the linear relationship between TCA axis (°) and magnitude.

To assess the agreement, we used the results only from the first measurement obtained by each device, and the following analysis was performed: (1) Differences in TCA magnitude, J_0, and J_{45}; (2) the 95% limits of agreement (LoA), defined as the mean difference for each pair of devices ±1.96 × standard deviations; and (3) pairwise comparisons of TCA measurements with Bonferroni adjustment.

To visualise the differences in the TCA magnitude of each pair of devices, Bland-Altman plots were generated.

To achieve 90% confidence in the estimate for repeatability analysis, we needed a sample size of 96 eyes for three repeated measurements.[33] In this study, we included 136 eyes which gives 91.6% confidence in the estimate.

3 | RESULTS

This study included 136 eyes (OD/OS: 81/55) of 136 patients [41.66 years ±15.15 (SD), range 16–75 years; male/female: 87/49]. According to Amsler-Krumeich KC classification,[34] the 136 eyes included in this study were Grade I: 103 eyes, Grade II: 30 eyes, Grade III: 3 eyes, and Grade IV: 0 eyes.

3.1 | Repeatability

Table 2 shows the S_w and repeatability limit r (2.77*S_w) for the TCA magnitude and its components J_0 and J_{45}. Anterion had the best S_w for TCA magnitude, J_0 and J_{45}, followed by Casia SS-1000, IOLMaster 700 and MS-39.

Table 3 shows the repeatability of the TCA axis (°) and its correlation with TCA magnitude (D). Anterion had the best S_w for TCA axis, followed by IOLMaster 700, MS-39 and Casia SS-1000. All of them had a S_w statistically significant ($p < 0.001$) negative correlation with the TCA magnitude, which means, that as the magnitude increases, the S_w tends to decrease (better repeatability).

3.2 | Agreement

Table 4 shows the mean of TCA measurements of all the 136 eyes obtained by the four devices. Casia SS-1000 had the lowest mean TCA magnitude with 1.52 ± 1.31 D, while IOLMaster 700 had the highest with 2.15 ± 1.81 D. The means of J_{45} values were similar for all four devices, while the mean of J_0 for Anterion and Casia SS-1000 was higher than for IOLMaster 700 and MS-39.

Table 5 shows the agreement of TCA magnitude and the components J_0 and J_{45} for each pair of devices. There were statistically significant differences in TCA magnitude in all pairs except for Anterion versus MS-39 and IOLMaster 700 versus MS-39, but only the difference between Casia SS-1000 and IOLMaster 700 was clinically significant by exceeding 0.50 D (0.631 D, $p = 0.000$). There were no statistically significant differences in TCA components in any pairs except in J_0 for IOLMaster 700 versus Anterion with a mean difference of −0.191 D ($p = 0.000$), and in Anterion versus MS-39 with a mean difference of 0.196 D ($p = 0.004$).

Bland–Altman plots for the agreement in TCA magnitude for all pairs of devices are shown in Figure 1.

3.3 | Axial length

Table 6 shows the repeatability and agreement of AL measurements of Anterion and IOLMaster 700.

Figure 2 shows the Bland–Altman plots for the agreement in AL measurements between Anterion and IOLMaster 700.

4 | DISCUSSION

In this prospective study, we tested the repeatability of TCA measurements in four devices (Table 2) in a group of eyes with KC. This analysis was performed by calculating the pooled within-subject SD (S_w), which represents the level of variability of three consecutive measurements, where lower values of S_w represent better repeatability.

Among the four devices, the Anterion had the best repeatability in measuring TCA magnitude and J_0 and J_{45} components. Previous studies[24,35,36] of TCA measurements in healthy eyes by Anterion reported a S_w for TCA magnitude varying from 0.07 D to 0.13 D, while Shajari et al.[37] reported a S_w of 0.15 D for IOLMaster 700. The worse repeatability in our study is presumably due to our population of KC corneas with irregular corneal optics. Gjerdrum et al.[25] evaluated the repeatability of Anterion and Casia SS-1000 in patients with hyperosmolar ($n = 31$) and normal ($n = 63$) tear film, showing a S_w for TCA mag-

TABLE 3 The repeatability of TCA axis (°) and its correlation with TCA magnitude (D).

Devices	Repeatability S_w	Pearson correlation r	p
Anterion	4.26	−0.491	<0.001
Casia SS-1000	9.23	−0.478	<0.001
IOLMaster 700	7.21	−0.359	<0.001
MS-39	8.73	−0.370	<0.001

Note: TCA, total corneal astigmatism; S_w, pooled within-subject standard deviation; r, the correlation coefficient.

TABLE 2 Repeatability of TCA measurements of the four devices.

	Repeatability, S_w (repeatability limit, r)			
	Anterion	Casia SS-1000	IOLMaster 700	MS-39
TCA magnitude (D)	0.12 (0.34)	0.18 (0.50)	0.19 (0.53)	0.23 (0.64)
J_0 (D)	0.07 (0.20)	0.10 (0.26)	0.10 (0.27)	0.14 (0.39)
J_{45} (D)	0.06 (0.15)	0.10 (0.26)	0.09 (0.25)	0.12 (0.33)

Note: TCA, total corneal astigmatism; S_w, pooled within-subject standard deviation; r (repeatability limit), 2.77 × S_w; J_0, cylinder at 0-degree meridian; J_{45}, cylinder at 45-degree meridian.

TABLE 4 The mean of TCA measurements obtained by each device.

	Mean ± SD			
	Anterion	Casia SS-1000	IOLMaster 700	MS-39
TCA magnitude (D)	1.89 ± 1.52	1.52 ± 1.31	2.15 ± 1.81	1.99 ± 1.73
J_0 (D)	0.258 ± 0.969	0.242 ± 0.916	0.067 ± 1.103	0.062 ± 1.067
J_{45} (D)	0.124 ± 0.677	0.127 ± 0.635	0.131 ± 0.859	0.189 ± 0.753

Abbreviations: SD, standard deviation; TCA, total corneal astigmatism.

nitude varying from 0.15 D to 0.16 D for the Anterion and from 0.18 D to 0.28 D for the Casia. Schiano-Lomoriello et al.[28] assessed the repeatability of MS-39 in KC eyes ($n = 44$), giving a S_w of 0.55 D for TCA magnitude, which is more than twice our results.

Concerning the TCA components J_0 and J_{45}, Piñero et al.[38] found a S_w of 0.09 D for J_0 and 0.07 D for J_{45} in healthy eyes ($n = 35$), using the Cassini system (i-Optics, The Hague, Netherlands, distributed by Ophthec). The Cassini system is a topographer based on the specular reflection of 679 coloured light-emitting diodes (LEDs) to construct topographic maps of the anterior corneal surface and seven additional infrared LEDs to measure the curvature of the posterior corneal surface. Their results with the Cassini showed superior repeatability to ours with MS-39 (S_w: 0.14 D for J_0 and 0.12 D for J_{45}), similar to ours with Casia SS-1000 (S_w: 0.10 D for J_0 and 0.10 D for J_{45}) and IOLMaster 700 (S_w: 0.10 D for J_0 and 0.09 D for J_{45}), but inferior to ours with Anterion (S_w: 0.07 D for J_0 and 0.06 D for J_{45}).

We assessed the repeatability of TCA axis (°) in the four devices. Our results had the best repeatability in Anterion with S_w 4.26° and the worst in Casia SS-1000 with S_w of 9.23°. So far, there are no publications about the repeatability of TCA axis measurements in KC eyes with the current four devices. de Luis Eguileor et al.[39,40] found a S_w range from 7.70° to 11.78° for astigmatism axis in KC eyes using Scheimpflug-based tomographer, Pentacam HR (Oculus; Optikgeräte GmbH, Wetzlar, Germany). Their results were close to ours with Casia SS-1000 (S_w: 9.23°), IOLMaster 700 (S_w: 7.21°), and MS-39 (S_w: 8.73°), while far worse than ours with Anterion. The different findings between the studies may be due to both the precision of the devices and the corneal irregularities of different grades in KC eyes.

We also correlated the repeatability of TCA axis (°) with TCA magnitude (D). We found the repeatability of the TCA axis measurement improved with increasing TCA magnitude across all four devices, possibly because the magnitude dominates the measurement despite irregularities. Similarly, Kanellopoulos and Asimellis,[41] using Cassini in normal eyes, reported that the greater the cylinder magnitude, the better the repeatability of the axis measurements. In our study, Anterion and Casia SS-1000 had a moderate correlation, while, IOLMaster 700 and MS-39 had a weak correlation (Table 3). The low cylinder measurements are generally more likely than high cylinder to be influenced by general noise in the readings, such as tear film surface irregularities,[42] which can obscure the precise detection of the axis.

Regarding the agreement in TCA measurements for any pair of devices in our study, most of them had statistically significant differences in TCA magnitude (Table 5). The mean difference between Casia SS-1000 and IOLMaster 700 was 0.631 D ($p < 0.001$), while the mean difference for the other pairs did not exceed 0.50 D. It should be noted that a difference of 0.50 D in the estimation of corneal power results in an error of IOL power calculations below 0.50 D at the corneal plane, while 0.50 D is the minimum IOL power step provided by most manufacturers.[43] Accordingly, only the TCA magnitude difference between Casia SS-1000 and IOLMaster 700 was clinically significant.

The Bland–Altman plots in Figure 1 showed that the mean difference was smallest between Anterion and MS-39 with 0.099 D ($p = 1.00$, adjusted by multiple comparisons by Bonferroni). However, the 95% LoA range for these two devices was wide, (−2.620, 2.422) D. The narrowest 95% LoA range was for Anterion and Casia SS-1000, (−0.469, 1.217) D. It is interesting to notice from the Bland–Altman plots when comparing MS-39 to any of the other three devices that the distribution of the points becomes much more scattered as their mean value increases (Figure 1C,E,F). This phenomenon was not observed for the other pairs. This might be due to the MS-39's technology, which combines Placido technology with the SD-OCT for the anterior corneal measurement. In addition, from the plots related to the IOLMaster 700 (Figure 1B,D), we can see an apparent bias towards a more negative difference (greater magnitude measured by IOLMaster 700) as the mean increases. We speculate that this might be due to the IOLMaster 700 combining telecentric keratometry and SS-OCT, while the Anterion and Casia SS-1000 utilise only SS-OCT technology. Furthermore, this changing bias could also be partly caused by differences in the diameters used for measurements.

TABLE 5 Agreement of TCA measurements for each pair of devices.

	Anterion vs. Casia SS-1000			Anterion vs. IOLMaster 700			Anterion vs. MS-39		
	Difference			Difference			Difference		
	Mean ± SD	*p*	95% LoA range	Mean ± SD (D)	*p*	95% LoA range	Mean ± SD	*p*	95% LoA range
TCA magnitude (D)	0.374 ± 0.430	0.000	−0.469 to 1.217	−0.258 ± 0.748	0.001	−1.724 to 1.208	−0.099 ± 1.286	1.000	−2.620 to 2.422
J_0 (D)	0.016 ± 1.156	1.000	−2.25 to 2.282	0.191 ± 0.424	0.000	−0.640 to 1.022	0.196 ± 0.653	0.004	−1.084 to 1.476
J_{45} (D)	−0.002 ± 0.786	1.000	−1.543 to 1.539	−0.007 ± 0.336	1.000	−0.666 to 0.652	−0.064 ± 0.658	1.000	−1.356 to 1.228
	Casia SS-1000 vs. IOLMaster 700			Casia SS-1000 vs. MS-39			IOLMaster 700 vs. MS-39		
	Difference			Difference			Difference		
	Mean ± SD	*p*	95% LoA range	Mean ± SD	*p*	95% LoA range	Mean ± SD	*p*	95% LoA range
TCA magnitude (D)	−0.631 ± 0.936	0.000	−2.462 to 1.204	−0.473 ± 1.381	0.001	−3.180 to 2.234	0.158 ± 1.171	0.705	−2.137 to 2.453
J_0 (D)	0.175 ± 1.222	0.584	−2.220 to 2.570	0.180 ± 1.300	0.657	−2.366 to 2.726	0.005 ± 0.574	1.000	−1.120 to 1.130
J_{45} (D)	−0.005 ± 0.927	1.000	−1.822 to 1.812	−0.062 ± 1.018	1.000	−2.057 to 1.933	−0.057 ± 0.735	1.000	−1.498 to 1.384

Note: TCA, total corneal astigmatism; SD, standard deviation; J_0, cylinder at 0-degree meridian; J_{45}, cylinder at 45-degree meridian; *p*, the mean difference is significant at the 0.05 level. Adjustment for multiple comparisons: Bonferroni.

Specifically, the IOLMaster 700 uses a 2.5 mm diameter, whereas the others use 3.0 mm. Therefore, consistent use of the same device is recommended for accurate and reliable monitoring of keratoconus progression.

We also assessed the repeatability and agreement of AL measurements acquired by Anterion and IOLMaster 700. Both devices had very high repeatability with a S_w of 0.007 mm for Anterion and 0.009 mm for IOLMaster 700. The difference in AL between the two was statistically significant (0.015 ± 0.033 mm, $p < 0.001$), but it would be clinically irrelevant and would produce a very negligible difference (less than 0.1 D) in postoperative refractive errors, the AL measured by the two instruments may be used interchangeably for IOL power calculation.[44] Panda et al.[23] reported a difference in AL of −0.02 ± 0.09 mm ($p = 0.001$, $n = 203$) between Anterion and IOLMaster 700. Schiano-Lomoriello et al.[24] found a S_w of 0.01 mm for Anterion, similar to our results. The latter group also compared the AL measured by Anterion and IOLMaster 500 (Carl Zeiss Meditec, Jena, Germany), which is an older generation of optical biometer than the IOLMaster 700 and reported a 95%LoA (−0.06, 0.05) mm for Anterion and IOLMaster 500, which was comparable to our results of 95%LoA (−0.08, 0.05) mm for Anterion and IOLMaster 700.

Differences in the measured diameter (2.5 mm used for IOLMaster 700 and 3.0 mm for the others), may have influenced the results. In our decision between utilising the 2.5 or 3.5 mm diameter for IOLMaster 700 (3.0 mm not being available), we were aware of the recent findings by Alpins et al.[45] advocating for larger zones in keratoconic eyes, but we chose 2.5 mm diameter since it has been widely used in clinical practice, as well as referred in the literature.[46–48] Additionally, Fredriksson et al.,[49] recommended a smaller zone to mitigate the influence of the cone on the measurement.

The eyes in this study had a confirmed keratoconus with 75.7% diagnosed as Grade I. As more corneal irregularities in higher grade KC lead to variable repeatability and agreement, the results in studies with KC eyes may be challenging to interpret.[50] Therefore, even if higher TCA magnitudes may improve repeatability, the presence of more irregularities in severer KC will always reduce the repeatability.[51]

Our study focused on keratoconic eyes, where the typical anterior/posterior curvature ratios observed in regular eyes may not be applicable. Using the ray-tracing type IOL-calculation, used in formulas, such as Okulix[52] and Olsen[53] may give better results since it involve the exact Snell's law and ray-tracing calculated TCA, not relying on any assumptions in the calculation. For more accurate IOL power calculation and astigmatism correction in keratoconic eyes, it is essential to employ

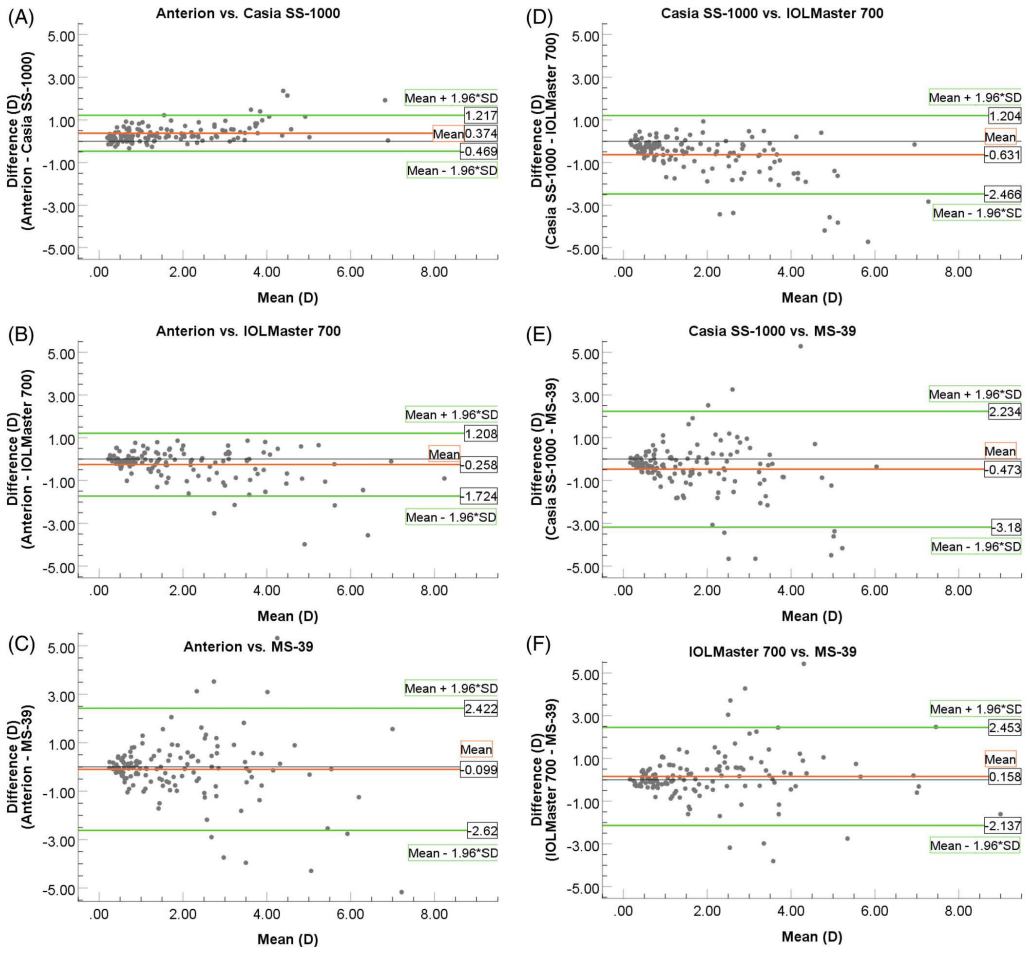

FIGURE 1 Bland–Altman plots showing agreement between total corneal astigmatism magnitude measured by (A) Anterion and Casia SS-1000, (B) Anterion and IOLMaster 700, (C) Anterion and MS-39, (D) Casia SS-1000 and IOLMaster 700, (E) Casia SS-1000 and MS-39, (F) IOLMaster 700 and MS-39. The red lines show the mean differences and the green lines show the lower and upper 95% limit of agreement.

TABLE 6 Repeatability and agreement of AL measurements of Anterion and IOLMaster 700.

			Difference (Anterion—IOLMaster 700)		
	Anterion	**IOLMaster 700**	**Mean ± SD**	***p***	**95% LoA range**
S_w (mm)	0.007	0.009	-	-	-
r (mm)	0.020	0.024	-	-	-
AL (mm)	24.120 ± 1.17	24.135 ± 1.17	−0.015 ± 0.033	<0.001	−0.080 to 0.049

Note: AL, axial length; S_w, pooled within-subject standard deviation; r (repeatability limit), 2.77 × S_w; LoA, limit of agreement; SD, standard deviation.

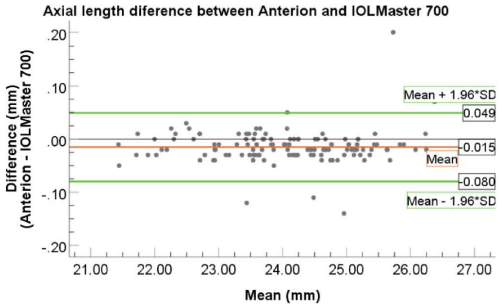

FIGURE 2 Bland–Altman plot showing the means plotted against the differences in axial length between Anterion and IOLMaster 700. The red line shows the mean differences and the green lines show the lower and upper 95% limit of agreement.

keratoconus-specific formulas. In addition to ray-tracing-based formulas, non-ray tracing formulas are used in keratoconic eyes, including the Barrett True-K for keratoconus, the Kane formula for keratoconus, the Holladay II keratoconus mode, the Toric Barrett True-K (for toric IOL), all utilising keratometry measurements. Commonly-used options based on TCP include the Barrett True-K keratoconus formula with total K (TK) for all severities of KC and Emmetropia Verifying Optical (EVO) formula with TK or K in eyes with non-severe disease ($K \leq 50.00$ D).[54] These specialised formulas take into account the unique corneal characteristics associated with keratoconus, providing more accurate and tailored results for IOL power and astigmatism correction. Thus, the use of personalised, device-specific A-constants is crucial to minimise systematic prediction errors.

Limitations of the current study: The cases were not divided into subgroups according to the grade of the KC due to the relatively small sample size. In addition, our sample included a few cases with severe keratoconus, where the quality of measurements is reduced.

4.1 | Conclusions

All four devices had good repeatability in the measurements of TCA in KC eyes, Anterion being the best. The agreement between the tested devices was generally low, and from this we identified two important consequences: a consistent use of the same device for accurate and reliable monitoring of keratoconus progression, and a use of personalised, device-specific A-constants, to minimise systematic prediction errors. We found that the larger the difference in the basic technology between the devices, the more disagreement in the results. For this reason, for the measurements of TCA, the SS-OCT-technology-only devices should not be used interchangeably with SS-OCT combined with telecentric keratometry (Anterion and Casia SS-1000 vs. IOLMaster 700) or with SD-OCT combined with Placido devices (Anterion and Casia SS-1000 vs. MS-39). Furthermore, devices using different hybrid technologies (IOLMaster 700 and MS-39) should not be used interchangeably. For AL measurements, Anterion and IOLMaster 700 had good repeatability and agreement and may be used interchangeably.

CONFLICT OF INTEREST STATEMENT

The authors declare no conflict of interest.

DATA AVAILABILITY STATEMENT

The data that support the findings of this study are available from the corresponding author upon reasonable request.

ORCID

Aleksandar Stojanovic https://orcid.org/0000-0003-1363-4689

REFERENCES

1. Zadnik K, Barr JT, Gordon MO, Edrington TB. Biomicroscopic signs and disease severity in keratoconus. *Cornea*. 1996;15:139-146.
2. Kennedy RH, Bourne WM, Dyer JA. A 48-year clinical and epidemiologic study of keratoconus. *Am J Ophthalmol*. 1986;101:267-273.
3. Naderan M, Jahanrad A, Balali S. Histopathologic findings of keratoconus corneas underwent penetrating keratoplasty according to topographic measurements and keratoconus severity. *Int J Ophthalmol*. 2017;10:1640-1646.
4. Sykakis E, Carley F, Irion L, Denton J, Hillarby MC. An in depth analysis of histopathological characteristics found in keratoconus. *Pathology*. 2012;44:234-239.
5. Andreassen TT, Simonsen AH, Oxlund H. Biomechanical properties of keratoconus and normal corneas. *Exp Eye Res*. 1980;31:435-441.
6. Nash IS, Greene PR, Foster CS. Comparison of mechanical properties of keratoconus and normal corneas. *Exp Eye Res*. 1982;35:413-424.
7. Wollensak G, Spoerl E, Seiler T. Riboflavin/ultraviolet-a-induced collagen crosslinking for the treatment of keratoconus. *Am J Ophthalmol*. 2003;135:620-627.
8. Spörl E, Huhle M, Kasper M, Seiler T. Increased rigidity of the cornea caused by intrastromal cross-linking. *Ophthalmologe*. 1997;94:902-906.
9. Zhang Y, Chen Y. Topography-guided corneal surface laser ablation combined with simultaneous accelerated corneal collagen cross-linking for treatment of keratoconus. *BMC Ophthalmol*. 2021;21:286.
10. Colin J, Cochener B, Savary G, Malet F. Correcting keratoconus with intracorneal rings. *J Cataract Refract Surg*. 2000;26:1117-1122.

11. Yahalomi T, Achiron A, Hecht I, et al. Refractive outcomes of non-toric and toric intraocular lenses in mild, moderate and advanced keratoconus: a systematic review and meta-analysis. *J Clin Med*. 2022;11(9):2456.
12. Marques RE, Guerra PS, Quintas AM, Rodrigues W. Characterization of posterior corneal astigmatism in a population with keratoconus. *Semin Ophthalmol*. 2020;35:352-357.
13. Piñero DP, Nieto JC, Lopez-Miguel A. Characterization of corneal structure in keratoconus. *J Cataract Refract Surg*. 2012;38: 2167-2183.
14. Feizi S, Delfazayebaher S, Javadi MA, Karimian F, Ownagh V, Sadeghpour F. Mean posterior corneal power and astigmatism in normal versus keratoconic eyes. *J Ophthalmic Vis Res*. 2018; 13:93-100.
15. Mendes J, Ribeiro FJ, Ferreira TB. Evaluation of posterior and total corneal astigmatism with colour-LED topography. *Eye*. 2021;35:2585-2593.
16. Savini G, Naeser K. An analysis of the factors influencing the residual refractive astigmatism after cataract surgery with toric intraocular lenses. *Invest Ophthalmol Vis Sci*. 2015;56:827-835.
17. Koch DD, Ali SF, Weikert MP, Shirayama M, Jenkins R, Wang L. Contribution of posterior corneal astigmatism to total corneal astigmatism. *J Cataract Refract Surg*. 2012;38:2080-2087.
18. Huang D, Tang M, Wang L, et al. Optical coherence tomography-based corneal power measurement and intraocular lens power calculation following laser vision correction (an American Ophthalmological Society thesis). *Trans Am Ophthalmol Soc*. 2013;111:34-45.
19. Kenny PI, Kozhaya K, Truong P, Wang L, Koch DD, Weikert MP. Performance of IOL calculation formulas that use measured posterior corneal power in eyes following myopic laser vision correction. *J Cataract Refract Surg*. 2024;50:7-11.
20. Abulafia A, Koch DD, Wang L, et al. New regression formula for toric intraocular lens calculations. *J Cataract Refract Surg*. 2016;42:663-671.
21. Balparda K, Maya-Naranjo MI, Mesa-Mesa S, Herrera-Chalarca T. Corneal and whole-eye higher order aberrations do not correlate with ocular residual astigmatism in prepresbyopic refractive surgery candidates. *Cornea*. 2023;42(7):867-873. doi: 10.1097/ICO.0000000000003160
22. Oh R, Oh JY, Choi HJ, Kim MK, Yoon CH. Comparison of ocular biometric measurements in patients with cataract using three swept-source optical coherence tomography devices. *BMC Ophthalmol*. 2021;21:62.
23. Panda A, Nanda A, Sahoo K. Comparison of ocular biometry and refractive outcome between ANTERION and IOL Master 700. *Indian J Ophthalmol*. 2022;70:1594-1598.
24. Schiano-Lomoriello D, Hoffer KJ, Abicca I, Savini G. Repeatability of automated measurements by a new anterior segment optical coherence tomographer and biometer and agreement with standard devices. *Sci Rep*. 2021;11:983.
25. Gjerdrum B, Gundersen KG, Lundmark PO, Aakre BM. Repeatability of OCT-based versus Scheimpflug- and reflection-based keratometry in patients with hyperosmolar and normal tear film. *Clin Ophthalmol*. 2020;14:3991-4003.
26. Feng Y, Reinstein DZ, Nitter T, et al. Epithelial thickness mapping in keratoconic corneas: repeatability and agreement between CSO MS-39, Heidelberg Anterion, and Optovue Avanti OCT devices. *J Refract Surg*. 2023;39:474-480.
27. Vega-Estrada A, Mimouni M, Espla E, Alió Del Barrio J, Alio JL. Corneal epithelial thickness intrasubject repeatability and its relation with visual limitation in keratoconus. *Am J Ophthalmol*. 2019;200:255-262.
28. Schiano-Lomoriello D, Bono V, Abicca I, Savini G. Repeatability of anterior segment measurements by optical coherence tomography combined with Placido disk corneal topography in eyes with keratoconus. *Sci Rep*. 2020;10:1124.
29. Savini G, Schiano-Lomoriello D, Hoffer KJ. Repeatability of automatic measurements by a new anterior segment optical coherence tomographer combined with Placido topography and agreement with 2 Scheimpflug cameras. *J Cataract Refract Surg*. 2018;44:471-478.
30. Thibos LN, Horner D. Power vector analysis of the optical outcome of refractive surgery. *J Cataract Refract Surg*. 2001;27: 80-85.
31. Bland JM, Altman DG. Measurement error. *BMJ*. 1996;313:744.
32. McAlinden C, Khadka J, Pesudovs K. Statistical methods for conducting agreement (comparison of clinical tests) and precision (repeatability or reproducibility) studies in optometry and ophthalmology. *Ophthalmic Physiol Opt*. 2011;31:330-338.
33. McAlinden C, Khadka J, Pesudovs K. Precision (repeatability and reproducibility) studies and sample-size calculation. *J Cataract Refract Surg*. 2015;41:2598-2604.
34. Amsler M. Classic keratocene and crude keratocene; unitary arguments. *Ophthalmologica*. 1946;111:96-101.
35. Tañá-Rivero P, Aguilar-Córcoles S, Ruiz-Mesa R, Montés-Micó R. Repeatability of whole-cornea measurements using a new swept-source optical coherence tomographer. *Eur J Ophthalmol*. 2021;31:1709-1719.
36. Cheng SM, Zhang JS, Shao X, et al. Repeatability of a new swept-source optical coherence tomographer and agreement with other three optical biometers. *Graefe's Arch Clin Exp Ophthalmol*. 2022;260:2271-2281.
37. Shajari M, Sonntag R, Ramsauer M, et al. Evaluation of total corneal power measurements with a new optical biometer. *J Cataract Refract Surg*. 2020;46:675-681.
38. Piñero DP, Molina-Martín A, Camps VJ, de Fez D, Caballero MT. Validation of corneal topographic and aberrometric measurements obtained by color light-emitting diode reflection topography in healthy eyes. *Graefe's Arch Clin Exp Ophthalmol*. 2019;257:2437-2447.
39. de Luis EB, Arriola-Villalobos P, Pijoan Zubizarreta JI, et al. Multicentre study: reliability and repeatability of Scheimpflug system measurement in keratoconus. *Br J Ophthalmol*. 2021; 105:22-26.
40. de Luis EB, Argaluza JE, Zubizarreta JIP, Carro AS, Ecenarro JE. Evaluation of the reliability and repeatability of scheimpflug system measurement in keratoconus. *Cornea*. 2018;37:177-181.
41. Kanellopoulos AJ, Asimellis G. Distribution and repeatability of corneal astigmatism measurements (magnitude and axis) evaluated with color light emitting diode reflection topography. *Cornea*. 2015;34:937-944.
42. Kanellopoulos AJ, Asimellis G. Forme fruste keratoconus imaging and validation via novel multi-spot reflection topography. *Case Rep Ophthalmol*. 2013;4:199-209.
43. Piñero DP, Camps VJ, Mateo V, Ruiz-Fortes P. Clinical validation of an algorithm to correct the error in the keratometric

estimation of corneal power in normal eyes. *J Cataract Refract Surg*. 2012;38:1333-1338.
44. Eibschitz-Tsimhoni M, Tsimhoni O, Archer SM, Del Monte MA. Effect of axial length and keratometry measurement error on intraocular lens implant power prediction formulas in pediatric patients. *J AAPOS*. 2008;12:173-176.
45. Alpins N, Ong JK, Stamatelatos G. New method of quantifying corneal topographic astigmatism that corresponds with manifest refractive cylinder. *J Cataract Refract Surg*. 2012;38:1978-1988.
46. Ma S, Gao R, Sun J, et al. Comparison of two swept-source optical coherence tomography devices, a Scheimpflug camera system and a ray-tracing aberrometer in the measurement of corneal power in patients with cataract. *Graefes Arch Clin Exp Ophthalmol*. 2023;262:1567-1578.
47. Salouti R, Kamalipour A, Masihpour N, et al. Effect of photorefractive keratectomy on agreement of anterior segment variables obtained by a swept-source biometer vs a Scheimpflug-based tomographer. *J Cataract Refract Surg*. 2020;46:1229-1235.
48. Sorkin N, Zadok T, Barrett GD, Chasid O, Abulafia A. Comparison of biometry measurements and intraocular lens power prediction between 2 SS-OCT-based biometers. *J Cataract Refract Surg*. 2023;49:460-466.
49. Fredriksson A, Behndig A. Measurement centration and zone diameter in anterior, posterior and total corneal astigmatism in keratoconus. *Acta Ophthalmol*. 2017;95:826-833.
50. Feng Y, Reinstein DZ, Nitter T, et al. Heidelberg Anterion swept-source OCT corneal epithelial thickness mapping: repeatability and agreement with Optovue Avanti. *J Refract Surg*. 2022;38:356-363.
51. Jack J, Kanski BB, Nischal KK, Pearson A. *Clinical Ophthalmology: A Systematic Approach*. Elsevier; 2011.
52. Ghoreyshi M, Khalilian A, Peyman M, Mohammadinia M, Peyman A. Comparison of OKULIX ray-tracing software with SRK-T and Hoffer-Q formula in intraocular lens power calculation. *J Curr Ophthalmol*. 2018;30:63-67.
53. Savini G, Taroni L, Hoffer KJ. Recent developments in intraocular lens power calculation methods-update 2020. *Ann Transl Med*. 2020;8:1553.
54. Heath MT, Mulpuri L, Kimiagarov E, et al. Intraocular lens power calculations in keratoconus eyes comparing keratometry, total keratometry, and newer formulae. *Am J Ophthalmol*. 2023;253:206-214.

How to cite this article: Feng Y, Nitter T, Bertelsen G, Stojanovic A. Repeatability and agreement of total corneal astigmatism measured in keratoconic eyes using four current devices. *Clin Exp Ophthalmol*. 2024;1-11. doi:10.1111/ceo.14423

Paper 2

Heidelberg Anterion Swept-Source OCT Corneal Epithelial Thickness Mapping: Repeatability and Agreement with Optovue Avanti

Heidelberg Anterion Swept-Source OCT Corneal Epithelial Thickness Mapping: Repeatability and Agreement With Optovue Avanti

Yue Feng, MSc, MD; Dan Z. Reinstein, MD, DABO, FRCOphth; Tore Nitter, MD, PhD; Timothy J. Archer, MA(Oxon) DipCompSci (Cantab), PhD; Colm McAlinden, MD, PhD, FRCOphth; Xiangjun Chen, MD, PhD; Geir Bertelsen, MD, PhD; Tor Paaske Utheim, MD, PhD; Aleksandar Stojanovic, MD, PhD

ABSTRACT

PURPOSE: To assess the repeatability of corneal epithelial thickness mapping in virgin, post-laser refractive surgery (PLRS), and keratoconic eyes using a novel swept-source optical coherence tomographer (SS-OCT), and to determine the agreement of the measurements with a validated spectral-domain (SD) OCT.

METHODS: Analysis of 90 virgin, 46 PLRS, and 122 keratoconic eyes was performed. Three consecutive measurements of each eye were acquired with the Anterion SS-OCT and Avanti SD-OCT devices, and averages of the epithelial thickness mapping were calculated in the central 2-mm zone and in the 2- to 5-mm and 5- to 7-mm diameter rings. The repeatability was analyzed using pooled within-subject standard deviation (S_w). The agreement was assessed by Bland-Altman analysis and paired *t* tests.

RESULTS: The repeatability ranges of the Anterion and Avanti epithelial thickness mapping measurements were S_w: 0.60 to 1.36 µm and S_w: 0.75 to 1.96 µm, respectively. The 95% limits of agreement of the Anterion and Avanti were 0.826 to 8.297. All values of the thickness measurements with the Anterion were lower than those of the Avanti, with the mean differences being 4.06 ± 1.81, 3.26 ± 2.52, and 3.68 ± 2.51 µm in virgin, PLRS, and keratoconic eyes, respectively ($P < .001$ for all).

CONCLUSIONS: The repeatability of the Anterion's epithelial thickness mapping was higher than that of the Avanti. In terms of the agreement between the Anterion and Avanti, the epithelium measured by the Anterion was always thinner than that of the Avanti, making their interchangeable use unsuitable without corrections.

[*J Refract Surg*. 2022;38(6):356-363.]

As its first cellular layer and refractive medium, the corneal epithelium has an important role in the refractive system of the eye. Being highly reactive to irregularities in the underlying stroma, it is always attempting to smooth the ocular surface by growing thicker over depressions and becoming thinner over bumps, a phenomenon described as epithelial remodeling.[1] This way, the epithelium regularizes the corneal optics and, in most cases, leads to less corneal astigmatism, less change of asphericity, and fewer higher order

From Institute of Community Medicine, Faculty of Health Sciences, University in Tromsø, Norway (YF, GB); London Vision Clinic, London, United Kingdom (DZR, TJA); the Department of Ophthalmology, Royal Gwent Hospital, Aneurin Bevan University Health Board, Newport, United Kingdom (CM); the Department of Ophthalmology, Arendal Hospital, Arendal, Norway (XC, TPU); the Department of Ophthalmology, Vestre Viken Hospital Trust, Drammen, Norway (XC); the Department of Ophthalmology, University Hospital North Norway, Tromsø, Norway (GB, AS); the Department of Ophthalmology, Oslo University Hospital, Oslo, Norway (TPU); the Department of Medical Biochemistry, Oslo University Hospital, Oslo, Norway (TPU); and Institute of Clinical Medicine, Faculty of Health Sciences, University in Tromsø, Tromsø, Norway (AS).

Submitted: November 26, 2021; Accepted: April 13, 2022

Disclosure: Dr. Reinstein is a consultant for Carl Zeiss Meditec AG and CSO Italia and has a proprietary interest in the Artemis Insight 100 technology (ArcScan, Inc), including patents administered by the Cornell Center for Technology Enterprise and Commercialization, Ithaca, New York. The remaining authors have no financial or proprietary interest in the materials presented herein.

Correspondence: Aleksandar Stojanovic, MD, PhD, Department of Ophthalmology, University Hospital North Norway, Sykehusveien 38, 9019 Tromsø, Norway. Email: aleks@online.no

doi:10.3928/1081597X-20220414-01

aberrations in both virgin and irregular corneas and as in eyes after refractive surgery,[2,3] compared to the same parameters measured on the stromal surface. The epithelium also decreases the refractive power of the eye by simply increasing the corneal radius of curvature by its thickness.[4] On the other hand, due to the effect of eyelid blinking mechanics, a slightly non-uniform epithelial thickness profile is induced.[5]

Epithelial thickness mapping (ETM) has recently become an indispensable tool in corneal and refractive surgery. It has contributed to the early diagnosis of keratoconus[1,6,7] and subsequently increased the safety of refractive surgery.[8,9] It is also valuable for therapeutic refractive surgery to help further understand irregular astigmatism.[10] ETM was pioneered by Reinstein et al, who were the first to measure[5] and map[11] the corneal epithelium across the whole cornea.[12] They also described the epithelial behavior[1,13-16] after corneal laser refractive surgery[17] and in keratoconus,[1,18] and were the first to use the term "epithelial remodeling."

Reinstein et al also introduced clinically applicable ETM using very high-frequency (VHF) digital ultrasound scanning (Artemis Insight 100; ArcScan, Inc) as early as 1994.[11] ETM based on optical coherence tomography (OCT) appeared in 2011. It did not surpass the former in terms of precision, but due to its ease of use, it became the most prevalent technology in current clinical practice. The first commercially available OCT-based instrument that provided 6-mm diameter epithelial mapping was the Optovue RT-100 (Optovue, Inc), featuring spectral-domain (SD) OCT technology, otherwise mainly used for the posterior segment diagnostics. SD-OCT technology has since been used for ETM on several devices, of which the Avanti (Optovue, Inc) is currently the most prevalent one.[19]

Swept-source (SS) OCT technology with a longer wavelength light source was introduced to allow a greater image depth and high-contrast imaging of the entire anterior segment.[20] The Anterion (Heidelberg Engineering) is a recently introduced, high-resolution anterior segment OCT device featuring SS-OCT technology.[21] However, the manufacturers of both the Anterion and the Casia2 (Tomey Corporation), another anterior segment OCT featuring SS-OCT technology, have yet to release their instruments' ETM capabilities commercially. The current study is the first to measure and analyze the ETM using SS-OCT technology, employing the Anterion's investigational software.

The purpose of this study was to assess the repeatability of ETM measurements with the Anterion across the central 7-mm diameter of the cornea and its agreement with the Avanti SD-OCT for healthy virgin, post-laser refractive surgery (PLRS), and keratoconic eyes. In addition, we analyzed the spatial variations in ETM with the two devices. By using the Avanti as the reference device in this study, we also assessed its repeatability, which previously has been reported only scarcely.[22]

PATIENTS AND METHODS

Ninety virgin eyes of 90 consecutive patients who were candidates for elective laser vision correction or cataract surgery (virgin eyes) and 46 eyes of 45 patients with a history of previous laser refractive surgery (PLRS eyes) were examined at Øyelegesenteret Eye Clinic (Tromsø, Norway), whereas 122 eyes of 118 patients with diagnosed keratoconus (keratoconic eyes) were examined at the Department of Ophthalmology of the University Hospital North Norway. In the virgin eyes, only one eye of each patient was used to avoid statistical bias. In the PLRS and keratoconic groups, we used both eyes from 1 and 4 patients, respectively, because there was a large difference between these patients' 2 eyes. All examinations were performed between March 2020 and February 2021. This was a prospective study approved by the Norwegian Regional Committee for Medical & Health Research Ethics (REK Nord 72084) and it complied with the tenets of the Declaration of Helsinki. All patients provided informed consent for the anonymous use of their data in scientific analyses and publications, following a detailed explanation of the study.

Inclusion criteria were age 18 years or older and healthy virgin corneas for the virgin eyes; age 18 years and older and previous corneal laser vision surgery (both myopic and hyperopic treated eyes) at least 3 months before the examination[23] for the PLRS eyes; and age 16 years or older and a diagnosis of keratoconus and spherical equivalent of myopia of 8.00 diopters (D) or less for the keratoconic eyes. Exclusion criteria were a history of other previous ocular surgery (except for PLRS eyes); patients with pterygium or other conjunctival, limbal, or corneal disease (except for keratoconus); poor fixation or inability to complete the examination; and use of hard contact lenses.

Age, sex, and personal and family history of eye diseases were recorded. Refraction, visual acuity, standard ophthalmological examination with the slit-lamp examination and funduscopy were performed before ETM measurements.

ETM Measurements

The sequence of the ETM measurements with the two devices was randomized. Three consecutive measurements were taken with each device. For both devices, each single measurement lasted approximately 20 seconds, including computer processing, and hanging from one device to the other took less than 10 min-

utes. All examinations were taken by the same experienced examiner (YF) between 10 AM and 2 PM.

The patients were asked to fixate on the device's fixation target to achieve a coaxial position with the infrared camera and the corneal vertex. For each measurement, the examiner centered the scan on the corneal vertex by adjusting the joystick until a bright vertical flare line was seen at the center of the real-time OCT image. Patients were instructed to blink immediately before each measurement to ensure that the tear film would be spread out evenly, and to keep their eyes wide open during the measurement. Patients were then asked to sit back and look away from the fixation light between the measurements. No eye drops were applied during testing.

ANTERION

The Anterion SS-OCT generates images using a laser light source with a 1,300-nm wavelength to obtain B-scans with an axial resolution of less than 10 µm and a transversal resolution of 45 µm. An active eye-tracker is used. The software version 1.2.2 with activated investigational epithelium feature provides corneal ETM and various derived statistics. The ETMs are acquired quickest using the "Cornea APP" mode on the device, but the same data are also acquired with the "Cataract APP" mode; both perform 65 radial scans with 256 A-scan lines centered on the corneal vertex over a 7-mm diameter. Acquisition time with the Cornea APP is less than 1 second.

After the acquisition, the instrument presents ETM, displaying mean thicknesses at 41 points, evenly distributed across the map, but the user may measure the epithelium thickness at any given point on the map by pointing the mouse. For comparison with the Avanti, we calculated averages of the same 17 zones/rings/sections that are used by Avanti, shown in **Figure A** (available in the online version of this article). Measurements from the 7- to 9-mm diameter ring on the Avanti were not used in this study. The technical specifications of the device are summarized in **Table A** (available in the online version of this article).

AVANTI

The Avanti SD-OCT operates using a super luminescent diode light source at a wavelength of 840 nm. It obtains B-scans with an axial resolution of 5 µm and a transversal resolution of 15 µm. It does not use an eye-tracker. Corneal thickness mapping and ETM are produced using the "pachymetry wide scan pattern" mode and attaching the "long adaptor lens" to the instrument (software v. 6.11.0.12). The ETM measurement consists of eight radial scans at 22.5-degree intervals repeated five times for each meridian, with 1,024 A-scan lines over a 9-mm diameter. Acquisition time is 0.58 second.

ETM and corneal pachymetry maps are generated by an automatic algorithm and divided into a total of 25 sections over a 9-mm diameter: a central 2-mm diameter zone and eight sections equally distributed (superior, superior temporal, temporal, inferior temporal, inferior, inferior nasal, nasal, and superior nasal) within three annular rings (2- to 5-, 5- to 7-, and 7- to 9-mm) (**Figure A**). Only the mean epithelial thickness of each section is presented. Only high-quality images centered at the corneal vertex, with complete coverage and free of motion artifacts, were accepted for analysis. The technical specifications of the device are summarized in **Table A**.

STATISTICAL ANALYSIS

We used vertically mirrored symmetry superimposition: thickness values for left eyes were reflected in the vertical axis and superimposed onto the right eye values so that the nasal/temporal characteristics could be combined.[16]

To assess the repeatability, we calculated pooled within-subject standard deviation (S_w) (lower values of S_w indicate higher repeatability).[24,25] The repeatability limit (r) defined as $1.96 \sqrt{2} \times S_w$ (= $2.77 \times S_w$) gives the value below which the absolute difference between two measurements would lie with 0.95 probability.[26]

To assess the agreement, we calculated the following parameters: difference in thickness readings (a positive difference indicates a thinner epithelium in the Anterion), 95% limits of agreement (LoA = mean ± 1.96 × standard deviation, and paired two-tailed *t* tests.

The Bland-Altman plot was added to visualize the agreement between the devices.

Data were entered into Microsoft Excel 2016 (Microsoft Corporation) and then imported into a statistical software (SPSS v25; IBM Corporation). A *P* value of less than .05 was considered to be statistically significant.

RESULTS

This study evaluated 258 eyes of 253 patients for both repeatability and agreement analyses. The demographic data are displayed in **Table 1**.

REPEATABILITY

The repeatability of the measurements (expressed as S_w) were calculated in the central 2-mm zone and in the 2- to 5-mm and 5- to 7-mm diameter rings with results displayed in **Table 2** for the three groups of eyes. The repeatability of all 17 sections is shown in **Table B** (available in the online version of this article). S_w ranges for the Anterion were 0.64 to 1.01 µm in virgin eyes, 0.60 to 1.36 µm in PLRS eyes, and 1.15 to 1.36

TABLE 1
Demographic Data

Parameter	Total (n = 258)	Virgin (n = 90)	PLRS (n = 46)	KC (n = 122)
Age (year)				
Mean ± SD	42.00 ± 15.51	48.77 ± 16.83	48.25 ± 13.41	34.53 ± 11.36
Range	16 to 76	18 to 76	21 to 72	16 to 75
Sex				
Male	173	46	29	98
Female	80	44	16	20
Eye				
Right	173	67	31	75
Left	85	23	15	47
Postop time (year)				
Mean ± SD	–	–	6.27 ± 6.51	–
Range	–	–	0.25 to 19.83	–

KC = keratoconus; PLRS = post-laser refraction surgery; postop = postoperative; SD = standard deviation

µm in keratoconic eyes. For the Avanti, S_w ranges were 0.98 to 1.11 µm in virgin eyes, 1.37 to 1.96 µm in PLRS eyes, and 1.37 to 1.60 µm in keratoconic eyes.

Agreement Between Anterion and Avanti Measurements

The mean difference in thickness (Avanti minus Anterion), 95% LoA, and paired, two-tailed *t* tests *P* values in the central 2-mm zone and the 2- to 5-mm and 5- to 7-mm diameter rings are displayed in **Table 3** for the three groups. The Anterion showed significantly thinner mean epithelium than the Avanti in all measured areas in all groups of eyes, with a mean difference ranging from 2.66 to 4.35 µm. The difference between the devices was most pronounced in the 2- to 5-mm ring in all three groups of eyes. If we look at the individual eyes, the Anterion measured the central 2-mm zone epithelium thickness thinner than the Avanti in 100% of virgin eyes, 93.48% (43 of 46 eyes) of PLRS eyes, and 87.70% (107 of 122 eyes) of keratoconic eyes.

In all of the 17 sections, the mean difference (Avanti minus Anterion), 95% LoA, and paired, two-tailed *t* tests *P* values are shown in **Table C** (available in the online version of this article). The mean ETM for each of the 17 sections for both Anterion and Avanti, and a map for the difference between the two devices in virgin, PLRS, and keratoconic eyes, are shown in **Figures B-D**, respectively.

Bland-Altman plots for the agreement between the epithelial thickness measured by the Anterion and Avanti for virgin, PLRS, and keratoconic eyes are shown in **Figures E-F**, respectively. The mean difference in epithelial thickness was larger in the virgin eyes than in the other two groups of eyes, whereas the range of 95% LoA was wider in the PLRS and keratoconic eyes than in the virgin eyes. Both the mean difference and the 95% LoA increased from the center to the periphery in all three groups. The epithelial thickness differences in the rings, as well as in the opposite corneal sections in the three groups of eyes, are shown in **Table 4**.

TABLE 2
Repeatability of ETM Measurements

Group	Repeatability, Sw (Repeatability Limit, r) Anterion	Avanti
Virgin		
Zone 0 to 2 mm	0.64 (1.77)	0.98 (2.72)
Ring 2 to 5 mm	0.79 (2.18)	1.14 (3.15)
Ring 5 to 7 mm	1.01 (2.80)	1.11 (3.08)
Area 0 to 7 mm	0.88 (2.44)	1.12 (3.10)
PLRS		
Zone 0 to 2 mm	0.60 (1.67)	0.75 (2.06)
Ring 2 to 5 mm	0.84 (2.33)	1.40 (3.88)
Ring 5 to 7 mm	1.36 (3.77)	1.96 (5.42)
Area 0 to 7 mm	1.08 (2.99)	1.62 (4.49)
KC		
Zone 0 to 2 mm	1.15 (3.19)	1.37 (3.78)
Ring 2 to 5 mm	1.18 (3.26)	1.45 (4.02)
Ring 5 to 7 mm	1.36 (3.76)	1.60 (4.44)
Area 0 to 7 mm	1.26 (3.49)	1.52 (4.21)
All		
Zone 0 to 2 mm	0.91 (2.52)	1.15 (3.19)
Ring 2 to 5 mm	1.00 (2.77)	1.34 (3.71)
Ring 5 to 7 mm	1.26 (3.49)	1.53 (4.24)
Area 0 to 7 mm	1.12 (3.10)	1.42 (3.39)

ETM = epithelial thickness mapping; KC= keratoconus; PLRS = post-laser refractive surgery
The Anterion is manufactured by Heidelberg Engineering and the Avanti is manufactured by Optovue.

DISCUSSION

The current study investigated for the first time the epithelial thickness mapping obtained by any SS-OCT–based instrument, notwithstanding a recent article[27] reporting ETM measured by the MS-39 (CSO), which is an SD-OCT device, erroneously described as SS-OCT.

The repeatability of the Heidelberg Anterion SS-OCT in the three groups of eyes (virgin, PLRS, and keratoconic) was good, and higher compared to the traditional SD-OCT (the Avanti), whereas the Anterion's

TABLE 3

Agreement of ETM Measurements Between the Two Devices

	Mean ± SD (µm)		Difference		95% LoA (µm)	
Group	Anterion	Avanti	Mean ± SD (µm)	*P*	Lower	Upper
Virgin						
Zone 0 to 2 mm	51.59 ± 3.27	55.60 ± 3.26	4.02 ± 1.38	< .001	1.307	6.73
Ring 2 to 5 mm	50.93 ± 3.31	55.28 ± 3.25	4.35 ± 1.73	< .001	0.95	7.75
Ring 5 to 7 mm	50.56 ± 3.70	54.34 ± 3.44	3.78 ± 1.93	< .001	-0.001	7.554
Area 0 to 7 mm	50.80 ± 3.49	54.86 ± 3.34	4.06 ± 1.81	< .001	0.523	7.598
PLRS						
Zone 0 to 2 mm	53.79 ± 6.07	56.96 ± 5.87	3.17 ± 1.99	< .001	-0.736	7.069
Ring 2 to 5 mm	54.05 ± 5.68	57.85 ± 5.45	3.80 ± 2.18	< .001	-0.475	8.071
Ring 5 to 7 mm	54.77 ± 6.53	57.50 ± 5.71	2.73 ± 2.93	< .001	-3.002	8.468
Area 0 to 7 mm	54.37 ± 6.10	57.63 ± 5.60	3.26 ± 2.52	< .001	-1.679	8.199
KC						
Zone 0 to 2 mm	50.49 ± 5.69	53.15 ± 5.61	2.66 ± 2.12	< .001	-1.501	6.829
Ring 2 to 5 mm	51.16 ± 4.90	55.12 ± 4.79	3.96 ± 2.14	< .001	-0.237	8.157
Ring 5 to 7 mm	52.55 ± 5.00	56.07 ± 4.36	3.52 ± 2.94	< .001	-2.238	9.273
Area 0 to 7 mm	51.78 ± 5.00	55.45 ± 4.64	3.68 ± 2.51	< .001	-1.253	8.604
All						
Zone 0 to 2 mm	51.46 ± 5.18	54.69 ± 5.19	3.23 ± 1.96	< .001	-0.62	7.07
Ring 2 to 5 mm	51.60 ± 4.86	55.66 ± 4.68	4.07 ± 2.04	< .001	0.075	8.059
Ring 5 to 7 mm	52.25 ± 5.15	55.72 ± 4.52	3.47 ± 2.66	< .001	-1.751	8.689
Area 0 to 7 mm	51.90 ± 5.02	55.63 ± 4.63	3.74 ± 2.33	< .001	-0.826	8.297

ETM = epithelial thickness mapping; KC = keratoconus; LoA = limits of agreement; PLRS = post-laser refractive surgery; SD = standard deviation
The Anterion is manufactured by Heidelberg Engineering and the Avanti is manufactured by Optovue.

TABLE 4

ETM Measurement Differences in the Rings and in the Opposite Sections for Both Devices

	Virgin				PLRS				KC			
	Anterion		Avanti		Anterion		Avanti		Anterion		Avanti	
Parameter	Mean ± SD (µm)	*P*	Mean ± SD (µm)	*P*	Mean ± SD (µm)	*P*	Mean ± SD (µm)	P	Mean ± SD (µm)	*P*	Mean ± SD (µm)	*P*
S-I	-4.08 ± 3.24	< .001	-3.16 ± 2.65	< .001	-3.76 ± 5.81	< .001	-3.40 ± 5.69	< .001	-0.43 ± 5.57	.230	-0.76 ± 5.04	.019
T-N	-0.36 ± 2.13	.024	-0.71 ± 1.86	< .001	0.35 ± 4.84	.492	0.10 ± 4.03	0.816	-1.76 ± 5.58	< .001	-1.93 ± 4.53	< .001
ST-IN	-3.1.0 ± 2.67	< .001	-2.93 ± 2.28	< .001	-1.93 ± 4.68	< .001	-1.67 ± 4.55	0.001	-0.57 ± 4.90	.069	-1.05 ± 4.06	< .001
SN-IT	-2.42 ± 3.15	< .001	-1.99 ± 2.53	< .001	-1.96 ± 5.39	.001	-1.93 ± 5.02	< .001	2.02 ± 6.42	< .001	1.55 ± 5.16	< .001
Center-Outer	1.02 ± 2.36	0.007	1.27 ± 2.19	.001	-0.98 ± 4.65	.342	-0.55 ± 4.11	.549	-2.06 ± 5.30	< .001	-2.92 ± 2.55	< .001
Inner-Outer	0.37 ± 2.06	< .001	0.96 ± 1.94	< .001	-0.73 ± 6.75	.041	0.34 ± 5.49	.231	-1.39 ± 4.73	< .001	-0.95 ± 4.13	< .001

Center = central 2 mm; ETM = epithelial thickness mapping; I = inferior; IN = inferior nasal; Inner = 2- to 5-mm diameter ring; IT = inferior temporal; KC = keratoconus; N = nasal; Outer = 5- to 7-mm diameter ring; PLRS = post-laser refractive surgery; S = superior; SN = superior nasal; ST = superior temporal; T = temporal
The Anterion is manufactured by Heidelberg Engineering and the Avanti is manufactured by Optovue.

measurements of the mean epithelial thickness in all 17 sections of all three groups of eyes were lower than the Avanti's.

The first ETM measurements by Reinstein et al[28] with the Artemis VHF digital ultrasound in 1994 showed an S_w of 0.58 µm at the corneal vertex, and 0.43 to 1.36 µm

in 90% of locations within the central 6-mm diameter after five consecutive measurements of 10 eyes of 10 patients 1 year after laser in situ keratomileusis.[28] Their S_w is similar to what we measured with the Anterion (0.60 to 1.36 µm) but lower (ie, higher repeatability) than what we measured with the Avanti (0.75 to 1.96 µm) in the PLRS eyes within the 7-mm diameter. However, repeatability should also be considered in the context of the measurement resolution of the device; VHF digital ultrasound can measure the epithelial thickness with less than 1 µm resolution, whereas OCT devices have a resolution of closer to approximately 5 µm for the Avanti and 8 µm for the Anterion. Therefore, although repeatability may be comparable, it could be expected that the accuracy of OCT devices might be lower than VHF digital ultrasound.

Although introduced 17 years later than the Artemis, ETM in virgin eyes measured by SD-OCT Optovue RT-100 showed an S_w as high as 0.70 µm within the central 2-mm zone and 0.7 to 0.9 µm in the paracentral ring (4 to 6 mm).[29] This is similar to what we obtained in virgin eyes with the Anterion (S_w: 0.64 to 1.01 µm), but lower than what we obtained with Avanti (S_w: 0.98 to 1.14 µm) for the central 2-mm zone and the outer 5- to 7-mm ring.

Sedaghat et al[22] calculated the repeatability of ETM with the Avanti within the 7-mm zone of 52 eyes before and after photorefractive keratectomy, and found an S_w of 1.73 µm preoperatively and 4.50 µm 6 months postoperatively. Within the 7 mm zone, our data showed a lower S_w (ie, higher repeatability) than theirs in our PLRS eyes obtained with both the Anterion (S_w: 0.60 to 1.36 µm) and Avanti (S_w: 0.75 to 1.96 µm). Even if we included all eyes, our data showed that the S_w of the Avanti (1.34 µm) was lower than that reported by Sedaghat et al (1.73 µm).

Using the MS-39 SD-OCT, Vega-Estrada et al[30] found in the central 3-mm zone an S_w of 1.24 µm in virgin eyes and an S_w of 2.03 µm in keratoconic eyes, whereas we, in the central 2-mm zone, found an S_w of 0.64 µm in virgin eyes and an S_w of 0.98 µm in keratoconic eyes with the Anterion and an S_w of 1.18 µm in virgin eyes and an S_w of 1.37 µm in keratoconic eyes with the Avanti. **Table D** (available in the online version of this article) summarizes the literature findings of the repeatability of ETM measurements in other studies.

We assume that 65 radial scans used by the Anterion versus eight radial scans used by Avanti, as well as the Anterion's eye-tracking ability, are the likely factors explaining the Anterion's better repeatability compared to the Avanti's.

Using VHF ultrasound, Reinstein et al[14,31,32] reported central epithelial thickness of 53.4 ± 4.6 µm in virgin eyes[32] and 45.7 ± 5.9 µm in eyes with keratoconus.[31] These measurements excluded the pre-corneal tear film thickness, whereas our measurements of the central epithelial thickness in virgin eyes with the Avanti that include the tear film[22] showed 55.60 ± 3.26 µm and the Anterion showed only 51.59 ± 3.27 µm. The manufacturer of the Anterior is neither claiming nor denying the inclusion of the tear film (Sandro Gunkel, Heidelberg Engineering, personal communication, November 19, 2021).

In both virgin and PLRS eyes, both devices measured a thicker epithelium inferiorly than superiorly (**Table 4** and **Figures B-C**), similar to other investigators.[22,31,33,34] In keratoconic eyes, both devices measured a thinner epithelium inferiorly than superiorly, and the differences in thickness between the superior and inferior sections were greater than for the other two groups of eyes (**Table 4**). In keratoconic eyes, the thinnest part of the epithelium, measured by both devices, was located in the inferior temporal section within the 2- to 5-mm ring (**Figure D**), which is also consistent with other researchers.[31,35]

Concerning the agreement between the Anterion and the Avanti, the mean epithelial thickness for all sections in all three groups of eyes was significantly different: 3.74 ± 2.33 µm ($P < .001$). We also calculated the agreement for each of the 17 sections (**Table C**) and showed maps of the difference between the measured thicknesses of the two devices in all three groups of eyes (**Figures B-D**), and we found a close correlation with respect to the thickness distribution. This close correlation results in registering similar recognizable ETM patterns that are important in the diagnosis of pathologic conditions in clinical practice. However, because one of the main applications for epithelial thickness measurement is keratoconus screening, where the thicknesses need to be measured on a scale of a few microns, the precise difference between the two devices must be known if their interchangeability is considered.

The Anterion and Avanti use their own proprietary methods for their respective segmentation algorithms. According to Heidelberg Engineering, their segmentation is looking for the highest intensity of the anterior surface, which can provide the ability to reliably find the underlying structure in a repeatable way (Sandro Gunkel, Heidelberg Engineering, personal communication, November 19, 2021). Because the axial resolution of the Anterion is limited to approximately 8 µm, the tear film cannot really be imaged/resolved, and that is why it is uncertain whether the tear film is included in the Anterion's OCT measurements. The Avanti has an axial resolution of approximately 5 µm and its ETM measurements include the tear film.[22]

Both the Anterion and Avanti use Fourier domain detection, but they feature different imaging wavelengths and bandwidths, whereas the Anterion uses a tunable

swept laser light source (center wavelength of 1,300 nm),[36,37] The Avanti uses broadband near-infrared super luminescent diode as its light source (center wavelength of 840 nm). This results in different lateral resolution (10 × 45 µm for the Anterion and 5 × 15 µm for the Avanti), which presumably leads to different performance. Both technologies record an interference spectrum that carries the information of the sample, but SS-OCT features a light source that sweeps the wavelength in time and SD-OCT uses a spectrometer for wavelength separation. SS-OCT imaging features a denser scan pattern, due to its higher acquisition speed, and a larger scan depth and area, due to the use of a longer wavelength and reduced sensitivity roll-off. Hence, SS-OCT may quickly acquire the images of the whole anterior segment,[36] whereas SD-OCT provides higher contrast and resolution within a shorter depth range. In addition, the Anterion features real-time eye-tracking during the acquisition of multiple B-scans, which allows precise alignment and enhanced detail imaging.[21] It appears that multiple factors may influence the repeatability of a device, such as axial resolution, image contrast and penetration rate, tracking, scanning speed, and scanning density (lateral resolution/data points). So, just by looking at the technical specifications, one cannot decide which device is superior, which emphasizes the importance of real-world clinical evaluation studies.

Although our study included a total of 258 eyes, we still did not have a sufficient sample size for our PLRS eyes to divide them according to the type of treated refractive error. Furthermore, we did not separately consider patients with other conditions such as dry eye disease and epithelial basement membrane dystrophy. Such considerations should be a subject for future studies.

We found that the repeatability of the ETM measurements with the Anterion SS-OCT was higher than with the Avanti SD-OCT in virgin, PLRS, and keratoconic corneas. However, the mean epithelial thickness measurements of the Anterion were always thinner than the Avanti's, something that must be considered if the devices are to be used interchangeably.

AUTHOR CONTRIBUTIONS

Study concept and design (XC, TPU, AS); data collection (YF); analysis and interpretation of data (YF, DZR, TN, TJA, CM, GB, AS); writing the manuscript (YF); critical revision of the manuscript (DZR, TN, TJA, CM, XC, GB, TPU, AS); statistical expertise (DZR, TN, TJA, CM, GB); supervision (XC, GB, TPU, AS)

REFERENCES

1. Reinstein DZ, Archer TJ, Gobbe M. Corneal epithelial thickness profile in the diagnosis of keratoconus. *J Refract Surg.* 2009; 25(7):604-610.
2. Zhou W, Reinstein DZ, Archer TJ, Chen X, Utheim TP, Feng Y, Stojanovic A. Intraoperative swept-source OCT-based corneal topography for measurement and analysis of stromal surface after epithelial removal. J Refract Surg. 2021, 37(7):484-492.
3. Reinstein DZ, Silverman RH, Sutton HF, Coleman DJ. Very high-frequency ultrasound corneal analysis identifies anatomic correlates of optical complications of lamellar refractive surgery: anatomic diagnosis in lamellar surgery. *Ophthalmology.* 1999;106(3):474-482. https://doi.org/10.1016/S0161-6420(99)90105-7 PMID:10080202
4. Simon G, Ren Q, Kervick GN, Parel JM. Optics of the corneal epithelium. *Refract Corneal Surg.* 1993;9(1):42-50. https://doi.org/10.3928/1081-597X-19930101-10 PMID:8481372
5. Reinstein DZ, Silverman RH, Coleman DJ. High-frequency ultrasound measurement of the thickness of the corneal epithelium. *Refract Corneal Surg.* 1993;9(5):385-387. https://doi.org/10.3928/1081-597X-19930901-12 PMID:8241045
6. Silverman RH, Urs R, RoyChoudhury A, Archer TJ, Gobbe M, Reinstein DZ. Combined tomography and epithelial thickness mapping for diagnosis of keratoconus. *Eur J Ophthalmol.* 2017;27(2):129-134. https://doi.org/10.5301/ejo.5000850 PMID:27515569
7. Reinstein DZ, Archer TJ, Urs R, Gobbe M, RoyChoudhury A, Silverman RH. Detection of keratoconus in clinically and algorithmically topographically normal fellow eyes using epithelial thickness analysis. J Refract Surg. 2015, 31(11):736-744.
8. Salomão MQ, Hofling-Lima AL, Lopes BT, et al. Role of the corneal epithelium measurements in keratorefractive surgery. *Curr Opin Ophthalmol.* 2017;28(4):326-336. https://doi.org/10.1097/ICU.0000000000000379 PMID:28399067
9. Khamar P, Rao K, Wadia K, et al. Advanced epithelial mapping for refractive surgery. *Indian J Ophthalmol.* 2020;68(12):2819-2830. https://doi.org/10.4103/ijo.IJO_2399_20 PMID:33229657
10. Reinstein DZ, Archer TJ, Dickeson ZI, Gobbe M. Transepithelial phototherapeutic keratectomy protocol for treating irregular astigmatism based on population epithelial thickness measurements by artemis very high-frequency digital ultrasound. *J Refract Surg.* 2014;30(6):380-387. https://doi.org/10.3928/1081597X-20140508-01
11. Reinstein DZ, Silverman RH, Trokel SL, Coleman DJ. Corneal pachymetric topography. *Ophthalmology.* 1994;101(3):432-438. https://doi.org/10.1016/S0161-6420(94)31314-5 PMID:8127563
12. Reinstein DZ, Silverman RH, Raevsky T, et al. Arc-scanning very high-frequency digital ultrasound for 3D pachymetric mapping of the corneal epithelium and stroma in laser in situ keratomileusis. J Refract Surg. 2000, 16(4):414-430. https://doi.org/10.3928/1081-597X-20000701-04
13. Reinstein DZ, Srivannaboon S, Gobbe M, et al. Epithelial thickness profile changes induced by myopic LASIK as measured by Artemis very high-frequency digital ultrasound. J Refract Surg. 2009, 25(5):444-450.
14. Reinstein DZ, Archer TJ, Gobbe M, Silverman RH, Coleman DJ. Epithelial thickness after hyperopic LASIK: three-dimensional display with Artemis very high-frequency digital ultrasound. J Refract Surg. 2010, 26(8):555-564. https://doi.org/10.3928/1081597X-20091105-02
15. Rocha KM, Perez-Straziota CE, Stulting RD, Randleman JB. SD-OCT analysis of regional epithelial thickness profiles in keratoconus, postoperative corneal ectasia, and normal eyes. *J Refract Surg.* 2013;29(3):173-179. https://doi.org/10.3928/1081597X-20130129-08 PMID:23446013
16. Zhou W, Stojanovic A. Comparison of corneal epithelial and stromal thickness distributions between eyes with keratoconus and healthy eyes with corneal astigmatism ≥ 2.0 D. *PLoS One.* 2014;9(1):e85994. https://doi.org/10.1371/journal.

pone.0085994 PMID:24489687

17. Huang D, Tang M, Shekhar R. Mathematical model of corneal surface smoothing after laser refractive surgery. *Am J Ophthalmol.* 2003;135(3):267-278. https://doi.org/10.1016/S0002-9394(02)01942-6 PMID:12614741
18. Silverman RH, Urs R, Roychoudhury A, Archer TJ, Gobbe M, Reinstein DZ. Epithelial remodeling as basis for machine-based identification of keratoconus. *Invest Ophthalmol Vis Sci.* 2014;55(3):1580-1587. https://doi.org/10.1167/iovs.13-12578 PMID:24557351
19. Reinstein DZ, Yap TE, Archer TJ, Gobbe M, Silverman RH. Comparison of corneal epithelial thickness measurement between fourier-domain OCT and very high-frequency digital ultrasound. *J Refract Surg.* 2015;31(7):438-445. https://doi.org/10.3928/1081597X-20150623-01
20. Shoji T, Kato N, Ishikawa S, et al. In vivo crystalline lens measurements with novel swept-source optical coherent tomography: an investigation on variability of measurement. *BMJ Open Ophthalmol.* 2017;1(1):e000058. https://doi.org/10.1136/bmjophth-2016-000058 PMID:29354706
21. Asam JSPM, Polzer M, Tafreshi A, Hirnschall N, Findl O. Anterior segment OCT. In: Bille JF, ed. *High Resolution Imaging in Microscopy and Ophthalmology: New Frontiers in Biomedical Optics.* Springer; 2019:285-298. https://doi.org/10.1007/978-3-030-16638-0_13
22. Sedaghat MR, Momeni-Moghaddam H, Gazanchian M, et al. Corneal epithelial thickness mapping after photorefractive keratectomy for myopia. *J Refract Surg.* 2019;35(10):632-641. https://doi.org/10.3928/1081597X-20190826-03
23. Reinstein DZ, Archer TJ, Gobbe M. Change in epithelial thickness profile 24 hours and longitudinally for 1 year after myopic LASIK: three-dimensional display with Artemis very high-frequency digital ultrasound. *J Refract Surg.* 2012;28(3):195-201. https://doi.org/10.3928/1081597X-20120127-02 PMID:22301100
24. Bland JM, Altman DG. Measurement error. *BMJ.* 1996;313(7059):744. https://doi.org/10.1136/bmj.313.7059.744 PMID:8819450
25. Schiano-Lomoriello D, Hoffer KJ, Abicca I, Savini G. Repeatability of automated measurements by a new anterior segment optical coherence tomographer and biometer and agreement with standard devices. *Sci Rep.* 2021;11(1):983. https://doi.org/10.1038/s41598-020-79674-4 PMID:33441703
26. McAlinden C, Khadka J, Pesudovs K. Statistical methods for conducting agreement (comparison of clinical tests) and precision (repeatability or reproducibility) studies in optometry and ophthalmology. *Ophthalmic & Physiological Optics.* 2011;31(4):330-338.
27. Georgeon C, Marciano I, Cuyaubère R, Sandali O, Bouheraoua N, Borderie V. Corneal and epithelial thickness mapping: comparison of swept-source- and spectral-domain-optical coherence tomography. *J Ophthalmol.* 2021;2021:3444083. https://doi.org/10.1155/2021/3444083 PMID:34650817
28. Reinstein DZ, Archer TJ, Gobbe M, Silverman RH, Coleman DJ. Repeatability of layered corneal pachymetry with the artemis very high-frequency digital ultrasound arc-scanner. *J Refract Surg.* 2010;26(9):646-659. https://doi.org/10.3928/1081597X-20091105-01 PMID:19928698
29. Ma XJ, Wang L, Koch DD. Repeatability of corneal epithelial thickness measurements using Fourier-domain optical coherence tomography in normal and post-LASIK eyes. *Cornea.* 2013;32(12):1544-1548. https://doi.org/10.1097/ICO.0b013e3182a7f39d PMID:24145634
30. Vega-Estrada A, Mimouni M, Espla E, Alió Del Barrio J, Alio JL. Corneal epithelial thickness intrasubject repeatability and its relation with visual limitation in keratoconus. *Am J Ophthalmol.* 2019;200:255-262. https://doi.org/10.1016/j.ajo.2019.01.015 PMID:30689987
31. Reinstein DZ, Gobbe M, Archer TJ, Silverman RH, Coleman DJ. Epithelial, stromal, and total corneal thickness in keratoconus: three-dimensional display with artemis very-high frequency digital ultrasound. *J Refract Surg.* 2010;26(4):259-271. https://doi.org/10.3928/1081597X-20100218-01
32. Reinstein DZ, Archer TJ, Gobbe M, Silverman RH, Coleman DJ. Epithelial thickness in the normal cornea: three-dimensional display with Artemis very high-frequency digital ultrasound. *J Refract Surg.* 2008;24(6):571-581.
33. Erie JC, Patel SV, McLaren JW, et al. Effect of myopic laser in situ keratomileusis on epithelial and stromal thickness: a confocal microscopy study. *Ophthalmology.* 2002;109(8):1447-1452. https://doi.org/10.1016/S0161-6420(02)01106-5 PMID:12153794
34. Patel SV, Erie JC, McLaren JW, Bourne WM. Confocal microscopy changes in epithelial and stromal thickness up to 7 years after LASIK and photorefractive keratectomy for myopia. *J Refract Surg.* 2007;23(4):385-392. https://doi.org/10.3928/1081-597X-20070401-11
35. Li Y, Tan O, Brass R, Weiss JL, Huang D. Corneal epithelial thickness mapping by Fourier-domain optical coherence tomography in normal and keratoconic eyes. *Ophthalmology.* 2012;119(12):2425-2433. https://doi.org/10.1016/j.ophtha.2012.06.023 PMID:22917888
36. Aumann S, Donner S, Fischer J, Müller F. Optical coherence tomography (OCT): principle and technical realization. In: Bille JF, ed. *High Resolution Imaging in Microscopy and Ophthalmology: New Frontiers in Biomedical Optics.* Springer; 2019:59-85.
37. Potsaid B, Baumann B, Huang D, et al. Ultrahigh speed 1050nm swept source/Fourier domain OCT retinal and anterior segment imaging at 100,000 to 400,000 axial scans per second. *Opt Express.* 2010;18(19):20029-20048. https://doi.org/10.1364/OE.18.020029 PMID:20940894

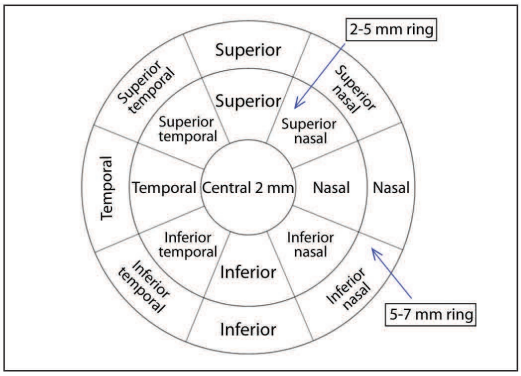

Figure A. 17 sections and two rings used in the analysis of the measurements.

TABLE A

Specifications of the OCT Devices for ETM

Device	Anterion	Avanti
Light source wavelength (nm)	1,300	840
A-scan speed (Hz)	50,000	70,000
Axial resolution (μm)	< 10	5
Transverse resolution (μm)	< 45	15
A-scan depth (mm)	14 ± 0.5	3
Maximum scan width (mm)	16.5	12
B-scan	65 × 1	8 × 5
No. of A-scans per B-scan	256	1,024

ETM = epithelial thickness mapping; OCT = optical coherence tomography
The Anterion is manufactured by Heidelberg Engineering and the Avanti is manufactured by Optovue.

TABLE B

Repeatability of ETM Measurements of All 17 Sections

	Repeatability, S_w (Repeatability Limit, r)							
	Virgin		PLRS		KC		All	
Parameter	Anterion	Avanti	Anterion	Avanti	Anterion	Avanti	Anterion	Avanti
Zone 0 to 2 mm								
Central	0.64 (1.77)	0.98 (2.72)	0.60 (1.67)	0.75 (2.06)	1.15 (3.19)	1.37 (3.78)	0.91 (2.52)	1.15 (3.19)
Ring 2 to 5 mm								
Nasal	0.73 (2.03)	1.08 (2.99)	0.85 (2.35)	1.48 (4.10)	1.23 (3.42)	1.32 (3.64)	1.02 (2.83)	1.27 (3.52)
Superior nasal	0.81 (2.24)	1.18 (3.26)	0.96 (2.65)	1.49 (4.12)	1.14 (3.16)	1.28 (3.56)	1.00 (2.77)	1.28 (3.55)
Superior	0.89 (2.46)	1.18 (3.26)	0.81 (2.25)	1.36 (3.76)	1.29 (3.56)	1.32 (3.65)	1.09 (3.02)	1.27 (3.52)
Superior temporal	0.86 (2.37)	1.19 (3.30)	0.79 (2.19)	1.43 (3.97)	1.00 (2.76)	1.72 (4.77)	0.91 (2.52)	1.51 (4.18)
Temporal	0.73 (2.03)	1.14 (3.16)	0.87 (2.41)	1.41 (3.91)	1.06 (2.95)	1.78 (4.94)	0.93 (2.58)	1.52 (4.21)
Inferior temporal	0.81 (2.25)	1.13 (3.12)	0.85 (2.35)	1.49 (4.11)	1.16 (3.21)	1.71 (4.74)	1.00 (2.77)	1.49 (4.13)
Inferior	0.76 (2.11)	1.13 (3.14)	0.82 (2.28)	1.07 (2.97)	1.24 (3.44)	1.37 (3.80)	1.03 (2.85)	1.24 (3.43)
Inferior nasal	0.69 (1.91)	1.08 (2.98)	0.77 (2.14)	1.49 (4.13)	1.28 (3.56)	1.10 (3.06)	1.03 (2.85)	1.17 (3.24)
Ring 2 to 5 mm total	0.79 (2.18)	1.14 (3.15)	0.84 (2.33)	1.40 (3.88)	1.18 (3.26)	1.45 (4.02)	1.00 (2.77)	1.34 (3.71)
Ring 5 to 7 mm								
Nasal	0.96 (2.65)	1.03 (2.84)	1.57 (4.36)	2.40 (6.66)	1.30 (3.61)	1.72 (4.75)	1.25 (3.46)	1.67 (4.63)
Superior nasal	1.11 (3.08)	1.25 (3.46)	1.43 (3.97)	1.97 (5.44)	1.37 (3.80)	1.90 (5.27)	1.31 (3.63)	1.72 (4.76)
Superior	1.01 (2.80)	1.27 (3.53)	2.05 (5.68)	1.70 (4.70)	1.50 (4.15)	1.99 (5.50)	1.47 (4.07)	1.71 (4.74)
Superior temporal	1.11 (3.07)	1.13 (3.14)	1.22 (3.39)	1.77 (4.89)	1.11 (3.07)	1.60 (4.42)	1.13 (3.13)	1.49 (4.13)
Temporal	1.03 (2.85)	1.10 (3.05)	1.27 (3.52)	1.95 (5.40)	1.20 (3.33)	1.50 (4.16)	1.16 (3.21)	1.47 (4.07)
Inferior temporal	0.99 (2.74)	0.96 (2.66)	1.07 (2.96)	1.93 (5.34)	1.37 (3.79)	1.56 (4.33)	1.20 (3.32)	1.46 (4.04)
Inferior	1.02 (2.83)	1.20 (3.32)	1.15 (3.18)	1.74 (4.83)	1.76 (4.89)	1.50 (4.16)	1.44 (3.99)	1.45 (4.02)
Inferior nasal	0.86 (2.39)	0.94 (2.60)	1.13 (3.13)	2.20 (6.08)	1.24 (3.44)	1.04 (2.88)	1.10 (3.05)	1.29 (3.57)
Ring 5 to 7 mm total	1.01 (2.80)	1.11 (3.08)	1.36 (3.77)	1.96 (5.42)	1.36 (3.76)	1.60 (4.44)	1.26 (3.49)	1.53 (4.24)

ETM = epithelial thickness mapping; KC = keratoconus; PLRS = post-laser refractive surgery; Repeatability limit = 2.77 × S_w; S_w = pooled within-subject standard deviation

TABLE C

Agreement of ETM Measurements Between the Two Devices in All 17 Sections

	Virgin				PLRS				KC				All			
	Difference		95% LoA (µm)		Difference		95% LoA (µm)		Difference		95% LoA (µm)		Difference		95% LoA (µm)	
Parameter	Mean ± SD (µm)	*P*	Lower	Upper	Mean ± SD (µm)	*P*	Lower	Upper	Mean ± SD (µm)	*P*	Lower	Upper	Mean ± SD (µm)	*P*	Lower	Upper
Zone 0 to 2 mm																
Central	4.02 ± 1.38	< .001	1.307	6.73	3.17 ± 1.99	< .001	-0.736	7.069	2.66 ± 2.12	< .001	-1.501	6.829	3.23 ± 1.96	< .001	-0.62	7.07
Ring 2 to 5 mm																
Nasal	4.43 ± 1.58	< .001	1.331	7.536	4.01 ± 2.23	< .001	-0.358	8.387	3.68 ± 2.07	< .001	-0.367	7.733	4.00 ± 1.97	< .001	0.15	7.86
Superior nasal	4.43 ± 1.63	< .001	1.239	7.62	3.75 ± 2.27	< .001	-0.698	8.191	3.87 ± 2.00	< .001	-0.047	7.79	4.04 ± 1.94	< .001	0.23	7.86
Superior	4.77 ± 1.75	< .001	1.335	8.213	3.95 ± 2.01	< .001	0.012	7.886	4.08 ± 2.15	< .001	-0.124	8.293	4.30 ± 2.02	< .001	0.35	8.25
Superior temporal	4.43 ± 1.58	< .001	1.337	7.53	3.85 ± 1.99	< .001	-0.062	7.757	3.61 ± 2.13	< .001	-0.563	7.793	3.94 ± 1.96	< .001	0.10	7.78
Temporal	4.22 ± 1.45	< .001	1.37	7.067	3.95 ± 2.04	< .001	-0.04	7.939	3.57 ± 2.04	< .001	-0.44	7.576	3.86 ± 1.87	< .001	0.19	7.54
Inferior temporal	4.04 ± 1.86	< .001	0.393	7.688	3.60 ± 2.32	< .001	-0.956	8.158	4.46 ± 2.66	< .001	-0.747	9.676	4.16 ± 2.36	< .001	-0.47	8.79
Inferior	4.29 ± 2.03	< .001	0.304	8.267	3.54 ± 2.25	< .001	-0.877	7.949	4.41 ± 2.13	< .001	0.245	8.575	4.21 ± 2.13	< .001	0.03	8.39
Inferior nasal	4.18 ± 1.99	< .001	0.287	8.076	3.74 ± 2.33	< .001	-0.818	8.297	3.98 ± 1.96	< .001	0.15	7.817	4.01 ± 2.03	< .001	0.02	8
Ring 2 to 5 mm total	4.35 ± 1.73	< .001	0.95	7.75	3.80 ± 2.18	< .001	-0.475	8.071	3.96 ± 2.14	< .001	-0.237	8.157	4.07 ± 2.04	< .001	0.075	8.059
Ring 5-7 mm																
Nasal	3.76 ± 1.79	< .001	0.255	7.263	2.80 ± 2.05	< .001	-1.222	6.831	3.34 ± 3.43	< .001	-3.38	10.05	3.39 ± 2.74	< .001	-1.97	8.75
Superior nasal	3.78 ± 2.05	< .001	-0.239	7.794	2.32 ± 3.10	< .001	-3.759	8.396	3.17 ± 3.43	< .001	-3.547	9.88	3.23 ± 2.99	< .001	-2.62	9.08
Superior	4.46 ± 2.31	< .001	-0.067	8.993	3.04 ± 3.28	< .001	-3.388	9.46	3.62 ± 2.88	< .001	-2.027	9.27	3.81 ± 2.81	< .001	-1.70	9.32
Superior temporal	3.94 ± 1.87	< .001	0.273	7.609	3.30 ± 3.28	< .001	-3.131	9.725	3.43 ± 2.59	< .001	-1.658	8.51	3.58 ± 2.52	< .001	-1.35	8.52
Temporal	3.28 ± 1.62	< .001	0.102	6.461	2.37 ± 3.35	< .001	-4.203	8.942	3.12 ± 2.31	< .001	-1.404	7.64	3.04 ± 2.34	< .001	-1.55	7.63
Inferior temporal	3.30 ± 1.75	< .001	-0.131	6.738	2.43 ± 2.91	< .001	-3.269	8.124	3.51 ± 2.99	< .001	-2.361	9.37	3.24 ± 2.63	< .001	-1.91	8.4
Inferior	3.83 ± 1.87	< .001	0.165	7.502	2.72 ± 2.01	< .001	-1.229	6.664	3.95 ± 2.86	< .001	-1.643	9.55	3.69 ± 2.44	< .001	-1.10	8.48
Inferior nasal	3.86 ± 2.15	< .001	-0.364	8.075	2.89 ± 3.42	< .001	-3.815	9.598	4.01 ± 3.01	< .001	-1.883	9.91	3.76 ± 2.84	< .001	-1.81	9.33
Ring 5-7 mm total	3.78 ± 1.93	< .001	-0.001	7.554	2.73 ± 2.93	< .001	-3.002	8.468	3.52 ± 2.94	< .001	-2.238	9.273	3.47 ± 2.66	.001	-1.75	8.689

ETM = epithelial thickness mapping; KC = keratoconus; LoA = limits of agreement; PLRS = post-laser refractive surgery; SD = standard deviation

TABLE D

Repeatability of ETM Measurements Reported by Previous Investigators

	Repeatability, Sw (Repeatability Limit, r) (μm)				
Authors	**Virgin**	**PLRS**	**KC**	**Diameter**	**Instrument Used**
Reinstein et al[29]	–	0.58 (1.61)	–	Corneal vertex	VHF-ultrasound Artemis
	–	0.43 to 1.36 (1.19 to 3.77)	Central 6 mm	–	–
Ma et al[22]	0.70 (1.94)	–	–	Central 2 mm	Optovue RT-100 SD-OCT
	0.7 to 0.9 (1.94 to 2.49)	–	–	4 to 6 mm	–
Sedaghat et al[23]	1.73 (4.79)	4.50 (12.47)	–	Central 7 mm	Avanti SD-OCT
Vega-Estrada et al[30]	1.24 (3.43)	–	2.03 (5.62)	Central 3 mm	MS 39 SD-OCT

ETM = epithelial thickness mapping; KC = keratoconus; OCT = optical coherence tomography; PLRS = post-laser refractive surgery; Repeatability limit = 2.77 × S_w; S_w = pooled within-subject standard deviation

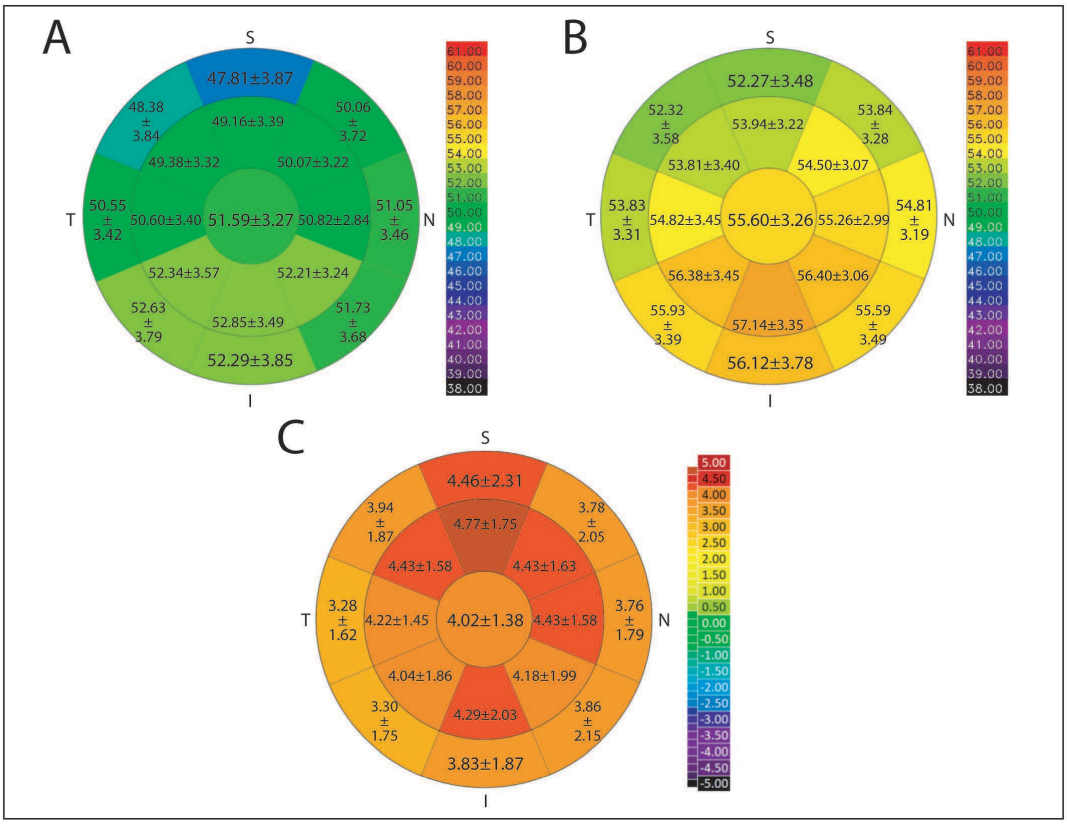

Figure B. Mean epithelial thickness mapping for the (A) Anterion (Heidelberg Engineering) and (B) Avanti (Optovue, Inc) between the two devices in virgin eyes over the central 7-mm diameter. N = nasal; S = superior; T = temporal; I = inferior; Unit: μm

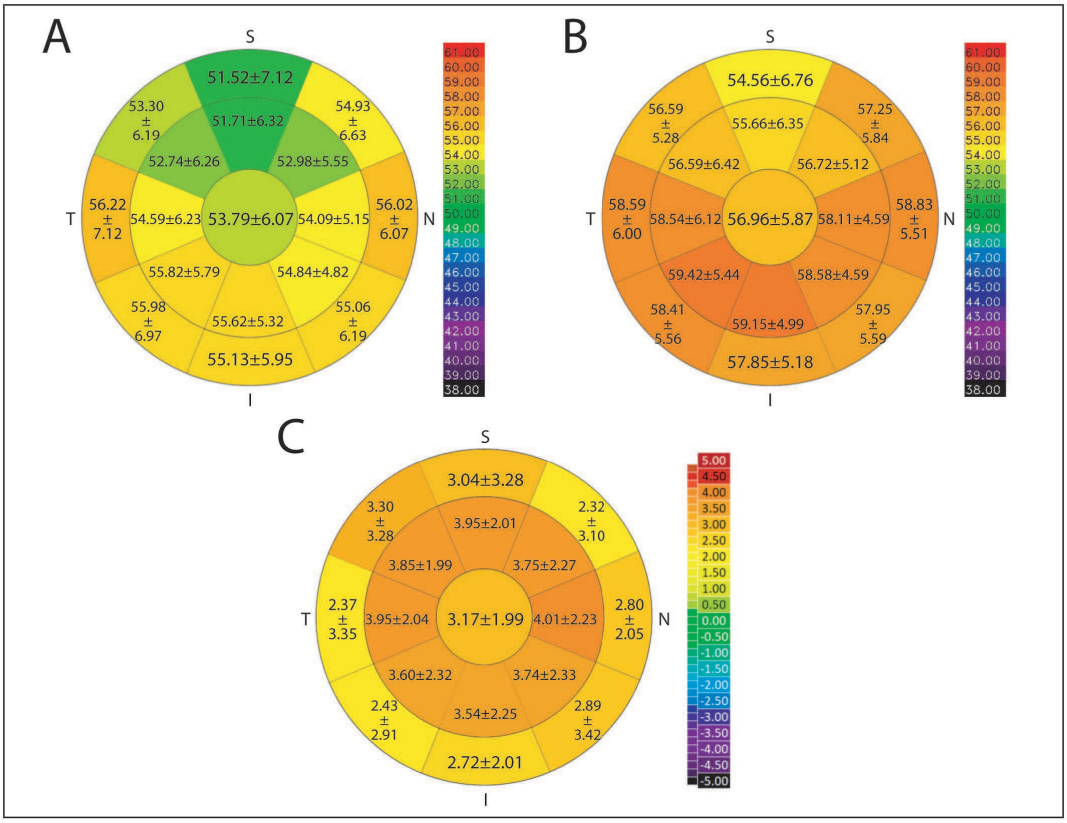

Figure C. Average epithelial thickness mapping for the (A) Anterion (Heidelberg Engineering) and (B) Avanti (Optovue, Inc) between the two devices in post-laser refractive surgery eyes over the central 7-mm diameter. N = nasal; S = superior; T = temporal; I = inferior; Unit: μm

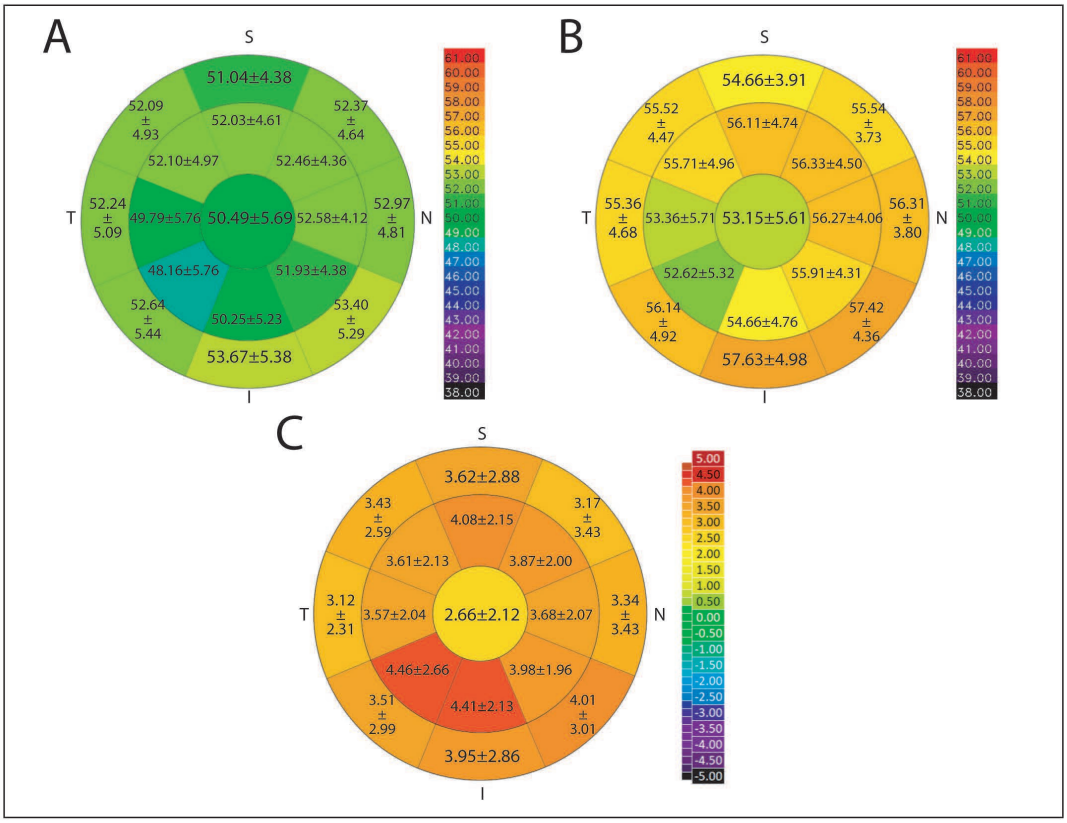

Figure D. Average epithelial thickness mapping for the (A) Anterion (Heidelberg Engineering) and (B) Avanti (Optovue, Inc), and differential mapping (C) between the two devices in keratoconic eyes over the central 7-mm diameter. N = nasal; S = superior; T = temporal; I = inferior; Unit: μm

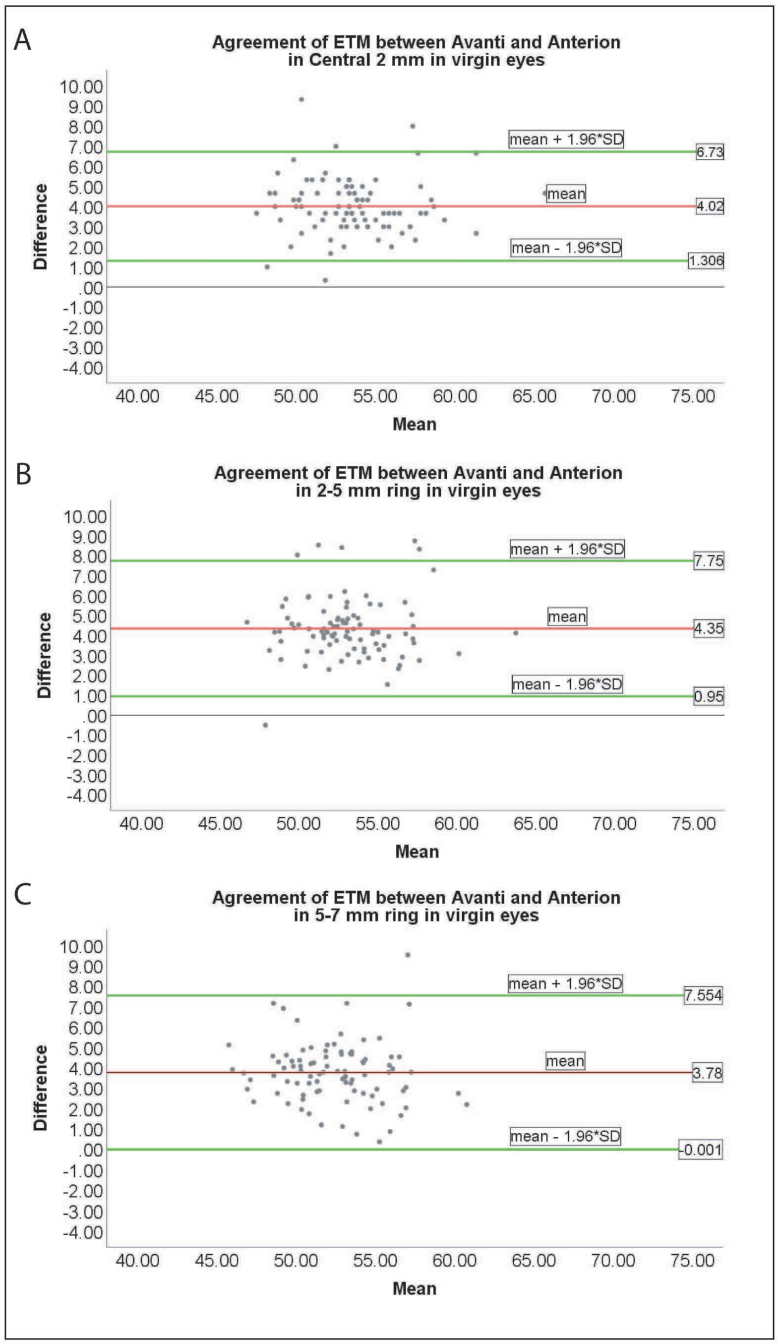

Figure E. Bland-Altman plots of virgin eyes, showing the difference in epithelial thickness measurements (ETM) (Avanti [Optovue, Inc] – Anterion [Heidelberg Engineering]), as a function of the mean epithelial thickness of both devices in the (A) central 2-mm zone, (B) 2- to 5-mm, and (C) 5- to 7-mm diameter rings, respectively. The red lines represent the mean difference; green lines represent the limits of agreement. SD = standard deviation; unit = μm

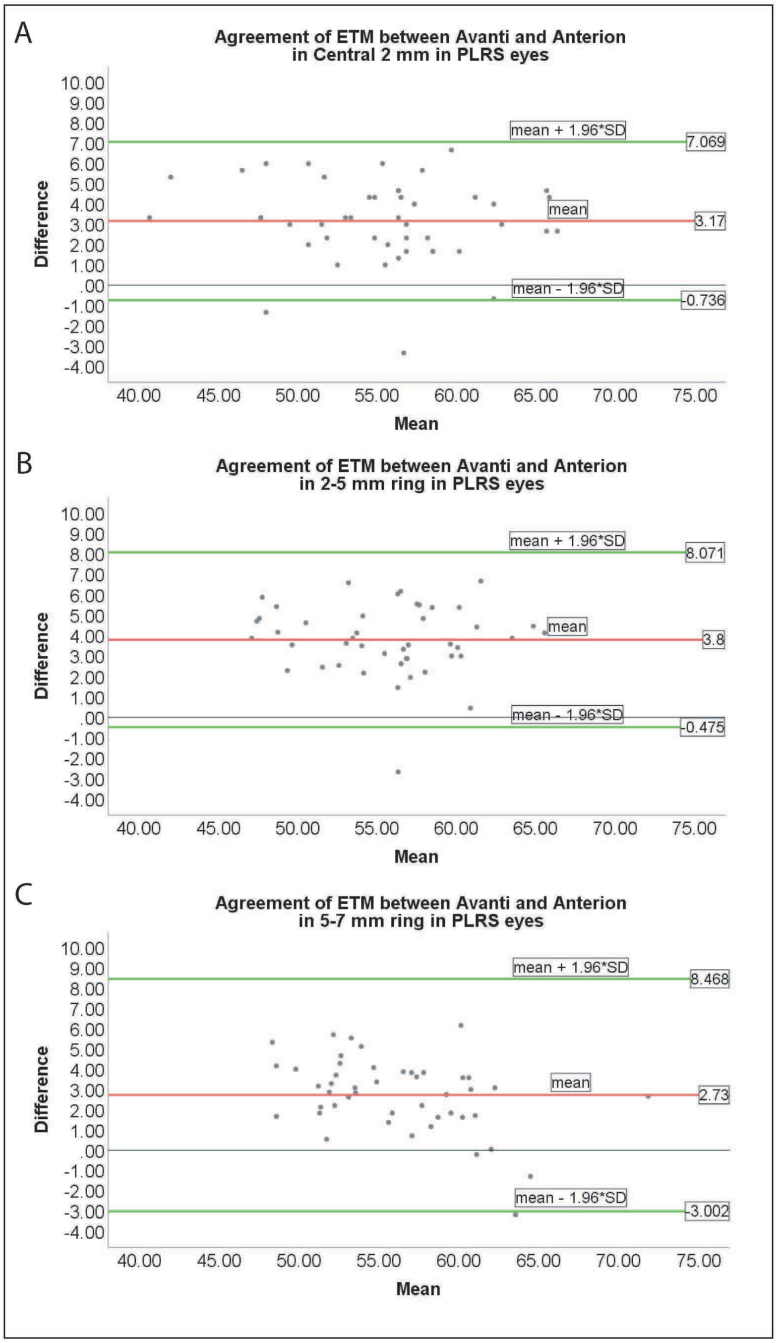

Figure F. Bland-Altman plots of post-laser refractive surgery (PLRS) eyes, showing the difference in epithelial thickness measurements (ETM) (Avanti [Optovue, Inc] − Anterion [Heidelberg Engineering]), as a function of the mean epithelial thickness of both devices in the (A) central 2-mm zone, (B) 2- to 5-mm, and (C) 5- to 7-mm diameter rings, respectively. The red lines represent the mean difference; green lines represent the limits of agreement. SD = standard deviation; unit = μm

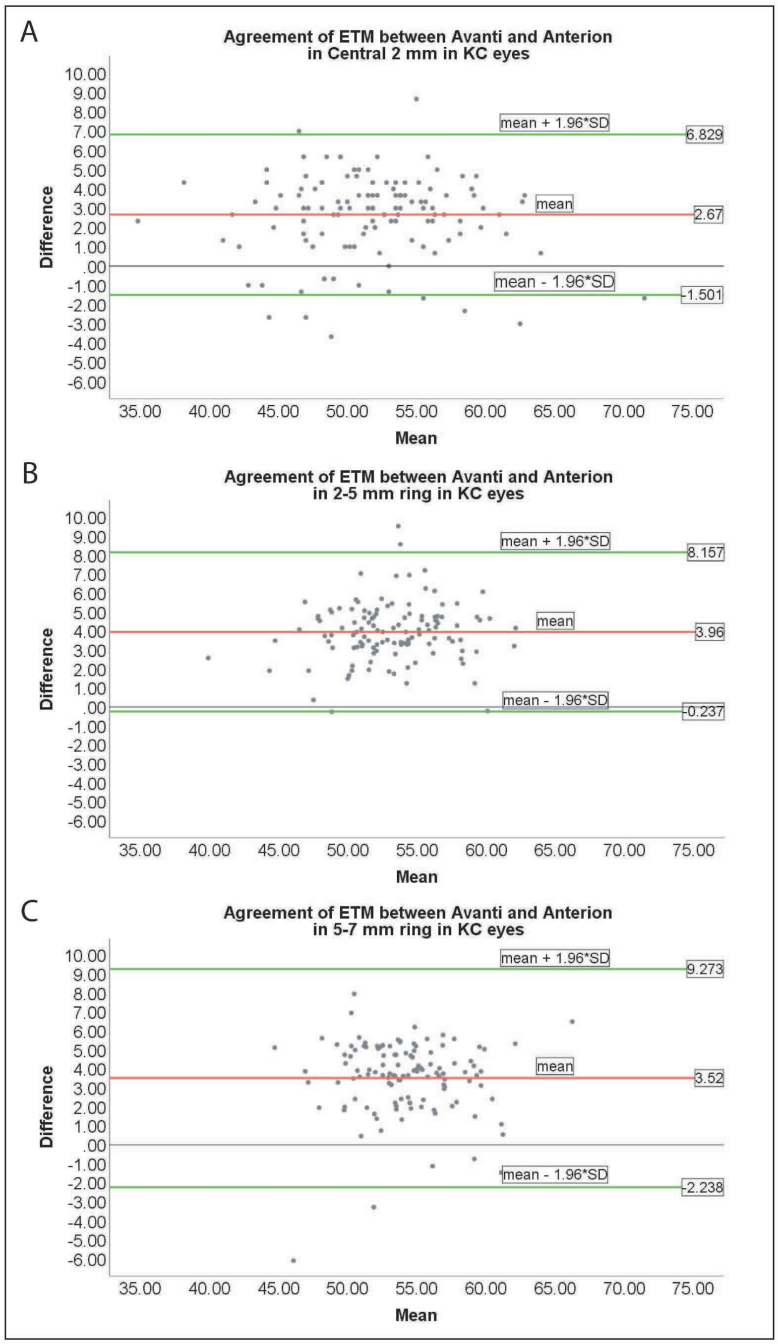

Figure G. Bland-Altman plots of keratoconic (KC) eyes, showing the difference in epithelial thickness measurements (ETM) (Avanti [Optovue, Inc] – Anterion [Heidelberg Engineering]), as a function of the mean epithelial thickness of both devices in the (A) central 2-mm zone, (B) 2- to 5-mm, and (C) 5- to 7-mm diameter rings, respectively. The red lines represent the mean difference; green lines represent the limits of agreement. SD = standard deviation; unit = μm

Paper 3

Epithelial Thickness Mapping in Keratoconic Corneas: Repeatability and Agreement Between CSO MS-39, Heidelberg Anterion and Optovue Avanti OCT Devices

ORIGINAL ARTICLE

Epithelial Thickness Mapping in Keratoconic Corneas: Repeatability and Agreement Between CSO MS-39, Heidelberg Anterion, and Optovue Avanti OCT Devices

Yue Feng, MD, MSc; Dan Z. Reinstein, MD, DABO, FRCOphth; Tore Nitter, MD, PhD; Timothy J. Archer, MA(Oxon) DipCompSci (Cantab), PhD; Colm McAlinden, MD, PhD, Geir Bertelsen, MD, PhD; Aleksandar Stojanovic, MD, PhD

ABSTRACT

PURPOSE: To assess repeatability and agreement of corneal epithelial thickness mapping in eyes with keratoconus using three optical coherence tomography (OCT) devices featuring different technologies: spectral-domain (SD) OCT combined with Placido disk corneal topography (MS-39), swept-source OCT (Anterion), and SD-OCT (Avanti).

METHODS: Three consecutive measurements were acquired with the three devices in 60 eyes with keratoconus. The mean epithelial thickness was calculated in the central 2-mm zone and in 2- to 5-mm and 5- to 7-mm diameter rings. The repeatability was calculated using pooled within-subject standard deviation (S_w). The agreement was assessed by paired *t* tests and Bland-Altman plots.

RESULTS: The repeatability (S_w) of the epithelial thickness for the central 2-mm zone was 0.91, 0.71, and 0.93 µm for the MS-39, Anterion, and Avanti, respectively. All thicknesses with the MS-39 were greater than those of the Anterion and Avanti, with mean differences of 4.11 ± 1.34 µm ($P < .001$) and 0.52 ± 1.30 µm ($P = .003$), respectively. The 95% limits of agreement were 1.484 to 6.736 µm for the MS-39 and Anterion, -3.068 to 2.028 µm for the Avanti and MS-39, and 1.258 to 5.922 µm for for the Avanti and Anterion.

CONCLUSIONS: Epithelial thickness mapping results were most repeatable with the Anterion, followed by the MS-39 and Avanti. The MS-39 gave the thickest values, followed by the Avanti and Anterion. The differences were significant, making the devices not interchangeable for epithelial thickness mapping in eyes with keratoconus.

[*J Refract Surg.* 2023;39(7):474-480.]

As its first cellular layer and refractive medium, the corneal epithelium has an important role in smoothing the ocular surface by actively growing thicker over stromal divots and becoming thinner over bumps, a phenomenon described as epithelial remodeling.[1] In this way, the epithelium regularizes the corneal refractive properties and, in most cases, leads to less corneal astigmatism, less prolate asphericity, and fewer higher order aberrations[2,3] compared to the same parameters measured on the stromal surface. The epithelium also decreases the eye's refractive power by simply increasing the corneal radius of curvature by the amount of its thickness.[4] Due to eyelid blinking mechanics, a slightly non-uniform epithelial thickness profile is induced in normal virgin eyes.[5]

Keratoconus is a progressive ectatic disease with localized biomechanical failure, which leads to a local protrusion and can lead to significant visual impairment due to irregular corneal optics.[6,7] The local protrusion causes intense epithelial remodeling, resulting in a donut-shaped epithelial pattern consisting of a compensatory thinning over the protruding part (cone) and a surrounding annulus of thicker epithelium.[1] One study also found that an overall epithelial thickness increase may be an early sign of keratoconus.[8] Epithelial thickness mapping (ETM) has become an important tool for the early diagnosis of keratoconus,[1,8-12] revealing the specific epithelial thickness pattern that hides the underlying stromal changes. Hence, the ETM may be thought of as an imprint of the protruding stromal surface from underneath the moldable epithelial tissue. ETM was pioneered by Reinstein et al in 1994,[1,5] and they have described "epithelial remodeling" across the whole cornea in eyes with keratoconus[1,9] using very high-frequency (VHF) digital ultrasound scanning (Artemis Insight 100; ArcScan, Inc). Since then, ETM has also become indispensable in therapeutic refractive surgery, assisting in analyzing irregular corneal optics[13] and identifying alternative treatment options. The epithelial thinning level over the cone has been used as a follow-up parameter to determine the progression of keratoconus before considering corneal cross-linking (CXL) and in evaluating its effect.

Optical coherence tomography (OCT)–based ETM appeared much later (2011),[10] without surpassing VHF digital ultrasound scanning in terms of repeatability, but it has become the most prevalent technology in current clinical practice due to its speed and ease of use. The first commercially available OCT-based instrument was the Optovue RT-100 (Optovue, Inc), featuring spectral-domain (SD) OCT technology, providing 6-mm diameter ETM, later replaced by a 9-mm ETM device (Avanti), which became the most commonly used ETM device.[14]

The more recently introduced swept-source (SS) OCT technology has a light source of longer wavelength than SD-OCT, allowing greater image depth and high-contrast imaging of the entire anterior segment.[15] The Anterion (Heidelberg Engineering) and Casia 2 (Tomey Corporation) are high-resolution anterior segment OCT devices featuring SS-OCT technology.[16] We recently reported the repeatability of ETM with the Anterion and its agreement with the Avanti for three different diagnostic groups (virgin, post-laser vision correction, and keratoconic eyes).[17]

The MS-39 (CSO) employs hybrid technology, combining SD-OCT with Placido disk imaging. It was released in 2018 and has been used for anterior segment imaging including ETM. So far, three studies[18-20] have investigated its repeatability for ETM, but no comparison with other devices was done. In the current study, we compared the repeatability and agreement between the MS-39 SD-OCT, Anterion SS-OCT, and Avanti SD-OCT. For data obtained by the MS-39, we used the manufacturer's recommended scanning mode (12 × 5 @ 10 mm), which has not been validated previously.

PATIENTS AND METHODS

Seventy-eight consecutive patients with keratoconus were examined at the eye department of the University Hospital of North Norway. All examinations were performed between March and December 2021. Inclusion criteria were: age 16 years or older; diagnosis of keratoconus; and spherical equivalent of myopia of 8.00 diopters (D) or less. Exclusion criteria were: history of previous ocular surgery (except for CXL); patients with conjunctival, limbal, or corneal disease (except for keratoconus); poor fixation or inability to complete the examination; and use of rigid gas permeable contact lens within 2 weeks of the examination day. One of each patient's eyes was randomly selected in patients where both eyes met the inclusion criteria; in cases where only one eye met the inclusion criteria, this eye was selected. Only one eye of each patient was used to avoid statistical bias, and, finally, 60 eyes of 60 patients were included.

From the Institute of Community Medicine, Faculty of Health Sciences, University in Tromsø, Norway (YF, GB); Reinstein Vision, London, United Kingdom (DZR, TJA); London Vision Clinic, EuroEyes Group, London, United Kingdom (DZR, TJA); Columbia University Medical Center, New York, New York (DZR); Sorbonne Université, Paris, France (DZR); and Biomedical Science Research Institute, Ulster University, Coleraine, United Kingdom (DZR); private practice (TN); the Department of Ophthalmology, Royal Gwent Hospital, Aneurin Bevan University Health Board, Newport, United Kingdom (CM); the Department of Ophthalmology, University Hospital North Norway, Tromsø, Norway (GB, AS); and Institute of Clinical Medicine, Faculty of Health Sciences, University in Tromsø, Norway (AS).

Submitted: January 3, 2023; Accepted: May 23, 2023

Disclosure: Dr. Reinstein is a consultant for Carl Zeiss Meditec (Carl Zeiss Meditec AG, Jena, Germany). Dr. Reinstein is also a consultant for CSO Italia (Florence, Italy) and has a proprietary interest in the Artemis technology (ArcScan, Inc, Golden, Colorado, USA) including patents administered by the Cornell Center for Technology Enterprise and Commercialization, Ithaca, New York. Dr. McAlinden has received consultancy fees/travel support from: Acufocus (Irvine, California, USA), Alcon Laboratories, Inc (Fort Worth, Texas, USA), Allergan (Irvine, California, USA), Atia Vision (Campbell, California, USA), Bausch and Lomb (Bridgewater, New Jersey, USA), Bayer (Leverkusen, Germany), Carl Zeiss Meditec (Dublin, California, USA), ClarVista (Aliso Viejo, California, USA), BVI (Liège, Belgium), Coopervision (Pleasanton, California, USA), CORD LLC (Laguna Beach, California, USA), Cutting Edge (Labége, France), European Society of Cataract and Refractive Surgeons (Dublin, Ireland), Eye and Vision Journal (Wenzhou, China), Eye Center Vista Alpina (Switzerland), Fudan University (Fudan, China), Glaukos (San Clemente, California, USA), Hoya (Frankfurt, Germany), Knowledge Gate Group (Copenhagen, Denmark), Johnson & Johnson Surgical Vision (Santa Ana, California, USA), Keio University (Tokyo, Japan), LensGen (Irvine, California, USA), Ludwig-Maximilians-University (München, Germany), Medevise Consulting SAS (Strasbourg, France), Novartis (Basel, Switzerland), Ocudyne (Roseville, Minnesota, USA), Ophtec BV (Groningen, The Netherlands) Ora (Andover, Massachusetts, USA), Perfect Lens (Irvine, California, USA), Pharmerit (Newton, Massachusetts, USA), PhysIOL (Liège, Belgium), Royal College of Ophthalmologists (London, UK), RxSight (Aliso Viejo, California, USA), Sun Yat-sen University (Guangzhou, China), Santen (Osaka, Japan), SCHWIND eye-tech-solutions (Kleinostheim, Germany), Scope (Crawley, UK), SightGlass Vision (Menlo Park, California, USA), Science in Vision (Bend, Oregan, USA), SpyGlass (Aliso Viejo, California, USA), STAAR Surgical (Monrovia, California, USA), Targomed GmbH (Bruchsal, Germany), Thea Pharmaceuticals (Clemont-Ferrand, France), University of Houston (Houston, Texas, USA), University of Michigan (Ann Arbor, Michigan, USA), University of São Paulo (São Paulo, Brazil), Vold Vision (Arkansas, USA), Wenzhou Medical University (Wenzhou, China), and Yoshida Eye Institute (Chiba, Japan). The remaining authors have no proprietary or financial interest in the materials presented herein.

Correspondence: Aleksandar Stojanovic, MD, PhD, Eye Department, University Hospital North Norway, Sykehusveien 38, 9019 Tromsø, Norway. Email: aleks@online.no

doi:10.3928/1081597X-20230606-01

Age, sex, and personal and family history of eye diseases were registered. Refraction, visual acuity, standard ophthalmological examination with slit-lamp examination, and funduscopy were performed before ETM measurements. This prospective study was approved by the Norwegian Regional Committee for Medical & Health Research Ethics (REK Nord 72084) and complied with the tenets of the Declaration of Helsinki. All patients provided informed consent for the anonymous use of their data in scientific analyses and publications.

Epithelial Thickness Measurements

The measurements with the three devices were obtained in a random order according to a randomized list generated by Microsoft Excel 2016 (Microsoft Corporation). Three consecutive measurements were taken with each device. All measurements with all three devices were acquired within 10 minutes between 10 AM and 2 PM.

Patients were asked to fixate on the fixation target while the examiner centered the OCT scan on the corneal vertex. Patients were instructed to blink immediately before each measurement and to keep their eyes wide open during the measurement. No eye drops were applied during testing.

The MS-39 (Phoenix software, v.4.1.1.5) uses a super luminescent diode at 845 nm as the illumination source for SD-OCT and a super luminescent diode at 635 nm for Placido disk. The "Corneal topography" mode "12 × 5 @10 mm" was used in this study because it provides a higher resolution than the "25 × 1 @16 mm" mode, which has been used in previous studies.[18-20] Data for the anterior surface from the Placido image and the elevation data of the anterior surface from OCT data are merged, using a proprietary method. After the acquisition, the MS-39 calculates the epithelial thickness within the 8-mm diameter and provides ETM, divided into a total of 25 sections.

The Anterion SS-OCT (software version 2.5.2) generates images using a laser light source of 1,300 nm wavelength and an active eye-tracker. It performs 65 radial scans with 256 A-scan lines centered on the corneal vertex within a 7-mm diameter.

The Avanti SD-OCT (software version 6.11.0.12) generates images using a SLed light source of 840 nm. ETM and the corneal pachymetry maps are divided into a total of 25 sections over a 9-mm diameter. The mean epithelial thickness of each section is presented.

For all three devices, the user may measure the epithelium thickness at any point on the map by mouse pointing. To compare the three devices, the mean values of the same 17 sections (including the central 2-mm zone) within a 7-mm diameter, as well as for the whole 2- to 5-mm and 5- to 7-mm rings, were calculated (**Figure A** available in the online version of this article). The technical specifications of the devices are summarized in **Table A** (available in the online version of this article)

Statistical Analysis

We used vertically mirrored symmetry superimposition so that nasal/temporal characteristics could be combined.[21] To assess the repeatability, we calculated the pooled within-subject standard deviation (S_w) (lower values of S_w indicate better repeatability).[22] The repeatability limit (r), defined as $1.96 \sqrt{2} \times S_w$ (= $2.77 \times S_w$), gives the value below which the absolute difference between two measurements of S_w would lie with 0.95 probability.[22]

To assess the agreement, we calculated the following parameters: difference in thickness readings; the 95% limits of agreement (LoA), defined as the mean difference in thickness ± 1.96 × standard deviation; and paired two-tailed *t* tests. Bland-Altman plots were generated to visualize the agreement between any two devices.

Data were entered into Microsoft Excel 2016 and then imported into statistical software (SPSS v25; IBM Corporation). A *P* value of less than .05 was considered to be statistically significant.

Sample Size Estimation

To achieve a 15% confidence in the estimate,[17-19] the required sample size is 43.[23] The current study comprised 60 eyes (n = 60), which gives 12% confidence.

RESULTS

This study evaluated 60 eyes (34 right eyes and 26 left eyes) of 60 patients (mean ± standard deviation age: 30.04 ± 9.50 years; range: 16 to 57 years; 50 men and 10 women) for both repeatability and agreement analyses.

Repeatability

The repeatability of the measurements was calculated for the 17 sections, as well as for the 2- to 5-mm, and 5- to 7-mm diameter rings (**Table B**, available in the online version of this article). Within the central 2-mm zone, S_w was 0.91 µm for the MS-39, 0.71 µm for the Anterion, and 0.93 µm for the Avanti. For the 2- to 5-mm diameter ring, the S_w range was 0.53 to 1.62 µm for the MS-39, 0.81 to 0.99 µm for the Anterion, and 1.04 to 1.68 µm for the Avanti. For the 5- to 7-mm diameter ring, the S_w range was 0.73 to 1.79 µm for the MS-39, 0.86 to 1.59 µm for the Anterion, and 0.75 to 1.79) µm for the Avanti.

Agreement Between MS-39, Anterion, and Avanti

The mean difference in epithelial thickness, the 95% LoA values, and paired, two-tailed *t* test *P* values were calculated for the 17 sections, the 2- to 5-mm and 5- to 7-mm diameter rings, and the total measured area (**Table C**, available in the online version of this article).

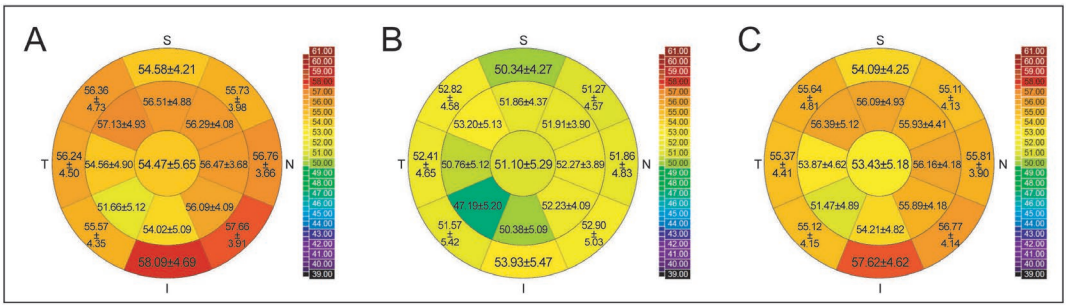

Figure 1. Average epithelial thickness mapping for the (A) MS-39 (CSO), (B) Anterion (Heidelberg Engineering), and (C) Avanti (Optovue, Inc) within the central 7-mm diameter. I = inferior; N = nasal; S = superior; T = temporal; unit: µm

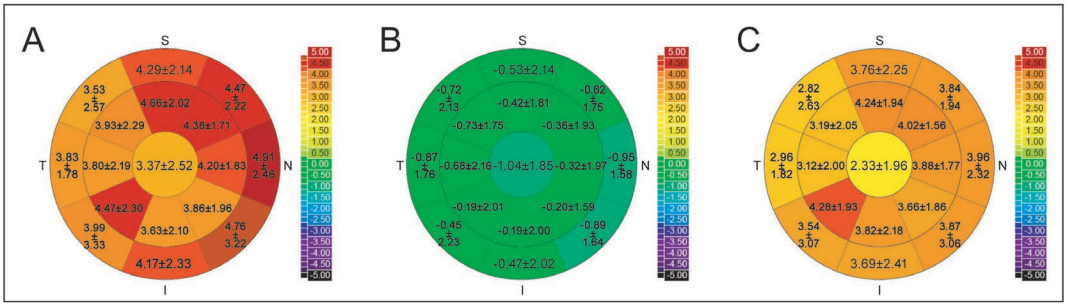

Figure 2. Differential mappings between each two devices within the central 7-mm diameter. (A) MS-39 – Anterion; (B) Avanti – MS-39; (C) Avanti – Anterion. The Avanti is manufactured by Optovue, Inc, the Anterion is manufactured by Heidelberg Engineering, and the MS-39 is manufactured by CSO. I = inferior; N = nasal; S = superior; T = temporal; unit: µm

The MS-39 measured significantly thicker epithelium than the Anterion in all sections, with a mean difference ranging from 3.37 to 4.91 µm ($P < .001$ for all). It also measured slightly thicker epithelium than the Avanti in all 17 sections except in the inferior section within the 2- to 5-mm ring, with a mean difference of 0.52 ± 1.30 µm ($P = .003$). Overall, the Anterion measured the thinnest, MS-39 the thickest, and the Avanti was in between.

The 95% LoAs were 1.484 and 6.736 µm for the MS-39 and Anterion, -3.068 and 2.028 µm for the Avanti and MS-39, and 1.258 and 5.922 µm for the Avanti and Anterion. The mean ETMs for the three devices are shown in **Figure 1**, and maps of the difference between the devices are shown in **Figure 2**. Bland-Altman plots for the agreement for the three pairs of devices are shown in **Figures B-D** (available in the online version of this article). For all three pairs of devices, the difference between the upper and lower 95% LoA was greater in the central 2-mm zone than in the 2- to 5-mm and 5- to 7-mm rings.

DISCUSSION

We compared repeatability of the MS 39 hybrid (SD-OCT + Placido disk) device with the SS-OCT Anterion and the SD-OCT Avanti in a group of 60 eyes with keratoconus. We also assessed the agreement between the three devices. The repeatability (S_w) values in the central 2-mm zone and 2- to 5-mm ring (**Table B**) were 0.91 and 1.06 µm for the MS-39, which was slightly worse than 0.71 and 0.91 µm for the Anterion but slightly better compared to 0.93 and 1.28 µm for the Avanti.

Repeatable corneal epithelial thickness measurements are important for the management of keratoconus,[1,9,12] as well as for safe corneal refractive surgery. The first ETM measurements by Reinstein et al with the Artemis VHF digital ultrasound showed S_w: 0.43 to 1.36 µm in 90% of the locations within the central 6-mm diameter after five consecutive measurements of 10 eyes 1 year after LASIK.[24] The repeatability should also be considered in the context of the measurement resolution of the device; VHF digital ultrasound can measure the epithelial thickness with less than 1 µm resolution, whereas OCT devices have a resolution of closer to 3.6 µm for the MS-39, 8 µm for the Anterion, and 5 µm for the Avanti.

Introduced 17 years later than the Artemis, the SD-OCT Optovue RT-100 has shown good repeatability and reproducibility of ETM in normal and not normal eyes

(dry eye syndrome, contact lens wear, post-laser refractive surgery, and keratoconic).[10,25,26] Ma et al[27] reported that the Avanti produced excellent repeatability and reproducibility for ETM measurements up to a 9-mm zone in normal eyes and eyes with different corneal conditions, showing S_w: 1.4 to 2.3 µm in 14 eyes with keratoconus. Lu et al[28] measured ETM with the Avanti within a 7-mm diameter, showing S_w: 1.31 to 2.43 µm in eyes with mild keratoconus and S_w: 1.90 to 3.89 µm in eyes with advanced keratoconus, whereas the current study found better repeatability of ETM measured with the Avanti, S_w: 0.75 to 1.68 µm, and Anterion, S_w: 0.71 to 1.59 µm within a 7-mm diameter in our group of 60 eyes with keratoconus. These results were consistent with the repeatability that we recently reported for the Avanti, S_w: 0.75 to 1.96 µm, and Anterion, S_w: 0.60 to 1.36 µm in eyes with keratoconus.[17]

Using the MS-39 in eyes with keratoconus, Vega-Estrada et al[18]found an S_w of 1.24 µm in the central 3-mm zone and ranges of 1.16 to 1.69 µm in the 3- to 6-mm ring and 1.42 to 2.70 µm in the 6- to 8-mm ring. Schiano-Lomoriello et al[19] reported an S_w of 1.57 µm in the central 3-mm zone in eyes with keratoconus with the MS-39. The current study showed better repeatability with the MS-39 with an S_w of 0.91 µm in the central 2-mm zone, and S_w ranges of 0.53 to 1.62 µm in the 2- to 5-mm and 0.73 to 1.79 µm in the 5- to 7-mm ring, which were better than the results from the two mentioned studies. **Table D** (available in the online version of this article) summarizes the literature findings on the repeatability of ETM studies.

We assume that 65 radial scans used by the Anterion versus the 12 radial scans used by the MS-39 and 8 radial scans used by the Avanti (both repeated five times for each meridian), as well as the Anterion's eye-tracking ability, are the likely factors explaining the better repeatability with the Anterion. We hypothesize that the repeated, wider-spread radial scans used by both the MS-39 and Avanti do not compensate for the denser coverage of the Anterion (**Table A**).

Concerning the agreement between any two devices, the epithelium measured by the MS-39 was significantly thicker than with the Anterion and slightly thicker than with the Avanti, whereas the measurements with the Anterion were significantly thinner than with the Avanti (**Table D**, **Figures 1-2**). The agreement between the Anterion and Avanti was consistent with the results we recently reported, with the Anterion measuring significantly thinner epithelium than the Avanti, with a mean difference of 3.68 ± 2.51 µm ($P < .001$).[17]

The three OCT devices use their own proprietary methods for their respective segmentation algorithms, and they treat differently the inclusion of the tear film in their ETM measurements. Corneal epithelial thickness measured by VHF ultrasound excludes the pre-corneal tear film thickness.[11] According to their respective manufacturers, the MS-39 measures the distance between the tear film layer and Bowman's layer, whereas the Anterion is "looking for the highest intensity of the anterior surface, which can provide the ability to reliably find the underlying structure in a repeatable way." The Avanti's manufacturer claims that its ETM measurements include the tear film.[29]

The CSO designers deemed it necessary to equip their SD-OCT device with a Placido disk and combine high-quality anterior curvature data with OCT-derived elevation data, to achieve the best possible resolution of the anterior surface morphology. However, conversion of curvature to elevation may be subject to errors inherent to the arc-step method.

All three devices use Fourier-domain detection, but they feature different imaging wavelengths and bandwidths. Although the Anterion uses a tunable swept laser light source (wavelength: 1,300 nm),[30] the Avanti and MS-39 use a broadband near-infrared SLed as their light source (wavelength: 840 nm and 845 nm, respectively). This results in different transversal and axial resolutions (3.6 × 35 µm for MS-39, 10 × 45 µm for Anterion, and 5 × 15 µm for Avanti), which presumably leads to different performance. Both SS-OCT and SD-OCT technologies record an interference spectrum that carries the information of the sample, but SS-OCT features a light source that sweeps the wavelength in time, whereas SD-OCT uses a spectrometer for wavelength separation. SS-OCT imaging features a denser scan pattern, due to its higher acquisition speed, as well as a larger scan depth, due to the use of a longer wavelength and reduced sensitivity roll-off. Hence, SS-OCT may quickly acquire the images of the whole anterior segment,[30] whereas SD-OCT provides higher contrast and resolution within a shorter depth range. In contrast to the other two devices, the Anterion features real-time eye-tracking during the acquisition of multiple B-scans, which allows precise alignment and enhanced detailed imaging.[16] For a given cornea, it appears that multiple factors may influence the repeatability of a device, such as axial resolution, image contrast, penetration rate, tracking, scanning speed, and scanning density. So, just by looking at the technical specifications, one cannot decide which device is superior, which emphasizes the importance of clinical evaluations.

As shown in **Table A**, the Anterion takes 0.33 second, followed by the Avanti with 0.58 second and the MS-39 with 1 second for acquisition. Concerning patient comfort, the red Placido rings lighting during the acquisition with the MS-39 may often cause the patient to blink. Overall, the Anterion has the advan-

tage of a shorter acquisition time and no issue with eye blinking, making it a more patient-friendly option.

Data within a 7-mm diameter were analyzed because all three devices covered that area (the maximum for Anterion, 1 mm off the maximum for MS-39, and 2 mm off the maximum for Avanti). Different coverage of the devices should be considered when comparing their clinical applicability, but there is no indication that this could affect our repeatability results within 7 mm.

A clinician will definitely recognize the same patterns on the ETMs of the three devices, which may be sufficient in most cases when used for diagnostics, but if used for surgical planning or scientific work, then the measurements of the three devices cannot be interchanged. Due to the complex relationship between the measurements, using a simple conversion factor is not advisable.

We found that the repeatability of the ETM measurements in eyes with keratoconus was high for all three devices, but the agreement between them was low. The repeatability with the MS-39 was slightly worse than with the Anterion, but better than with the Avanti. The mean epithelium thicknesses measured with the three devices were significantly different, making them not interchangeable for ETM in eyes with keratoconus.

AUTHOR CONTRIBUTIONS

Study concept and design (GB, AS); data collection (YF); analysis and interpretation of data (YF, DZR, TN, TJA, CM, AS); writing the manuscript (YF); critical revision of the manuscript (DZR, TN, TJA, CM, GB, AS); statistical expertise (CM); administrative, technical, or material support (TJA); supervision (DZR, TN, GB, AS)

REFERENCES

1. Reinstein DZ, Archer TJ, Gobbe M. Corneal epithelial thickness profile in the diagnosis of keratoconus. *J Refractive Surg.* 2009;25:604-610. https://doi.org/10.3928/1081597X-20090610-06
2. Zhou W, Reinstein DZ, Archer TJ, Chen X, Utheim TP, Feng Y, Stojanovic A. Intraoperative swept-source OCT-based corneal topography for measurement and analysis of stromal surface after epithelial removal. *J Refractive Surg.* 2021;37:484-492.
3. Reinstein DZ, Silverman RH, Sutton HF, Coleman DJ. Very high-frequency ultrasound corneal analysis identifies anatomic correlates of optical complications of lamellar refractive surgery: anatomic diagnosis in lamellar surgery. *Ophthalmology.* 1999;106(3):474-482. https://doi.org/10.1016/S0161-6420(99)90105-7 PMID:10080202
4. Simon G, Ren Q, Kervick GN, Parel JM. Optics of the corneal epithelium. *Refract Corneal Surg.* 1993;9(1):42-50. https://doi.org/10.3928/1081-597X-19930101-10 PMID:8481372
5. Reinstein DZ, Silverman RH, Coleman DJ. High-frequency ultrasound measurement of the thickness of the corneal epithelium. *Refract Corneal Surg.* 1993;9(5):385-387. https://doi.org/10.3928/1081-597X-19930901-12 PMID:8241045
6. Rabinowitz YS. Keratoconus. *Surv Ophthalmol.* 1998;42(4):297-319. https://doi.org/10.1016/S0039-6257(97)00119-7 PMID:9493273
7. Padmanabhan P, Lopes BT, Eliasy A, Abass A, Elsheikh A. In vivo biomechanical changes associated with Keratoconus progression. *Curr Eye Res.* 2022;47(7):982-986. https://doi.org/10.1080/02713683.2022.2058020 PMID:35385372
8. Kanellopoulos AJ, Aslanides IM, Asimellis G. Correlation between epithelial thickness in normal corneas, untreated ectatic corneas, and ectatic corneas previously treated with CXL: is overall epithelial thickness a very early ectasia prognostic factor? *Clin Ophthalmol.* 2012;6:789-800. https://doi.org/10.2147/OPTH.S31524 PMID:22701079
9. Silverman RH, Urs R, Roychoudhury A, Archer TJ, Gobbe M, Reinstein DZ. Epithelial remodeling as basis for machine-based identification of keratoconus. *Invest Ophthalmol Vis Sci.* 2014;55(3):1580-1587. https://doi.org/10.1167/iovs.13-12578 PMID:24557351
10. Li Y, Tan O, Brass R, Weiss JL, Huang D. Corneal epithelial thickness mapping by Fourier-domain optical coherence tomography in normal and keratoconic eyes. *Ophthalmology.* 2012;119(12):2425-2433. https://doi.org/10.1016/j.ophtha.2012.06.023 PMID:22917888
11. Reinstein DZ, Gobbe M, Archer TJ, Silverman RH, Coleman DJ. Epithelial, stromal, and total corneal thickness in keratoconus: three-dimensional display with Artemis very-high frequency digital ultrasound. *J Refractive Surg.* 2010;26:259-271. https://doi.org/10.3928/1081597X-20100218-01
12. Haque S, Jones L, Simpson T. Thickness mapping of the cornea and epithelium using optical coherence tomography. *Optom Vis Sci.* 2008;85:E963-E976. https://doi.org/10.1097/OPX.0b013e318188892c
13. Reinstein DZ, Archer TJ, Dickeson ZI, Gobbe M. Transepithelial phototherapeutic keratectomy protocol for treating irregular astigmatism based on population epithelial thickness measurements by Artemis very high-frequency digital ultrasound. *J Refractive Surg.* 2014;30:380-387. https://doi.org/10.3928/1081597X-20140508-01
14. El Wardani M, Hashemi K, Aliferis K, Kymionis G. Topographic changes simulating keratoconus in patients with irregular inferior epithelial thickening documented by anterior segment optical coherence tomography. *Clin Ophthalmol.* 2019;13:2103-2110. https://doi.org/10.2147/OPTH.S208101 PMID:31802839
15. Shoji T, Kato N, Ishikawa S, et al. In vivo crystalline lens measurements with novel swept-source optical coherent tomography: an investigation on variability of measurement. *BMJ Open Ophthalmol.* 2017;1(1):e000058. https://doi.org/10.1136/bmjophth-2016-000058 PMID:29354706
16. Asam JS, Polzer M, Tafreshi A, Hirnschall N, Findl O. Anterior segment OCT. In: Bille JF, ed. *High Resolution Imaging in Microscopy and Ophthalmology: New Frontiers in Biomedical Optics.* Springer; 2019:285-299. https://doi.org/10.1007/978-3-030-16638-0_13
17. Feng Y, Reinstein DZ, Nitter T, Archer TJ, McAlinden C, Chen X, Bertelsen G, Utheim TP, Stojanovic A. Heidelberg Anterion swept-source OCT corneal epithelial thickness mapping: repeatability and agreement with Optovue Avanti. *J Refractive Surg.* 2022;38:356-363.
18. Vega-Estrada A, Mimouni M, Espla E, Alió Del Barrio J, Alió JL. Corneal epithelial thickness intrasubject repeatability and its relation with visual limitation in keratoconus. *Am J Ophthalmol.* 2019;200:255-262. https://doi.org/10.1016/j.ajo.2019.01.015 PMID:30689987
19. Schiano-Lomoriello D, Bono V, Abicca I, Savini G. Repeatability of anterior segment measurements by optical coherence tomography combined with Placido disk corneal topography in eyes with keratoconus. *Sci Rep.* 2020;10(1):1124. https://doi.org/10.1038/s41598-020-57926-7 PMID:31980662
20. Savini G, Schiano-Lomoriello D, Hoffer KJ. Repeatability of automatic measurements by a new anterior segment optical coherence tomographer combined with Placido topography and agreement with 2 Scheimpflug cameras. *J Cataract Refract Surg.*

2018;44(4):471-478. https://doi.org/10.1016/j.jcrs.2018.02.015 PMID:29705008

21. Zhou W, Stojanovic A. Comparison of corneal epithelial and stromal thickness distributions between eyes with keratoconus and healthy eyes with corneal astigmatism ≥ 2.0 D. *PLoS One*. 2014;9(1):e85994. https://doi.org/10.1371/journal.pone.0085994 PMID:24489687
22. Bland JM, Altman DG. Measurement error. *BMJ*. 1996;313(7059):744. https://doi.org/10.1136/bmj.313.7059.744 PMID:8819450
23. McAlinden C, Khadka J, Pesudovs K. Precision (repeatability and reproducibility) studies and sample-size calculation. *J Cataract Refract Surg*. 2015;41(12):2598-2604. https://doi.org/10.1016/j.jcrs.2015.06.029 PMID:26796439
24. Reinstein DZ, Archer TJ, Gobbe M, Silverman RH, Coleman DJ. Repeatability of layered corneal pachymetry with the Artemis very high-frequency digital ultrasound arc-scanner. *J Refractive Surg*. 2010;26:646-659. https://doi.org/10.3928/1081597X-20091105-01
25. Ma XJ, Wang L, Koch DD. Repeatability of corneal epithelial thickness measurements using Fourier-domain optical coherence tomography in normal and post-LASIK eyes. *Cornea*. 2013;32(12):1544-1548. https://doi.org/10.1097/ICO.0b013e3182a7f39d PMID:24145634
26. Sella R, Zangwill LM, Weinreb RN, Afshari NA. Repeatability and reproducibility of corneal epithelial thickness mapping with spectral-domain optical coherence tomography in normal and diseased cornea eyes. *Am J Ophthalmol*. 2019;197:88-97. https://doi.org/10.1016/j.ajo.2018.09.008 PMID:30240724
27. Ma JX, Wang L, Weikert MP, Montes de Oca I, Koch DD. Evaluation of the repeatability and reproducibility of corneal epithelial thickness mapping for a 9-mm zone using optical coherence tomography. *Cornea*. 2019;38(1):67-73. https://doi.org/10.1097/ICO.0000000000001806 PMID:30379719
28. Lu NJ, Chen D, Cui LL, Wang L, Chen SH, Wang QM. Repeatability of cornea and sublayer thickness measurements using optical coherence tomography in corneas of anomalous refractive status. *J Refract Surg*. 2019;35:600-605. https://doi.org/10.3928/1081597X-20190806-03
29. Azartash K, Kwan J, Paugh JR, Nguyen AL, Jester JV, Gratton E. Pre-corneal tear film thickness in humans measured with a novel technique. *Mol Vis*. 2011;17:756-767. PMID:21527997
30. Aumann S, Donner S, Fischer J, Müller F. Optical coherence tomography (OCT): principle and technical realization. In: Bille JF ed, *High Resolution Imaging in Microscopy and Ophthalmology: New Frontiers in Biomedical Optics*. Springer; 2019:59-85.

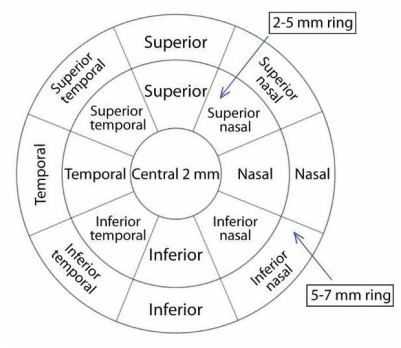

Figure A. Epithelial thickness mapping 17 sections and two rings used in the analysis of the measurements.

Table A
Technical Specifications of the Three Devices for ETM

Parameter	MS-39	Anterion	Avanti
Light source wavelength (nm)	OCT: 845 Placido: 635	1300	840
A-scan speed	102,400	50000	70000
Axial resolution (μm)	3.6	<10	5
Transverse resolution (μm)	35	<45	15
A-scan depth (mm)	7.5	14	3
Maximum Scan width (mm)	16	16.5	12
B scan	10 × 5[a]	65 × 1	8 × 5
Number of A-scans per B-scan	1024[b]	256	1024
Acquisition time (s)	1	0.33	0.58

ETM = epithelial thickness mapping; OCT = optical coherence tomography
[a]*Customized in this study as recommended by the manufacturer.*
[b]*1600 A-scan on 16 mm and 800 A-scan on 8 mm.*

Table B Repeatability of ETM (μm) Measurements of the Three Devices			
Repeatability, S_w (Repeatability Limit, r)[a]	**MS-39**	**Anterion**	**Avanti**
Zone 0 to 2 mm			
Central	0.91 (2.53)	0.71 (1.97)	0.93 (2.59)
Ring 2- to 5-mm			
Nasal	0.53 (1.46)	0.81 (2.24)	1.11 (3.08)
Superior nasal	0.97 (2.68)	0.90 (2.48)	1.22 (3.39)
Superior	0.90 (2.49)	0.99 (2.73)	1.15 (3.18)
Superior temporal	1.13 (3.12)	0.98 (2.72)	1.04 (2.89)
Temporal	1.27 (3.52)	0.94 (2.59)	1.68 (4.65)
Inferior temporal	1.62 (4.48)	0.92 (2.56)	1.45 (4.00)
Inferior	1.39 (3.84)	0.91 (2.53)	1.33 (3.69)
Inferior nasal	0.72 (1.98)	0.82 (2.29)	1.28 (3.55)
Ring 2-5 mm total	1.06 (2.95)	0.91 (2.52)	1.28 (3.55)
Ring 5- to 7-mm			
Nasal	0.80 (2.22)	0.86 (2.39)	1.11 (3.07)
Superior nasal	1.36 (3.76)	1.13 (3.12)	1.07 (2.97)
Superior	1.41 (3.92)	1.28 (3.54)	1.19 (3.28)
Superior temporal	1.22 (3.38)	1.34 (3.71)	1.34 (3.70)
Temporal	0.94 (2.61)	1.21 (3.35)	1.44 (3.99)
Inferior temporal	1.79 (4.95)	1.17 (3.25)	1.79 (4.97)
Inferior	1.37 (3.80)	1.59 (4.40)	0.99 (2.75)
Inferior nasal	0.73 (2.02)	1.21 (3.36)	0.75 (2.07)
Ring 5- to 7-mm total	1.20 (3.33)	1.22 (3.39)	1.21 (3.35)

ETM = epithelial thickness mapping; S_w = pooled within-subject standard deviation

[a]*Repeatability limit= 2.77 × S_w*

The Anterion is manufactured by Heidelberg Engineering, the Avanti is manufactured by Optovue, Inc, and the MS-39 is manufactured by CSO.

TABLE C

Agreement of ETM Measurements Between Two Devices

	Epithelial Thickness, Mean ± SD (µm)			MS-39 – Anterion			Avanti - MS-39			Avanti - Anterion		
				Difference			Difference			Difference		
Parameter	MS-39	Anterion	Avanti	Mean ± SD (µm)	*P*	95% LoA Range (µm)	Mean ± SD (µm)	*P*	95% LoA Range (µm)	Mean ± SD (µm)	*P*	95% LoA Range (µm)
Zone 0 to 2 mm												
Central	54.47 ± 5.65	51.10 ± 5.29	53.43 ± 5.18	3.37 ± 2.52	< .001	-1.569 to 8.309	-1.04 ± 1.85	< .001	-4.666 to 2.586	2.33 ± 1.96	< .001	-1.512 to 6.172
Ring 2-5 mm												
Nasal	56.47 ± 3.68	52.27 ± 3.89	56.16 ± 4.18	4.20 ± 1.83	< .001	0.613 to 7.787	-0.32 ± 1.97	.219	-4.181 to 3.541	3.88 ± 1.77	< .001	0.411 to 7.349
Superior nasal	56.29 ± 4.08	51.91 ± 3.90	55.93 ± 4.41	4.38 ± 1.71	< .001	1.028 to 7.732	-0.36 ± 1.93	.153	-4.143 to 3.423	4.02 ± 1.56	< .001	0.962 to 7.078
Superior	56.51 ± 4.88	51.86 ± 4.37	56.09 ± 4.93	4.66 ± 2.02	< .001	0.701 to 8.619	-0.42 ± 1.81	.079	-3.968 to 3.128	4.24 ± 1.94	< .001	0.438 to 8.042
Superior temporal	57.13 ± 4.93	53.20 ± 5.13	56.39 ± 5.12	3.93 ± 2.29	< .001	-0.558 to 8.418	-0.73 ± 1.75	.002	-4.160 to 2.700	3.19 ± 2.05	< .001	-0.828 to 7.208
Temporal	54.56 ± 4.90	50.76 ± 5.12	53.87 ± 4.62	3.80 ± 2.19	< .001	-0.492 to 8.092	-0.68 ± 2.16	.017	-4.914 to 3.554	3.12 ± 2.00	< .001	-0.800 to 7.040
Inferior temporal	51.66 ± 5.12	47.19 ± 5.20	51.47 ± 4.89	4.47 ± 2.30	< .001	-0.038 to 8.978	-0.19 ± 2.01	.457	-4.130 to 3.750	4.28 ± 1.93	< .001	0.497 to 8.063
Inferior	54.02 ± 5.09	50.38 ± 5.09	54.21 ± 4.82	3.63 ± 2.10	< .001	-0.486 to 7.746	0.19 ± 2.00	.466	-3.730 to 4.110	3.82 ± 2.18	< .001	-0.453 to 8.093
Inferior nasal	56.09 ± 4.09	52.23 ± 4.09	55.89 ± 4.18	3.86 ± 1.96	< .001	0.018 to 7.702	-0.20 ± 1.59	.334	-3.316 to 2.916	3.66 ± 1.86	< .001	0.014 to 7.306
Ring 2- to 5-mm total	55.34 ± 3.51	51.22 ± 3.31	55.00 ± 3.52	4.12 ± 1.54	< .001	1.102 to 7.138	-0.34 ± 1.43	.071	-3.143 to 2.463	3.78 ± 1.30	< .001	1.232 to 6.328
Ring 5- to 7-mm												
Nasal	56.76 ± 3.66	51.86 ± 4.83	55.81 ± 3.90	4.91 ± 2.46	< .001	0.088 to 9.732	-0.95 ± 1.58	< .001	-4.047 to 2.147	3.96 ± 2.32	< .001	-0.587 to 8.507
Superior nasal	55.73 ± 3.98	51.27 ± 4.57	55.11 ± 4.13	4.47 ± 2.22	< .001	0.119 to 8.821	-0.62 ± 1.75	.008	-4.050 to 2.810	3.84 ± 1.94	< .001	0.038 to 7.642
Superior	54.58 ± 4.21	50.34 ± 4.27	54.09 ± 4.25	4.29 ± 2.14	< .001	0.096 to 8.484	-0.53 ± 2.14	.061	-4.724 to 3.664	3.76 ± 2.25	< .001	-0.650 to 8.170
Superior temporal	56.36 ± 4.73	52.82 ± 4.58	55.64 ± 4.81	3.53 ± 2.57	< .001	-1.507 to 8.567	-0.72 ± 2.13	.011	-4.895 to 3.455	2.82 ± 2.63	< .001	-2.335 to 7.975
Temporal	56.24 ± 4.50	52.41 ± 4.65	55.37 ± 4.41	3.83 ± 1.78	< .001	0.341 to 7.319	-0.87 ± 1.76	< .001	-4.320 to 2.580	2.96 ± 1.82	< .001	-0.607 to 6.527
Inferior temporal	55.57 ± 4.35	51.57 ± 5.42	55.12 ± 4.15	3.99 ± 3.33	< .001	-2.537 to 10.517	-0.45 ± 2.23	.123	-4.821 to 3.921	3.54 ± 3.07	< .001	-2.477 to 9.557
Inferior	58.09 ± 4.69	53.93 ± 5.47	57.62 ± 4.62	4.17 ± 2.33	< .001	-0.397 to 8.737	-0.47 ± 2.02	.075	-4.429 to 3.489	3.69 ± 2.41	< .001	-1.034 to 8.414
Inferior nasal	57.66 ± 3.91	52.90 ± 5.03	56.77 ± 4.14	4.76 ± 3.22	< .001	-1.551 to 11.071	-0.89 ± 1.64	< .001	-4.104 to 2.324	3.87 ± 3.06	< .001	-2.128 to 9.868
Ring 5- to 7-mm total	56.40 ± 3.69	52.18 ± 3.70	55.73 ± 3.64	4.22 ± 1.30	< .001	1.672 to 6.768	-0.67 ± 1.44	.001	-3.492 to 2.152	3.56 ± 1.25	< .001	1.110 to 6.010
Total 17 sections	55.81 ± 3.27	51.70 ± 3.16	55.29 ± 3.26	4.11 ± 1.34	< .001	1.484 to 6.736	-0.52 ± 1.30	.003	-3.068 to 2.028	3.59 ± 1.19	< .001	1.258 to 5.922

ETM = epithelial thickness mapping; LoA = limits of agreement; SD = standard deviation

[a]*According to the paired* t *test.*

The Anterion is manufactured by Heidelberg Engineering, the Avanti is manufactured by Optovue, Inc, and the MS-39 is manufactured by CSO.

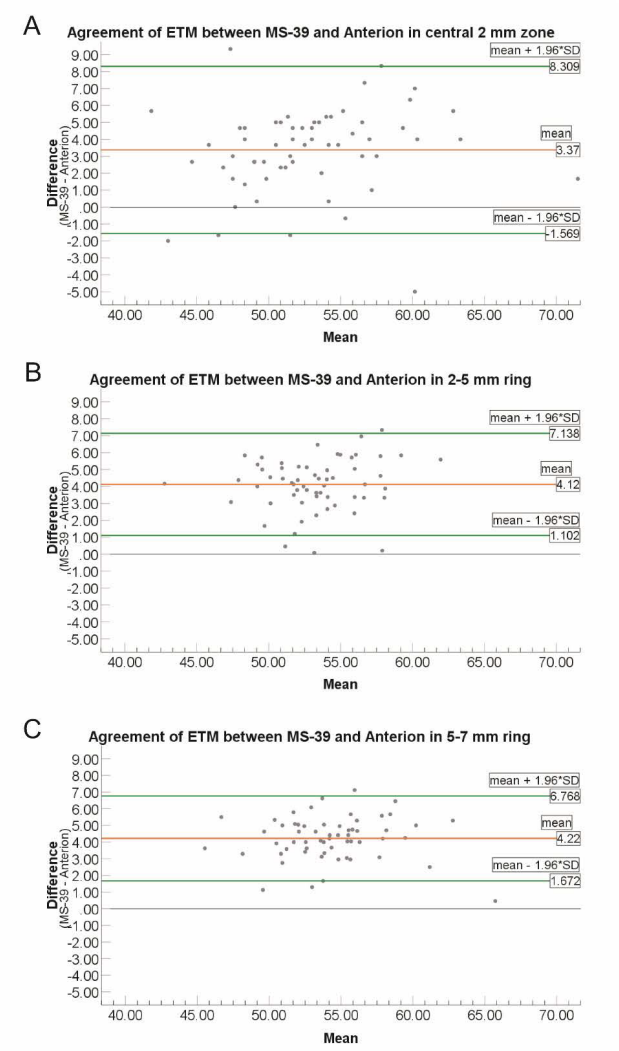

Figure B. Bland-Altman plots showing the difference in epithelial thickness measurements (MS-39 – Anterion) as a function of the mean epithelial thickness of the two devices in the (A) central 2-mm zone, (B) 2- to 5-mm diameter rings, and (C) 5- to 7-mm diameter rings, respectively. The red lines represent the mean difference and green lines represent the 95% limits of agreement. The Anterion is manufactured by Heidelberg Engineering and the MS-39 is manufactured by CSO. Unit: μm

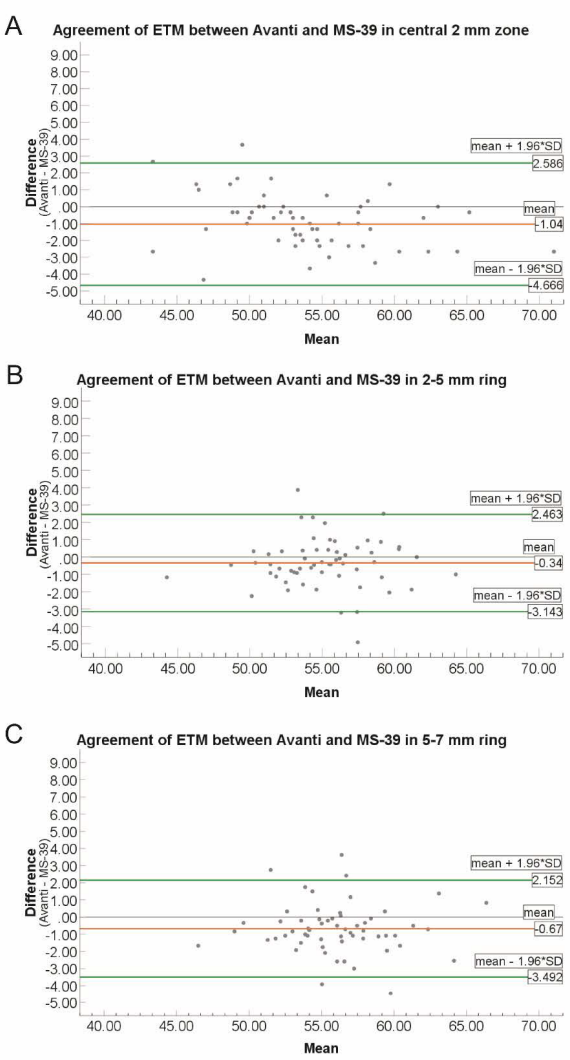

Figure C. Bland-Altman plots showing the difference in epithelial thickness measurements (Avanti – MS-39) as a function of the mean epithelial thickness of the two devices in the (A) central 2-mm zone, (B) 2- to 5-mm diameter rings, and (C) 5- to 7-mm diameter rings, respectively. The red lines represent the mean difference and green lines represent the 95% limits of agreement. The Avanti is manufactured by Optovue, Inc and the MS-39 is manufactured by CSO. Unit: μm

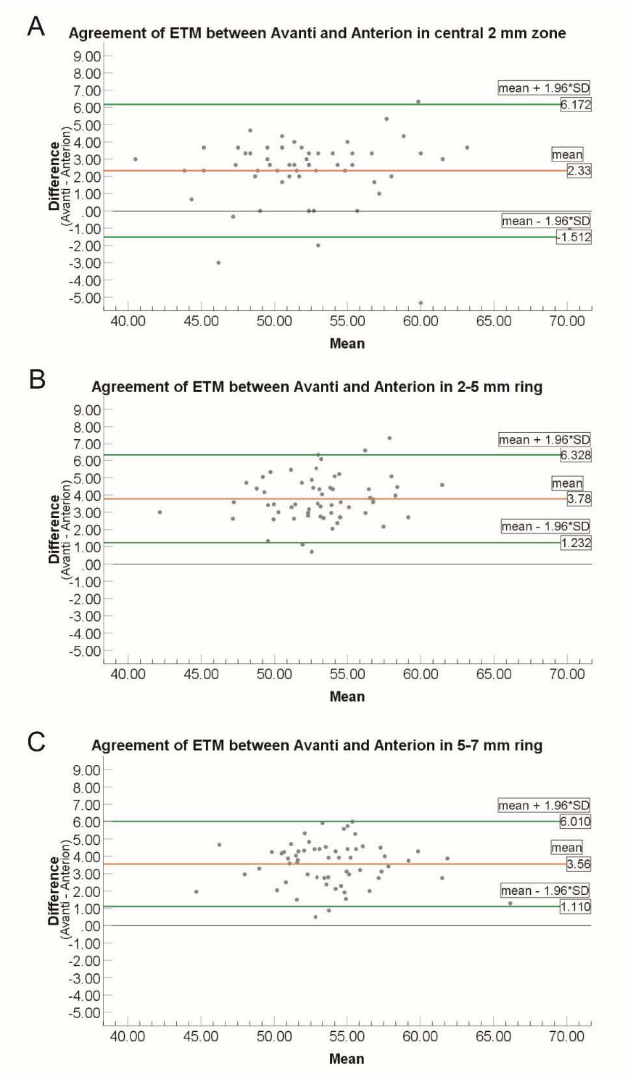

Figure D. Bland-Altman plots showing the difference in epithelial thickness measurements (Avanti – Anterion) as a function of the mean epithelial thickness of the two devices in the (A) central 2-mm zone, (B) 2- to 5-mm diameter rings, and (C) 5- to 7-mm diameter rings, respectively. The red lines represent the mean difference and green lines represent the 95% limits of agreement. The Avanti is manufactured by Optovue and the Anterion is manufactured by Heidelberg Engineering. Unit: μm

Table D
Repeatability of ETM Measurements Reported by Previous Investigators

		Repeatability, S_w				
Authors/ Year	**Eyes (n)**	**Normal**	**PLRS**	**KC**	**Areas**	**Instrument used**
Reinstein and colleagues (2010)	KC: 10		0.58		vertex	Very-high frequency ultrasound
			0.43-1.36		central 6 mm	
Ma and colleagues (2013)	Normal: 35 PLRS: 45	0.7	0.7		central 2 mm	Optovue RT-100 SD-OCT
		0.6-0.9	0.8-1.7		2-5 mm	
		0.8-1.2	1.4-2.2		5-6 mm	
Sella and colleagues (2019)	Normal: 12 PLRS: 48	0.9	1.2		central 2 mm	
		0.9-1.3	1.3-1.5		2-5 mm	
		1.0-1.4	1.5-1.9		5-6 mm	
Lu and colleagues (2019)	Normal: 75 PLRS: 204 KC:73	0.89	1.35-2.34	1.41-2.42	central 2 mm	Optovue Avanti SD-OCT
		0.99-1.24	1.2-3.56	1.36-3.89	2-5 mm	
		1-1.26	1.42-3.04	1.31-3.83	5-7 mm	
		0.92-1.62	1.57-2.94	1.02-4.01	7-9 mm	
Savini and colleagues (2018)	Normal: 96 PLRS: 43	0.99	1.84		central 3 mm	MS-39 SD OCT
		1.06-1.57	1.50-2.10		3-6 mm	
Vega-Estrada and colleagues (2019)	Normal: 60 KC:170	2.03		1.24	central 3 mm	
		0.84-1.18		1.16-1.69	3-6 mm	
		0.99-2.72		1.42-2.70	6-8 mm	
Schiano-Lomoriello and colleagues (2020)	KC: 43			1.57	central 3 mm	
Feng and colleagues (2022)	Normal: 90 PLRS: 46 KC:122	0.98	0.75	1.15	central 2 mm	Optovue Avanti SD-OCT
		1.08-1.19	1.07-1.49	1.17-1.52	2-5 mm	
		0.94-1.27	1.70-2.40	1.29-1.72	5-7 mm	
		0.64	0.6	0.91	central 2 mm	Anterion SS- OCT
		0.69-0.89	0.79-0.96	0.91-1.09	2-5 mm	
		0.86-1.11	1.07-2.05	1.10-1.47	5-7 mm	
Current study	KC: 60			0.93	central 2 mm	Optovue Avanti SD-OCT
				1.04-1.68	2-5 mm	
				0.75-1.79	5-7 mm	
				0.71	central 2 mm	Anterion SS- OCT
				0.81-0.98	2-5 mm	
				0.86-1.59	5-7 mm	
				0.91	central 2 mm	MS-39 SD OCT
				0.53-1.62	2-5 mm	
				0.73-1.79	5-7 mm	

ETM = epithelial thickness mapping; KC = keratoconus; OCT = optical coherence tomographer; PLRS = post-laser refractive surgery; SD = spectral-domain; SS = swept-source; S_w = pooled within-subject standard deviation
The Avanti is manufactured by Optovue and the Anterion is manufactured by Heidelberg Engineering.